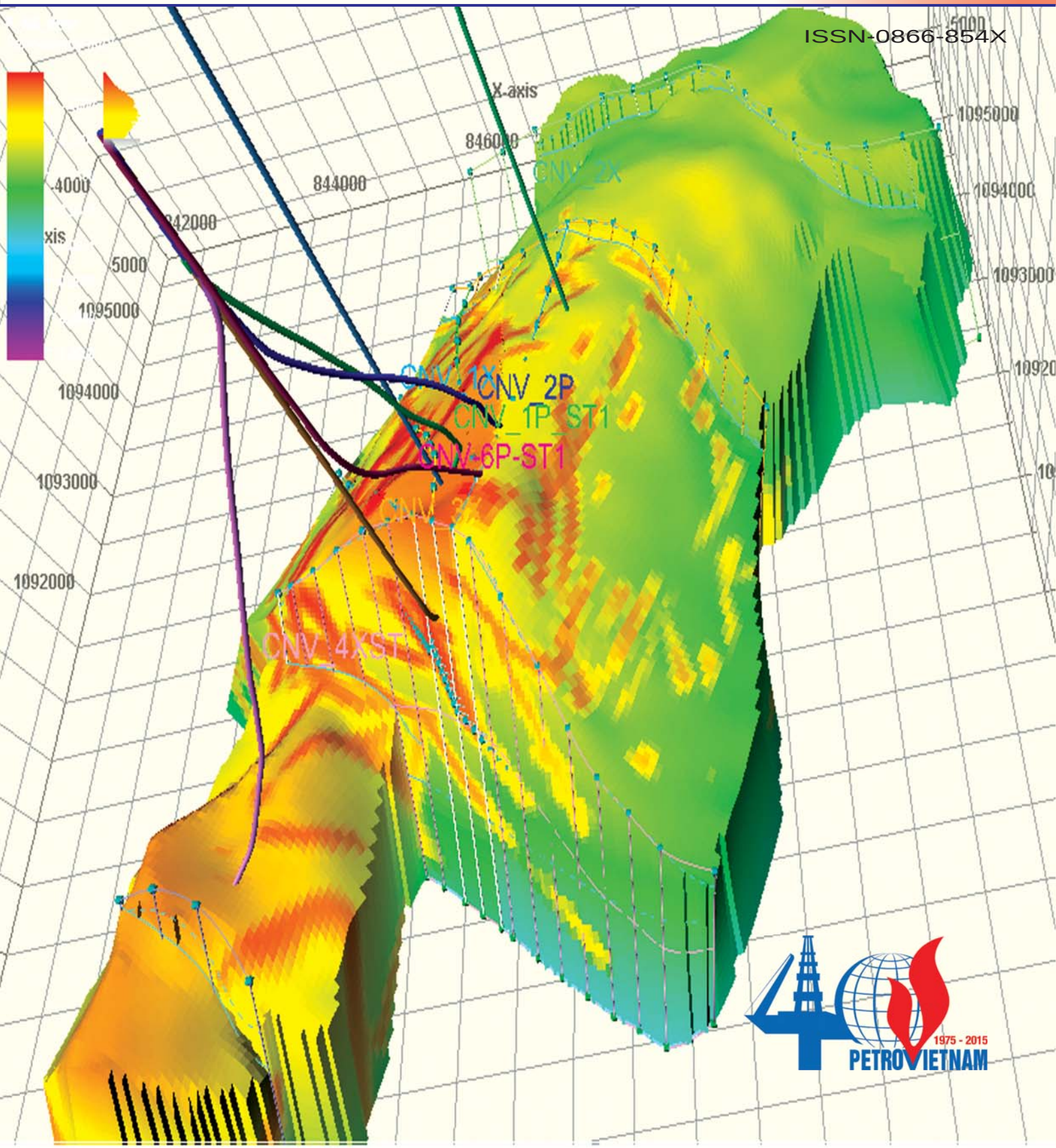
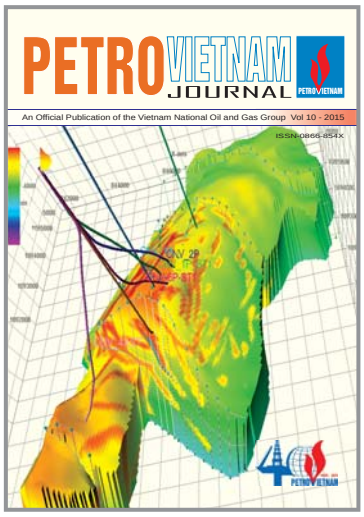
# PETROVIETNAM JOURNAL

An Official Publication of the Vietnam National Oil and Gas Group Vol 10 - 2015

ISSN-0866-854X



PETROVIETNAM JOURNAL IS PUBLISHED MONTHLY BY VIETNAM NATIONAL OIL AND GAS GROUP




**EDITOR-IN-CHIEF**
Dr. Nguyen Quoc Thap

**DEPUTY EDITOR-IN-CHIEF**
Dr. Le Manh Hung
Dr. Phan Ngoc Trung

**EDITORIAL BOARD MEMBERS**
Dr. Hoang Ngoc Dang
Dr. Nguyen Minh Dao
BSc. Vu Khanh Dong
Dr. Nguyen Anh Duc
MSc. Tran Hung Hien
MSc. Vu Van Nghiem
MSc. Le Ngoc Son
Eng. Le Hong Thai
MSc. Nguyen Van Tuan
Dr. Phan Tien Vien
MSc. Tran Quoc Viet
Dr. Nguyen Tien Vinh
Dr. Nguyen Hoang Yen

**SECRETARY**
MSc. Le Van Khoa
M.A. Nguyen Thi Viet Ha

**DESIGNED BY**
Le Hong Van

**MANAGEMENT**
Vietnam Petroleum Institute

**CONTACT ADDRESS**
*16th Floor, VPI Tower, Trung Kinh street, Yen Hoa ward, Cau Giay district, Ha Noi*
*Tel: (+84-4) 37727108 * Fax: (+84-4) 37727107 * Email: tapchidk@vpi.pvn.vn*
*Mobile: 0982288671*

*Cover photo: The promise of dual porosity model in Ca Ngu Vang fractured basement reservoir*
*Source: Hai An (PVEP)*

Publishing Licence No. 100/GP-BTTTT dated 15 April 2013 issued by Ministry of Information and Communications

# PETROVIETNAM CONCENTRATES EFFORTS
## for sound and sustainable development

***After 40 years of establishment and development, the Vietnam National Oil and Gas Group has grown into a leading economic group in Vietnam, contributing to the assurance of national energy security. Petrovietnam has developed a complete oil and gas industry which covers hydrocarbon exploration, production, petroleum processing, gas industry, power generation industry and petroleum services. According to its Development Strategy until 2025 and vision to 2035, Petrovietnam will focus on developing synchronously and sustainably into a group having sound financial, scientific and technological strength and high competitiveness.***



*Mr. Nguyen Quoc Khanh, Acting Chairman, President and CEO of Petrovietnam, and PVEP leaders welcome first oil from H5-Te Giac Trang. Photo: PVEP*

According to Mr. Nguyen Quoc Khanh, Acting Chairman, President and CEO of Petrovietnam, the Group has built up a complete and modern system of facilities for the petroleum industry from hydrocarbon exploration and production to petroleum processing, gas industry, power generation industry and petroleum services, contributing importantly to ensuring the country's energy security. From the first gas production landmark in June 1981 and the first ton of crude oil produced in June 1986, Petrovietnam is currently producing oil and gas from 25 domestic fields and 10 overseas fields with total output to date reaching 455 million tons of oil equivalent (over 346 million tons of crude oil and over 108 billion $m^3$ of gas).

Activities of atracting and implementing investments have been promoted; the progress of investment projects assured; and projects put into operation with high socio-economic efficiency. Petrovietnam is implementing 66 petroleum contracts, attracting nearly USD 15 billion of foreign investment into Vietnam. A system of modern facilities has been built for the gas industry with 4 gas pipeline systems: Cuu Long basin - Dinh Co, Nam Con Son 1 - Nam Con Son 2 (Phase 1), PM3 - Ca Mau, and Ham Rong - Thai Binh, which are attached to the gas processing factories, and the low-pressure gas infrastructure which is being operated safely and efficiently, providing over 10 billion $m^3$ of gas/year.

Power plants with installed capacity of over 4,200MW have been put into operation, and so far produced and supplied to the national grid more than 100 billion kWh of electricity. Petrovietnam is actively promoting investments in power projects, striving to bring the total capacity of power plants invested by Petrovietnam to over 9,000MW and to produce 15 - 20% of the nation's electricity output. Its fertiliser plants (Phu My and Ca Mau) have produced over 11 million tons of urea, meeting 70% of the country's demand for urea fertiliser. Dung Quat Refinery and Dung Quat Polypropylene Plant have been put into operation since 2009, marking the completion of the construction process of the Vietnam oil and gas industry.

Key projects, e.g. the Gas Development Project in Blocks B, 48/95 and 52/97; Nghi Son Refinery and Petrochemical Complex, Southern Petrochemical Complex, Nam Con Son gas pipeline (phase 2), and Block B - O Mon gas pipeline, are being actively deployed by Petrovietnam in order to put them into early operation to meet the growing demand of socio-economic development.

Besides promotion of development investments at home, Petrovietnam has also been seeking and expanding

overseas investments. The Group is implementing 19 oil and gas contracts in 14 countries in the world, and currently producing oil and gas from 10 fields abroad. The total overseas production has reached almost 7 million tons of oil.

Over 40 years, Petrovietnam has operated efficiently, in both production and business, making great contribution to the State Budget and the country's socio-economic development. Petrovietnam has earned an estimated total revenue of nearly USD 290 billion, maintaining an average revenue growth rate of almost 20% per year, and creating a total owner's equity of roughly VND 405 billion and total assets of VND 750 trillion. The Group has contributed to the State Budget over USD 87 billion, representing 25 - 28% of the annual State Budget.

On 23 July 2015, the Politburo issued Resolution no. 41-NQ/TW on orientations for the development strategy until 2025 and vision to 2035. The overall objectives defined in the Resolution are to develop the oil and gas industry into a complete and modern mainstay economic-technical sector which covers exploration, production, transportation, processing, storage, distribution, import and export services; contribute importantly to the cause of national construction and defence; mobilise all resources to invest in the oil and gas industry development; and build Petrovietnam into a group with sound financial, scientific and technological strength and high competitiveness, being proactive and active in international integration. On that basis, the Group will concentrate all resources and efforts to achieve the specific objectives in each domain of production and business.


Hai Thach - Moc Tinh fields

In the field of hydrocarbon exploration and production, Petrovietnam is accelerating basic surveys and exploration activities in Vietnam, especially in deepwater and offshore acreages, in linkage with safeguarding the national sovereignty on the sea; actively carrying out further exploration of existing fields, research and exploration of new fields, new sedimentary basins, and unconventional hydrocarbons (coal gas, shallow gas, shale gas and gas hydrate) to increase the hydrocarbon reserves for long-term production. The Group is efficiently and effectively exploiting the existing fields, rationally and effectively developing and putting fields with hydrocarbon discoveries into production for long-term utilisation of domestic petroleum resources. Petrovietnam is boosting oil and gas exploration and production activities abroad on the principle of economic efficiency.

Petrovietnam has been developing a complete gas industry from production, collection, transportation and processing to export and import, storage, distribution and consumption of gas products; gradually reducing the share of gas used for power generation and fuel, and increasing deep processing. The Group is studying and looking for new markets as well as building warehouse and port infrastructures to get ready for import of gas and gas products after 2020. Petrovietnam is also investigating the option to build a pipeline system to link different areas and develop a national gas pipeline system.

Petrovietnam continues to study and evaluate the possibility for Vietnam to become a regional refining and petrochemical hub; with emphasis on petroleum processing to maximally meet the domestic demand and move towards exporting products; concentrating on development of the petrochemical sector (including transformation of gas) and chemicals in order to increase the added value of petroleum products, providing



materials and fuels for the development of domestic industrial production. Foreign investment and domestic investment from the society will be mobilised to develop the petroleum processing sector. Integration and combination of refining and petrochemical complex with natural gas production are promoted in order to enhance the efficiency of existing projects and facilities, and new projects are developed in both scale and level of deep processing which are capable to compete in the regional and international markets.

Petrovietnam will develop a rational system for storage and distribution of petroleum products to ensure circulation and stabilisation of the consumption market, satisfy the domestic demand for petroleum products; strengthen measures to ensure increase of reserves of crude oil and petroleum products; and vigorously implement the policy to utilise bio-fuels in order to minimise the dependence on fossil fuels and protect the environment. The maximum participation of different economic sectors in the distribution of petroleum products will be encouraged.

Petrovietnam has also promoted investments in development of petroleum services, building supporting mechanisms to develop petroleum services abroad. Investment will be made in modern equipment and facilities to ensure pro-active delivery of services for the main business domains and investment projects within the sector. The following key professional services have been identified: drilling and well technical services; seismic survey, processing and interpretation services; geotechnical services, survey and repair of underground structures; design, fabrication, construction and installation of petroleum structures; building and operation of floating facilities; operation, maintenance and repair services for petroleum plants/structures. The different economic sectors are encouraged to participate in petroleum service development in order to increase the competitiveness and concentrate


Bach Ho field, Cuu Long basin

capital to reinvest in the core business domain of the industry.

Petrovietnam is strengthening the management, operation, maintenance and repair of existing power plants and ongoing power projects to ensure their investment efficiency, and developing some new gas-fired power projects.

In the immediate future, Petrovietnam will continue to strictly control the progress of exploration, field development and production projects both at home and abroad to ensure the fulfilment of the plan to increase oil and gas reserves and production. At the same time, Petrovietnam will focus on enterprise restructuring, research and application of scientific and technological achievements, investment in new technologies to improve production and business efficiency, and increase the added value of petroleum products in the value chain.

**Ngoc Phuong**

## PETROVIETNAM'S OIL AND GAS PRODUCTION IN 2015 ESTIMATED AT OVER 27 MILLION TONS OF OIL EQUIVALENT

*In the first 9 months of 2015, the Vietnam National Oil and Gas Group produced a total of 21.86 million tons of oil equivalent (13.96 million tons of crude oil and 7.9 billion $m^3$ of gas), which is equal to 111% of the 9-month plan and 82.2% of the yearly plan, representing an increase of 7.4% over the same period of 2014. Besides, Petrovietnam has produced and contributed 16.19 billion kWh of electricity to the national grid, at the same time produced 1.2 million tons of urea fertiliser, 61 thousand tons of fibre and 5.22 million tons of petroleum products. By the end of September 2015, Petrovietnam has earned a total revenue of VND 428.3 trillion and contributed to the State Budget VND 89.1 trillion.*

*In the coming period, Petrovietnam will continue to strictly control the progress of exploration, field development and production projects both at home and abroad to ensure the fulfilment of the plan to increase oil and gas reserves and production in 2015. The Group continues to strengthen external relations and international co-operation in the field of oil and gas in order to find good overseas projects for investment, at the same time to invite large, reputable foreign oil and gas companies to jointly invest in Petrovietnam's projects; and promote co-operation with oil and gas companies in the region to study areas of mutual interest on the sea and jointly invest in good projects in a third country.*

*At the same time, Petrovietnam will continue to implement the restructuring plan for the 2012 - 2015 period which was approved by the Prime Minister in Decisions no. 46/QD-TTg and no. 1011/QD-TTg, as well as monitor the serious implementation of its member units. In particular, the key tasks will be equitisation, divestments, and enhancement of competitiveness and operational efficiency. Besides, it will ensure the safe operation of Dung Quat Refinery, gas transportation systems, power plants and fertiliser plants; as well as the implementation progress of its key projects; and focus on developing markets for the new products (fibre and biofuel).*

| Content | Unit | Goal set by Government for 2015 | Goal for 4th quarter of 2015 |
|---|---|---|---|
| Oil and gas production | Million tons of oil equivalent | 26.60 | 6.92 |
| Oil | Million tons | 16.80 | 4.22 |
| - *Vietnam* | Million tons | 14.74 | 3.66 |
| - *Abroad* | Million tons | 2.06 | 0.56 |
| Gas | Billion $m^3$ | 9.80 | 2.70 |
| Electricity | Billion kWh | 18.50 | 4.95 |
| Urea | Million tons | 1.525 | 0.393 |
| Petroleum products | Million tons | 5.55 | 1.31 |
| Total revenue | Trillion VND | 718.4 | 220.1 |
| Contribution to State Budget | Trillion VND | 159.0 | 54.2 |

## EXPLORATION AND PRODUCTION

***With a view to increasing oil and gas reserves and discovering new fields to meet the domestic demand and export, the Vietnam National Oil and Gas Group has been effectively deploying and implementing hydrocarbon exploration and production activities both at home and abroad, making important petroleum discoveries, quickly bringing the discovered fields into production and applying state-of-the-art technologies to increase oil and gas production and recovery rate, as well as to protect the environment and natural resources.***

***During the 2015 - 2020 period, Petrovietnam has set the goal to increase reserves by 165 - 200 million tons of oil equivalent and produce 130 - 150 million tons of oil equivalent. Petrovietnam will continue to strictly control the progress of exploration, field development and production projects both at home and abroad to ensure the fulfilment of the plan to increase oil and gas reserves and production.***





Dai Hung field



Su Tu Vang field



Hai Thach - Moc Tinh fields



Rang Dong field


Bach Ho field


Nenets field, Russia


Bir Seba field, Algieria


Thang Long field


Block 67, Peru



Dinh Co Gas Processing Plant

## GAS INDUSTRY

***Petrovietnam has built a system of modern facilities for the gas industry with 4 gas pipeline systems: Cuu Long basin - Dinh Co, Nam Con Son 1 - Nam Con Son 2 (Phase 1), PM3 - Ca Mau, and Ham Rong - Thai Binh. Many mega-gas projects are also being deployed by Petrovietnam to supply gas for power plants, chemical and fertiliser plants, and for transportation and household consumption.***



Thi Vai Refrigerated LPG Storage





Thi Vai Refrigerated LPG Storage





Nam Con Son Gas Processing Plant



Tien Hai Gas Distribution Centre



Ca Mau Gas Distribution Centre

## PETROLEUM PROCESSING

***Petrovietnam is actively accelerating the progress of refinery and petrochemical projects while at the same time studying the possibility of expanding and upgrading its existing plants to bring added value to petroleum resources in order to meet the domestic demand for fuel, petrochemicals and petrochemical materials.***





*Ca Mau Fertilizer Plant*



*Dung Quat Bio-fuel Plant*




*Phu My Fertilizer Plant*



*Dung Quat Refinery*



*Dung Quat Polypropylene Plant*

## PETROLEUM SERVICES

***Petroleum services have been greatly expanded and recorded high growth rates, representing a large proportion (over 30%) of the total revenues of Petrovietnam and step by step reaching out to foreign markets.***



*PV Drilling V TAD*



*PQP-HT topside farbricated by PTSC*



*PV Drilling I jack up*




*Binh Minh 02 seismic research vessel*



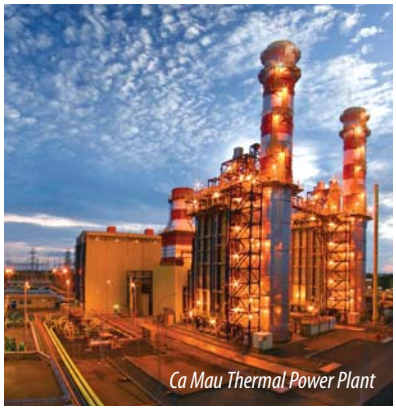

*FPSO Ruby II*


Ca Mau Thermal Power Plant

## POWER GENERATION

***Petrovietnam's power plants with installed capacity of over 4,200MW have been put into operation, and have so far produced and supplied to the national grid more than 100 billion kWh of electricity, contributing to ensuring the national electricity security. Petrovietnam is actively promoting investments in power projects with the target of bringing the total capacity of power plants invested by Petrovietnam to over 9,000MW and producing 15 - 20% of the nation's electricity output.***


Vung Ang 1 Thermal Power Plant


Ca Mau Thermal Power Plant


Nhon Trach 1 Thermal Power Plant


Nhon Trach 2 Thermal Power Plant

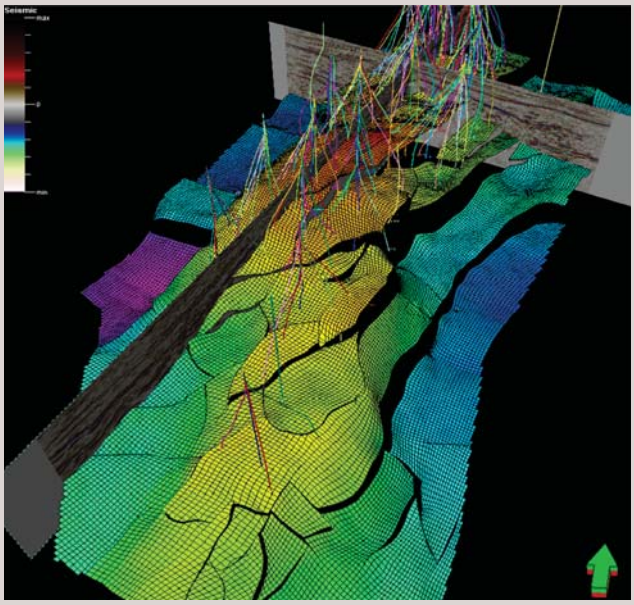
## SCIENCE AND TECHNOLOGY

***The Vietnam National Oil and Gas Group (Petrovietnam) will hold a Conference and Exhibition with the theme "Petrovietnam - 40 years of integration and development" on 21 - 23 October 2015 in Ho Chi Minh city. This is an important event to mark significant milestones through four decades of development - its emergence and contribution to Vietnam's economy in general as well as to Vietnam's oil and gas industry in particular.***

***At this important event, more than 80 Vietnamese and international companies will introduce the latest scientific and technological achievements in the petroleum industry, exchange experience, seek opportunities for investment and co-operation and promote technology transfer.***

***The conference will create a forum for oil and gas companies to discuss current issues in the petroleum industry in both regional and international perspectives. The plenary session of the Conference will concentrate on 2 topics, namely sustainable development of Vietnam's petroleum industry and innovation and new technology trend for the future petroleum industry. At the same time, the Conference will discuss other topics, including unlocking hydrocarbon resources from deep water areas, challenging reservoir development, unconventional hydrocarbon resources potential and development, improving efficiency of refineries and petrochemical plants, natural gas deep processing, bringing natural gas' high potential onstream, and corporate governance and portfolio management.***

***In the new stage of development, Petrovietnam affirms that science and technology will be the foundation, motivation and one of the three breakthrough measures for Vietnam's oil and gas industry to achieve sustainable development.***



### EXPLORATION, DISCOVERY AND EFFICIENT EXPLOITATION OF OIL RESERVOIRS IN PRE-TERTIARY GRANITOID BASEMENT OF CUU LONG BASIN IN THE CONTINENTAL SHELF OF VIETNAM

The most significant scientific and technological achievement of Petrovietnam over 40 years of establishment and development is the scientific research and technological innovation works entittled "Exploration, discovery and efficient exploitation of oil reservoirs in pre-Tertiary granitoid basement of Cuu Long basin in the continental shelf of Vietnam", which has been awarded the noble "Ho Chi Minh Prize for Science and Technology".

### ASSESSMENT OF HYDROCARBON POTENTIAL OF VIETNAM'S TERRITORIAL WATERS AND CONTINENTAL SHELF

The "Assessment of hydrocarbon potential of Vietnam's territorial waters and continental shelf" project conducted by the Vietnam Petroleum Institute (VPI) has been considered one of the projects having made new and valuable contributions to petroleum geology. VPI has conducted 7 sub-topics on "Assessment of hydrocarbon potential and reserves" of 8 sedimentary basins (Song Hong, Phu Khanh, Cuu Long, Nam Con Son, Malay - Tho Chu - Phu Quoc, and Truong Sa - Tu Chinh - Vung May) and a general topic on "Overall assessment of hydrocarbon potential of the entire continental shelf and orientation for oil and gas exploration and production". The geological structure of sedimentary basins, zones and regions, composition and trap are made precise with new data and modern technology and software applied, ensuring adequate reliability for research on zoning and assessment of oil and gas potential.

The structure units of grade I and II in the sedimentary basins have been established and standardised. For the first time, the boundary between the Cenozoic sedimentary basins is determined on the basis of handling and interpreting a large volume of documents and geological - geophysical survey data, with sufficient scientific arguments and reliability necessary to guide oil and gas exploration activities.

This is a comprehensive collection of scientific research and technological innovation works which involved both the Vietnamese and Russian scientists over a period of 24 years. The exploration and discovery of oil in Bach Ho field have paved the way for basements to become the major exploration target in the continental shelf of Vietnam (accounting for over 80% of the total oil production) and it took only a short time before various fields with commercial reserves were discovered in the fractured basements.

The discovery and identification of the geological structure, formation mechanism, unprecedented characteristics of structure, permeability and porosity, amongst other things, have helped guide the exploration activities and determined the appropriate production system involving optimal technologies for the fractured basement reservoir. It has also become a crucial contribution that the oil and gas industry of Vietnam has made to the global petroleum science, changing the traditional perspectives on petroleum exploration and production. The success story of Bach Ho has opened a whole new direction for petroleum exploration in the Cuu Long basin particularly and in the continental shelf of Vietnam generally, attracting the interests of international oil and gas companies and promoting exploration activities in Vietnam.

From the basic surveys and studies conducted, the Vietnam Petroleum Institute has developed a reliable and constantly-updated scientific database of hydrocarbon potential and reserves in the territorial waters and the continental shelf of Vietnam. The project has provided data to facilitate the formulation of policies and development of strategies for oil and gas prospecting, exploration and production; as well as proposed measures for the State to manage and rationally exploit the marine resources and environment in a scientific, effective and efficient manner, satisfying the requirements for sustainable economic development and contributing to safeguarding the national sovereignty and security.



*Bach Ho field, Cuu Long basin*

## CRUDE OIL RECOVERY, TREATMENT AND TRANSPORTATION TECHNOLOGY IN THE PARTICULAR CONDITIONS OF VIETSOVPETRO'S OIL FIELDS

Accompanying the development of Vietsovpetro over 30 years is the process of research and development of technologies and continuous improvement of the oil recovery, treatment and transportation systems in Bach Ho, Rong and adjacent fields. The continual and diligent intellectual works of the scientific and technical staff of Vietsovpetro in this field have been compiled in the "Research, development and completion of crude oil recovery, treatment and transportation technologies under the particular conditions of Vietsovpetro's oil fields and tie-in fields on the continental shelf of Vietnam".

From the findings of this study, Vietsovpetro has innovatively developed oil treatment and transportation technologies which are economically efficient, consistent with the actual conditions of Vietsovpetro and different from the traditional technology of the world. These technologies are the combination of various solutions such as combination of heat treatment and pour point depressants; utilisation of condensate to increase fluid mobility; and utilisation of the geothermal gradient of wells for chemical treatment of oil, etc. These technological solutions have been applied by Vietsovpetro with flexibility, depending on the area and the production phases of the fields, and have been highly efficient in enabling the safe transportation of crude oil through long distance at low cost by subsea pipelines offshore.

The successful research and development of the crude oil recovery, treatment and transportation technology applied in Vietsovpetro's oil fields and tie-in fields have introduced a complete and scientific process of research and application, which not only effectively facilitates the continued production development of the fields in Block 09-1 in a systematic way but also can be applied to similar fields in the Cuu Long basin and Vietnam's continental shelf in general.

**Hien Trang**

# BETTER EXPLORATION PROSPECTIVITY UNDERSTANDING THROUGH THE USE OF ADVANCED 3D BROADBAND SEISMIC

Pham Vu Chuong, Pham Minh Hai, Paul Begg, Timur Manapov
*Rosneft Vietnam*
*Email: chuong.pham@vn.rosneft.com*

**Summary**

*Nam Con Son basin is one of the most prolific oil and gas rich basins in Vietnam. Oil and gas is produced in a number of fields, i.e. Dai Hung, Hai Thach/Moc Tinh, Lan Tay/Lan Do, Dua/Chim Sao and Rong Doi/Rong Doi Tay. Despite many successful wells, there are opportunities to improve exploration CoS (chance of success) in a basin by better prediction of trap definition, reservoir and seal risks. This paper presents the use of advanced 3D broadband data to help better understanding the exploration prospectivity in the centre of the Nam Con Son basin.*

*3D broadband seismic was acquired and processed in 2013 - 2014, and conventional and special seismic interpretation techniques (Amplitude Versus Offset - AVO) were conducted to provide a better geological understanding of the prospectivity. In particular: i) traps were well defined in both structural and stratigraphic plays, ii) reservoir was better predicted through a combination of sequence stratigraphy and special seismic studies, iii) seal potential across major faults was determined by combination of conventional geological methods and using the seismic character response across the faults.*

*The presented results may be helpful for geoscientists exploring in the Nam Con Son basin and other areas of the Vietnam shelf.*

***Key words:*** *3D broadband seismic, AVO, Nam Con Son basin.*

## 1. Introduction

Block 05-3/11 operated by Rosneft Vietnam is located at the centre of the Nam Con Son basin, offshore Vietnam, approximately 330km to the South-East from Vung Tau city (Figure 1). In 2013, 1,179.81km$^2$ of 3D broadband seismic data and 75.8km of 2D were acquired; the data was processed to both pre-stack time migration (PSTM) and pre-stack depth migration (PSDM) and was completed in 2014. Conventional and special seismic interpretation has defined a number of prospects including both structural (Middle Miocene) and stratigraphic traps (Upper Miocene). The understanding of prospect potential was significantly improved by a number of studies including: i) regional geological integrated analysis, ii) regional structure and tectonic activity evaluation, iii) 3D petroleum system basin modelling, iv) seismic sequence stratigraphic interpretation, and v) fault/top seal analysis based on the new 3D broadband seismic data.

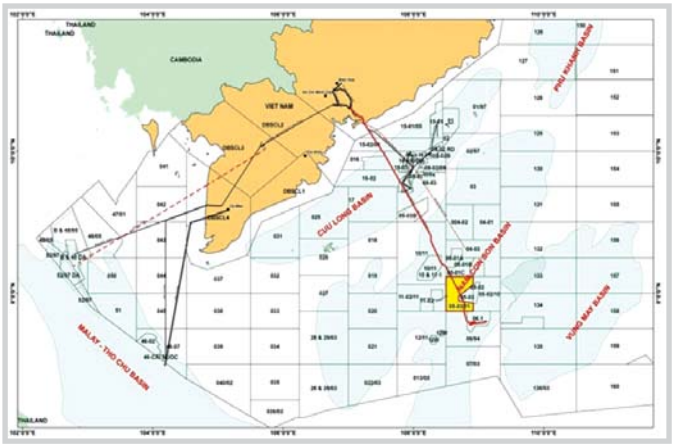



***Figure 1.*** *Block 05-3/11 location map*

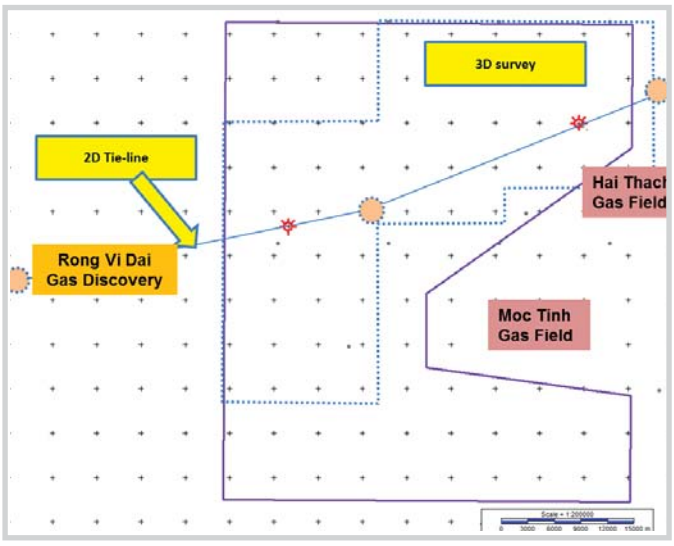



***Figure 2.*** *3D broadband seismic area*

## 2. Trap understanding

The 2013 3D broadband was acquired and processed by CGG (Figure 2). Eight horizons from T100 to T30 have been interpreted. In addition to the conventional interpretation, AVO and inversion studies were also undertaken, which helped to define two trap styles on the Block 05-3/11. These include the following:

- Upper Miocene stratigraphic traps

They were defined as i) seismic AVO Fluid Factor (ABFF) anomalies, and ii) conventional PSDM amplitude extractions that show greater chaotic character (Figure 3). The AVO anomalies are not conforming to structure interpretation. The ABFF data is used to highlight areas with good potential gas and reservoir characteristics that also show strong negative ABFF amplitudes. Reduced ABFF amplitudes are interpreted as possible increase in sub-seismic resolution scale faulting, small shale partitioning, decrease in gas saturation, or poorer reservoir quality (i.e. net to gross, porosity, permeability). Sedimentary environmental studies suggest that these seismic facies represent slump/ turbidities and/or ponded and amalgamated channels feature deposited in shelf/slope and deep marine environment. Seismic sequence stratigraphy analysis of the 3D data suggests these channels have their provenance to the west of the Block.

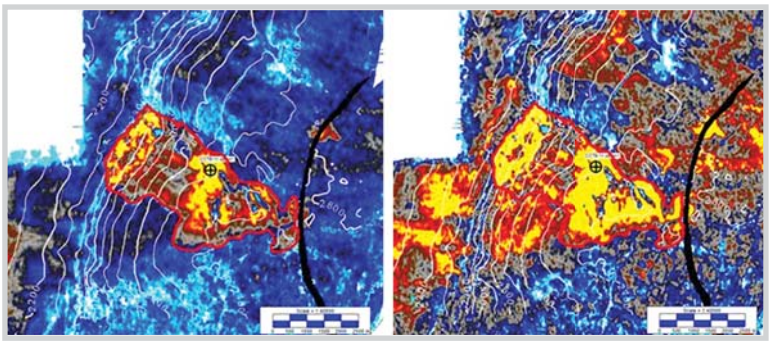


***Figure 3.*** *ABFF amplitude anomaly (left) vs. Conventional PSDM amplitude extraction (right)*

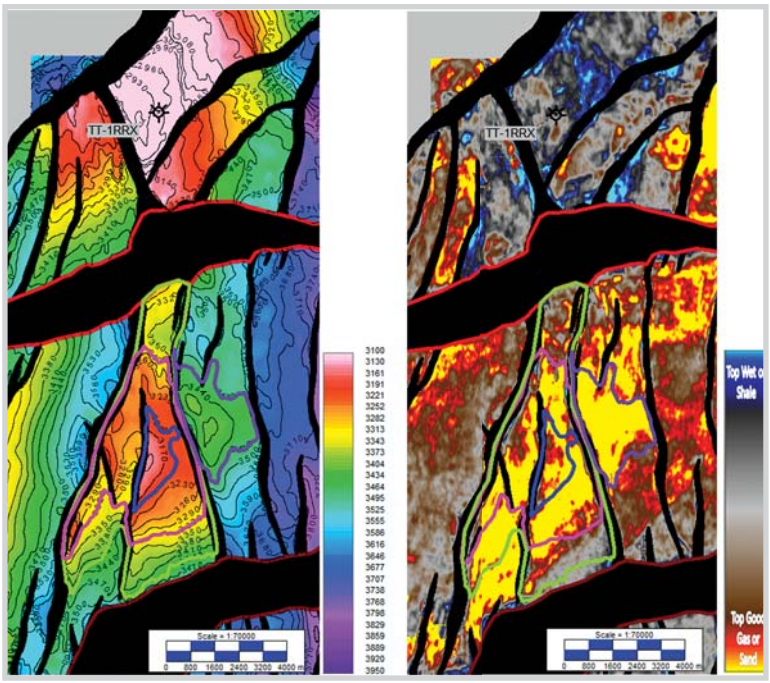



***Figure 4.*** *Top depth structure map (left) and good sand with high gas saturation predicted by AVO Fluid Factor attributes (right)*

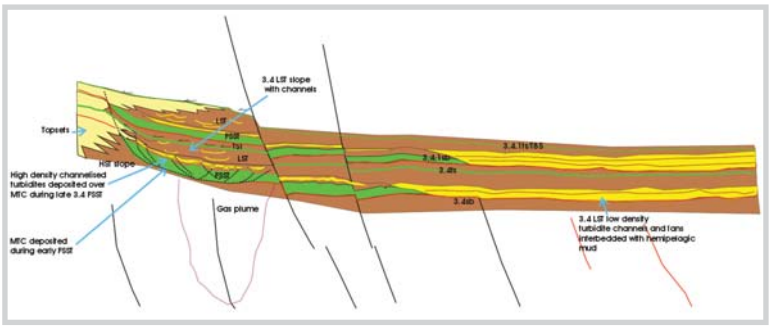



***Figure 5.*** *Schematic diagram of reservoir in Upper Miocene*

- Middle Miocene structural traps

They are 2-way or 3-way fault-bounded structures that have been defined on the high quality 3D data. The majority of the faults are oriented in a NE-SW or N-S direction and demonstrate large fault throws, and a lesser number are oriented in NW-SE direction with smaller fault throws (Figure 4). The orientation and magnitude of the faults are consistent with this regional stress regime in the Nam Con Son basin. There are complex imaging issues associated with the larger faults, which increases the potential risk for defining accurate fault geometries and trap definition.

## 3. Reservoir understanding

Clastic reservoirs are formed in both Middle and Upper Miocene sections:

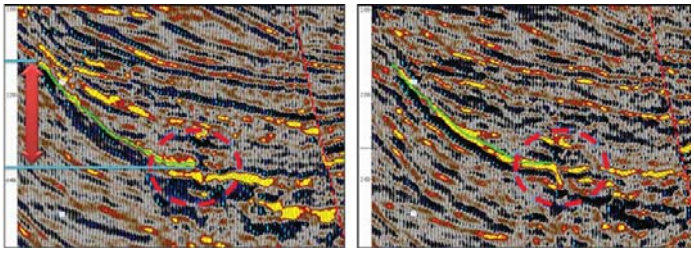
- Upper Miocene reservoirs constitute deep marine slope/turbidite sands. Sandstone is present at depth 2,500 - 3,500m with porosity from 18 - 30%, average 20 - 22%. Reservoir thickness varies from 20 - 80m, average thickness of 40 - 50m from adjacent wells data. Seismic sequence stratigraphy study shows Upper Miocene reservoir in the Block has been identified as a combination of a slump deposit in the early falling stage systems tract (FSST) overlain by turbidite channel sands of the late FSST and lowstand systems tract (LST) (Figure 5). Seismic amplitude mapping identifies slump/turbidite and ponding of amalgamated channel facies. These illustrate chaotic geometry indicating variable reservoir

or partially cohesive mass flow deposits covered by high density turbidite channels. The slump/turbidite channel feature is limited down-dip by significant N-S faults that are surrounded to the north, south and east by marine shale deposits. From the AVO analysis, we observe that the PSDM intercept polarity changes whilst the gradient polarity remains unchanged, suggesting the possible gas water contact (GWC) indicator (Figure 6). Sand thickness evaluation is also supported by AVO derived isopach vs. drilled well thickness analyses.

- Middle Miocene reservoirs are shelfal, synrift turbidite sands, or were deposited in a slope or deep marine environment. These reservoirs are present at depth range of 3,000 - 5,000m with average porosity of 13 - 16% deduced from adjacent wells. Seismic sequence stratigraphy shows there is the possibility of widely deposited sands within stacked sand units with average thickness of each reservoir of between 15 - 20m. It is interpreted that these shelfal sand packages were flanked by incised valleys formed during FSST, thereafter these were filled during LST, transgressive systems tract (TST) and highstand systems tract (HST) with a range of paralic facies associations and later blanketed by marine flooding shale to form an effective top seal (Figure 7). Within this sequence, there are several interspersed high-amplitude seismic events that may represent carbonate facies that were deposited during HST transgression. There is a higher prevalence of seismic amplitudes within this section suggesting higher number of sands within the southern structure. The T60 and T58 reservoirs in Tho Tinh Nam prospect have fair to good AVO lithology indicators that are reasonably conformable with the structure. We believe the AVO lithology response is better than that seen at the TT-1RRX well, suggesting the possibility of similar to better quality sands. Below T50, the AVO response is dim and is interpreted as tight sand with low gas saturation. Sand thickness is supported by AVO amplitude and wavelength analysis using TT-1RRX as a constraint.

## 4. Seal understanding

Seal evaluation includes both top and lateral (side) seal evaluation. While top seal is proven within the Nam Con Son basin with a thick marine shale of up to 300m within the Upper Miocene and 140m in Middle Miocene, the lateral seal remains the key risk



(a) (b)

***Figure 6.*** *PSDM Intercept Polarity (a) changes while Gradient Polarity (b) remains unchanged at the bottom, suggesting the potential GWC indicator*

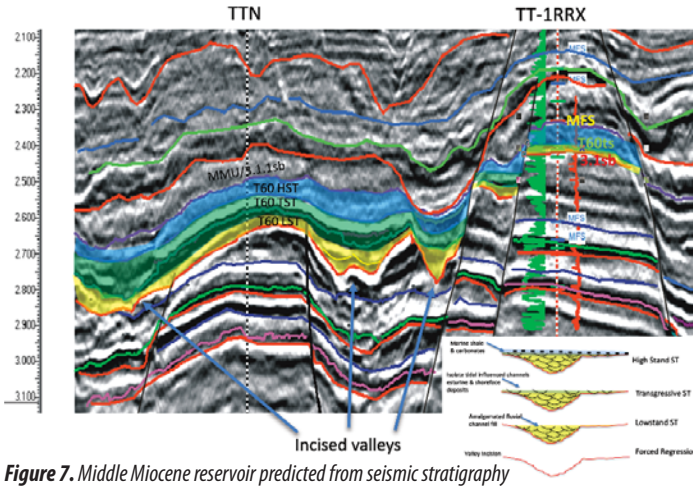



***Figure 7.*** *Middle Miocene reservoir predicted from seismic stratigraphy*

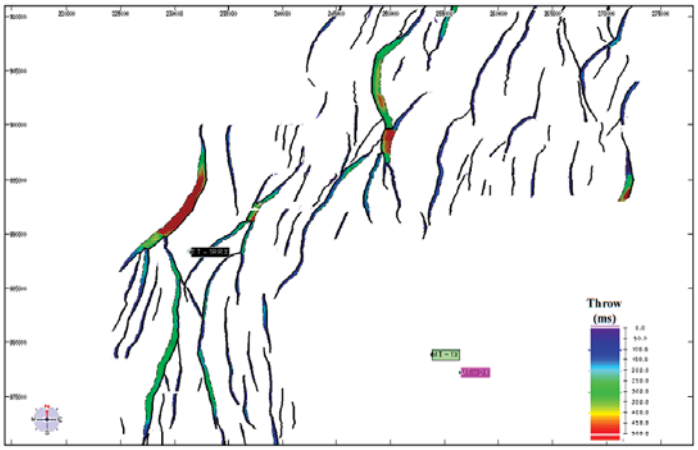



***Figure 8.*** *Block 05-3/11 fault throw in Middle Miocene*

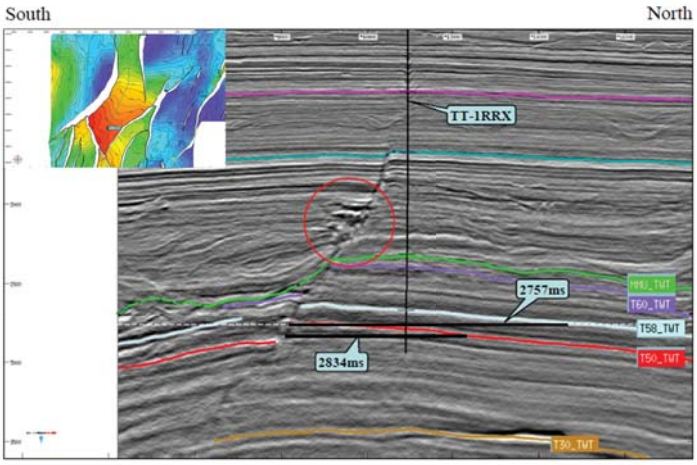



***Figure 9.*** *Evidence of gas leaking along fault in TT-1RRX*

for several prospects in this area. The sealing potential across major faults is better determined by combination of conventional geological methods and using the seismic response across the faults.

Conventional fault seal study includes modelling of the fault throw, Allan diagrams, calculation of the Shale Gouge Ratio and prediction of the hydrocarbon height. Most of faults in the Block have fault throw of more than 100m within sections of abundant shale where there is more chance of sand against shale. Calculated shale gouge ratio is mostly higher than 50% and max hydrocarbon height supported by fault seal is up to 180 - 210m (Figure 8).

Conventional method shows all the faults are sealing, however the question is raised why the TT-1RRX well failed. Detailed investigation was undertaken using new broadband seismic data where we believe there is possible "seal damage" arising from complex fault linkages and the intersection of several faults bounding the Tho Tinh prospect, in particular the faults defining the SW and NW edge of the prospect where high amplitude anomalies are located close to and abut against the fault traces (Figure 9). These suggest that beside conventional interpretational methods, we need to carefully investigate the seismic image above the fault for any evidence of gas leaking, especially where there are complex fault intersections where effective seal could be damaged. A prospect with simple fault geometry with no fault linkages or confluences and no evidence of gas leaking up dip along fault is a much preferable drilling candidate.

**5. Conclusions**

Prospectivity understanding of the prospects in the Nam Con Son basin and Block 05-3/11 was significantly improved with the help from 3D broadband seismic:

- The structural traps were better defined, and the new seismic data helped better define the stratigraphic trap within the Upper Miocene section. These traps are believed to be formed by slump/turbidite and ponded amalgamated channel features in the shelf/slope and deep marine environment that are supported by good AVO characteristics.

- Reservoir risks are mitigated by an understanding of the sedimentary environment through seismic sequence stratigraphy studies, by AVO analysis, and with analog and well data correlation.

- Sealing potential has been identified using both conventional and detailed investigation of seismic image along and up dip of mapped faults. Structures with no fault confluences and no evidence of gas leaking up dip along fault are likely to be the best drilling candidates.

**References**

1. Badleys. *Fault and top seal analysis*. 2014.

2. Black Gold. *Regional structure and tectonic activity evaluation*. 2014.

3. Hasegawa. *Post-MMU stratigraphic play in the Nam Con Son basin offshore Vietnam*. PVEP Technical Forum. 2005.

4. ISIS. *Seismic sequence stratigraphic interpretation of Block 05-3/11*. 2014.

5. Rosneft Vietnam. *Regional geological integrate analysis*. 2014.

6. Su-Yeong Yang, Michelle Kim. *A success of a new play concept offshore Northwestern Myanmar: Pliocene deepmarine turbidites of the Eastern Bengal Fan*. SEAPEX Exploration Conference. 24 - 26 April, 2007.

7. Tyumen Petroleum Research Center (TNNC). *Regional & prospect scale formation evaluation for Block 05-3/11*. 2014.

8. Nguyen Thanh Tung, Nguyen Quang Tuan, Vu The Anh. *Updated seismic interpretation and the implication for evolution of Nam Con Son basin*. Proceedings of the Science and Technology Conference: The Intellect of Petrovietnam - Integration and Sustainable Development. 2013: p. 261 - 269.

9. G.Yielding, B.Freeman, D.T.Needham. *Quantitative fault seal prediction*. AAPG Bulletin. 1997; 81(6): p. 897 - 917.

# FORECASTING THE PRESENCE OF HYDROCARBON IN MOC TINH TAY PROSPECT, BLOCK 05-3, NAM CON SON BASIN BY 3D PETROLEUM SYSTEM MODELLING

Nguyen Huy Giang[1], Le Thi Vu Ngan[2]
[1]*Vietnam Petroleum Institute*
[2]*Bien Dong Petroleum Operating Company*
*Email: giangnh@vpi.pvn.vn*

**Summary**

*Moc Tinh Tay is located to the west of the Moc Tinh discovery, Block 05-3, Nam Con Son basin. Results of exploration wells and production wells clarified the petroleum potential of Block 05-3, especially Moc Tinh area, including Moc Tinh Tay structure.*

*The purpose of this paper is to understand, by 3D basin modelling, the generation, migration and accumulation histories of oil and gas from source rock; and evaluate the presence of hydrocarbons in Moc Tinh Tay prospect to minimise the risk of oil and gas exploration in the study area.*

*In this study, Lower Miocene and Oligocene source rocks are fair to very good source richness and essentially contain kerogen type III and a mix of type III and type II and has fair to good gas generation potential. Oligocene source rock has generated hydrocarbon since 24Ma. It is in oil window at 13Ma, and reached dry gas phase at 10Ma to the present time. The Lower Miocene source rock has generated hydrocarbon since 12Ma. It is in oil window from 5.5Ma and in gas phase in almost the entire area at the present.*

***Key words:*** *Petroleum system modelling, Moc Tinh Tay, Petromod software, hydrocarbon potential, Nam Con Son basin.*

## 1. Introduction

The Moc Tinh Tay prospect is located to the west of Moc Tinh discovery, Block 05-3, central part of Nam Con Son basin. It consists of two segments, West and East. The West segment is a faulted three-way dip closure against a large-throw, N-S trending fault. The East segment is a two-way dip closure against a large throw, NE-SW trending fault and another small N-S trending fault at T30 level (Figure 1).

The potential of Moc Tinh Tay structure is proved by the results from the exploration well in Block 05-3. The expected reservoir section is fluvio-deltaic Late Oligocene to Early - Middle Miocene deltaic/shallow marine sandstones and turbidite sandstone in the upper syn-rift.

The principal aims of this study are to evaluate the petroleum system and estimate the volume of hydrocarbon accumulations in Upper Miocene turbidite, Lower Miocene and Oligocene plays on Moc Tinh Tay structure by 3D basin modelling.

The Tertiary structural history of the Nam Con Son basin, and Block 05-3 in particular, can be divided into distinct episodes of tectonic activities, namely first rift phase (Eocene - Early Oligocene), intra rift phase (Late Oligocene - Early Miocene), second extensional phase (Middle Miocene), and post rift phase (Late Miocene - Pliocene). The Middle Miocene faulting related to rifting created intensive faulted blocks and a major structural depression through Block 05-3 and the adjacent areas [2]. The chrono-stratigraphy chart summarising the history of the Nam Con Son basin is shown in Figure 2.

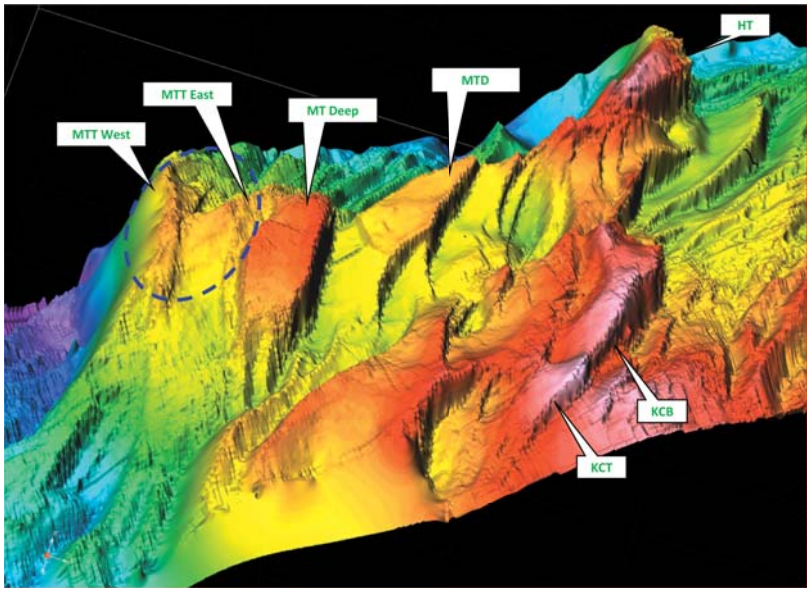



***Figure 1.*** *Moc Tinh Tay location*

## 2. Model building

### *2.1. Geometry*

To begin with, the present geometry for 3D Petroleum System Modelling is based on the input structural model in Petromod, covering an area in Block 05-3. Geometry (faults and horizons) modelling for the 3D model incorporates data from a range of disciplines including regional geological frame-work, seismic interpretation as well as wireline, environment and source rock characteristics. The structural model is built from simple grid and faults which are converted to depth domain from seismic interpretation results correlated with well markers. The horizontal grid increment is defined by 200 x 200 metre grid (I increment and J increment) due to a large study area. The fault model is built from forty-three (43) interpreted faults, in which fault stick is provided from seismic interpretation (Figure 3). Moreover, the properties of fault are assigned into the model that faults opened during the active time and closed when they became inactive (Figure 4).

The horizon modelling is the creation of main stratigraphic horizons based on seismic interpretation and subdivision of structural model (Figure 3). The sub-horizons between the main horizons are conformably followed base which are constrained by well correlations.

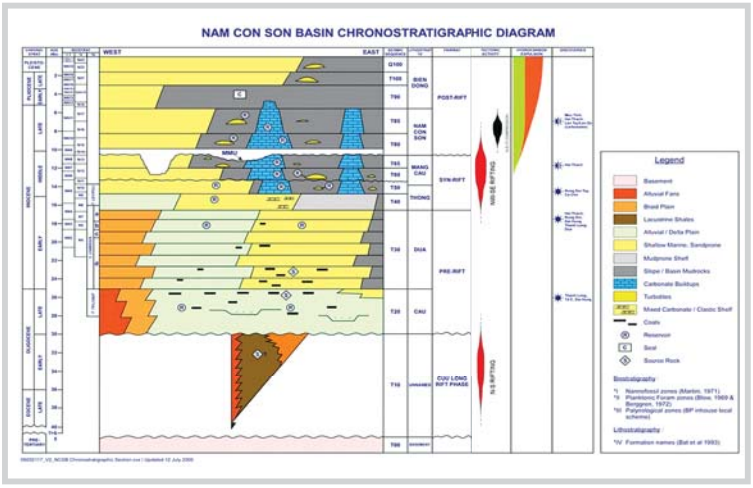



***Figure 2.*** *Nam Con Son basin chrono-stratigraphic chart*

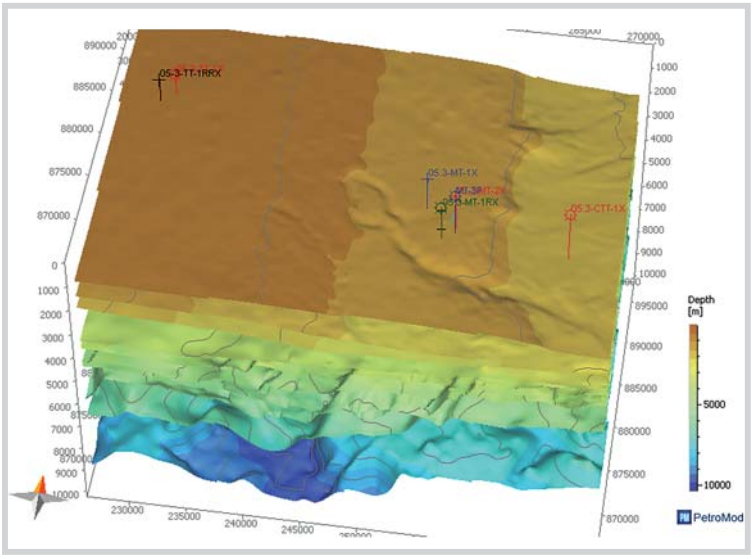
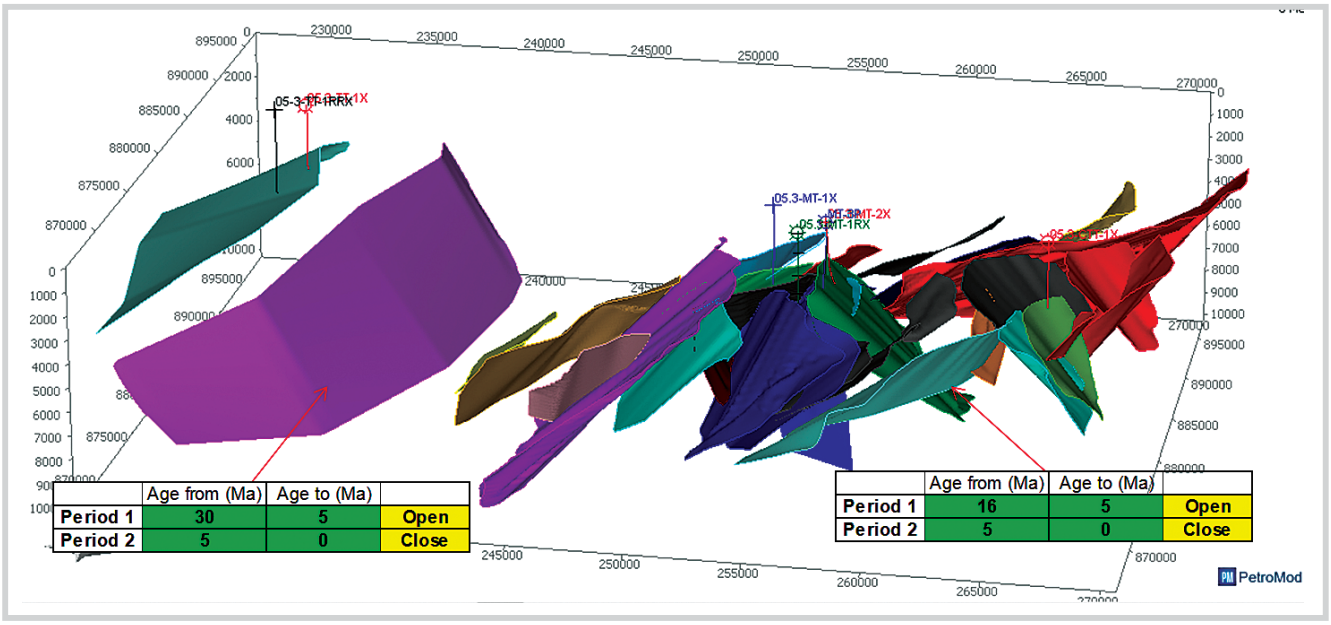



***Figure 3.*** *The 3D view of grids of 10 main horizons derived from seismic interpretations*




| | Age from (Ma) | Age to (Ma) | |
|---|---|---|---|
| Period 1 | 30 | 5 | Open |
| Period 2 | 5 | 0 | Close |

| | Age from (Ma) | Age to (Ma) | |
|---|---|---|---|
| Period 1 | 16 | 5 | Open |
| Period 2 | 5 | 0 | Close |

***Figure 4.*** *43 key faults were selected for building the fault model*

### 2.2. Lithology and facies distribution

*2.2.1. Stratigraphy/age assignment*

Cenozoic stratigraphy in the basin was subdivided into four major mega-sequences based on tectonic stages of basin evolution: syn-rift 1, intra-rift, syn-rift 2 and post-rift (RN/EPC Joint Study 2012). These mega-sequences were subdivided into thinner zones equivalent to vertical resolution of the models. Ages of mega-sequences were derived from the available biostratigraphic data of Vietnam Petroleum Institute and other analyses from different oil/gas companies (Table 1).

*2.2.2. Lithologies/facies definitions*

Lithologies used in 3D models were generated by mixing fundamental lithologies in the Petromod library e.g. sandstone, shale, and coal, etc. For sandstone, previous studies suggested that it is mainly arkoses to lithic arkoses in Folk (1974) [6] classification. The basement mainly contains granitic intrusive such as granite, granodiorite with extrusive and metamorphic rocks in places, so in the Petromod models basement was simply assigned to be granite (150Ma old).

*2.2.3. Facies maps*

Facies map for the area covered by 3D models have been constructed based on the integration of key information including the well-log interpretation, the isopach maps and the depositional frame-work of the Nam Con Son basin.

### 2.3. Boundary Condition

*2.3.1. Paleo-water depth*

The PWD was inferred from the interpreted facies maps by the following relationships: Delta front-shore face (0 - 30m); shallower marine (> 30 - 200m) and deep marine (> 200m). Figure 5 shows the estimated PWD maps for 3D modelling areas of key events.

*2.3.2. Sedimentary water interface temperature (SWIT)*

Sedimentary water interface temperature or Paleo-water interface temperature in this modelling was extrapolated from pseudo trends created by assigning the location at latitude 8°, South East Asia to Petromod software (Figure 6).

*2.3.3. Heat flow (1D modelling)*

The Nam Con Son basin is a rifting basin, the heat

***Table 1.*** *List of interpreted horizons and assigned ages*

| Horizons | Nano | Foram | Age | Ma |
|---|---|---|---|---|
| WB | | | Holocene | 0.0 |
| T100 | NN3 - NN4 | N19 - N20 | Pliocene | 1.7 |
| T90 | | | Intra Pliocene | 2.5 |
| T80 | NN10 - NN11 | N15 - N18 | Late Miocene | 5.5 |
| T65 | NN5 - NN9 | N9 - N14 | Middle Miocene | 10.5 |
| T30 | NN2 - NN4 | N6 - N8 | Early Miocene | 16 |
| T20 | ? - NP24 | | Late Oligocene | 24.5 |
| T10 | ? | | ? - Early Oligocene | 30.0 |
| T00 | | | | 40.00 |

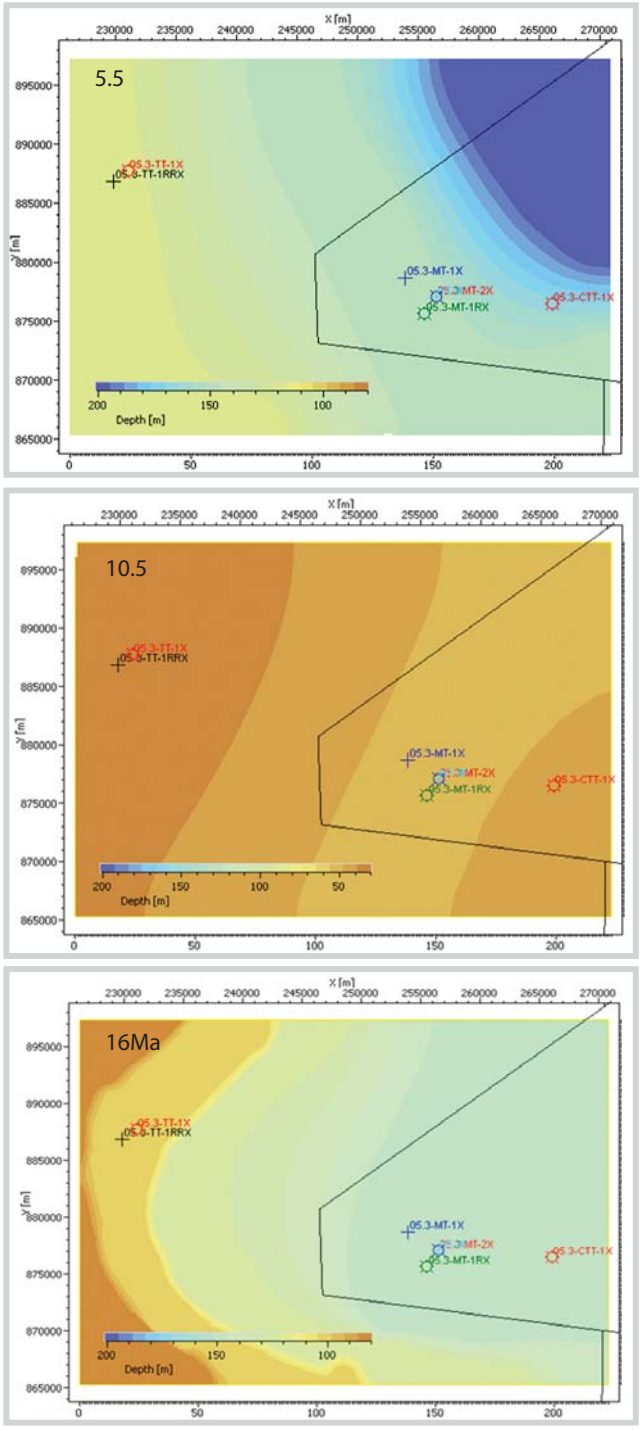



***Figure 5.*** *Paleo water depth (PWD) maps at key events*

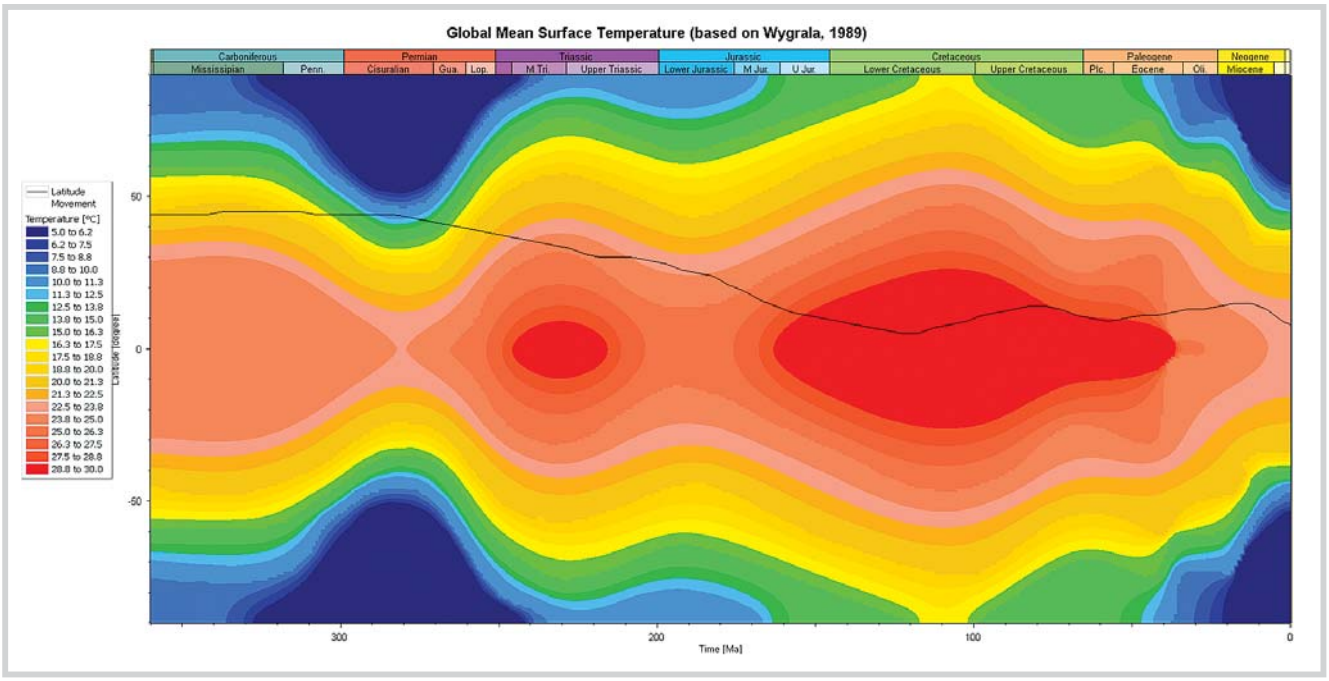



***Figure 6.*** *Sedimentary Water Interface Temperature (SWIT) at latitude 8°, South East Asia*

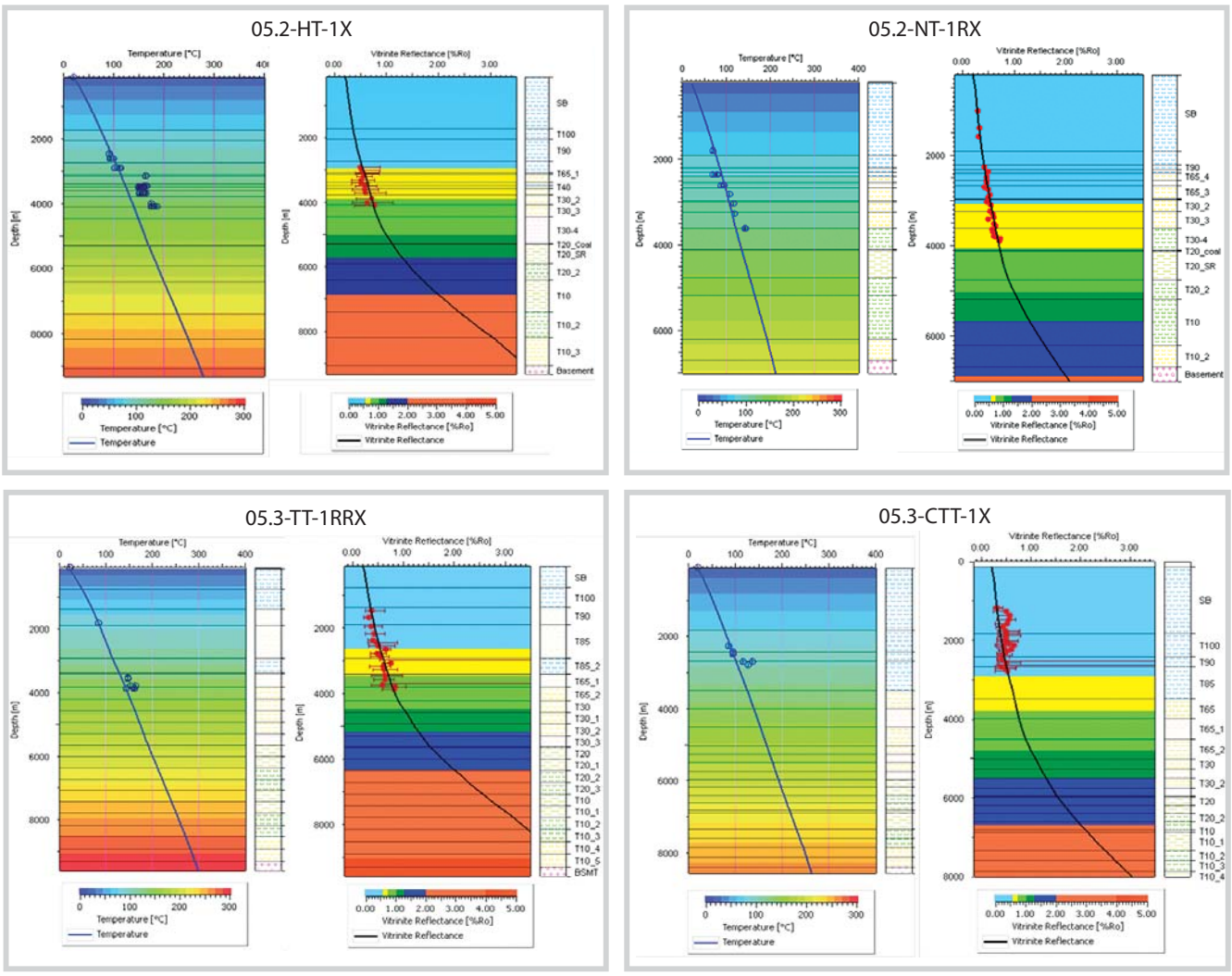



***Figure 7.*** *Vitrinite calibration of key wells in Blocks 05-2 & 05-3*

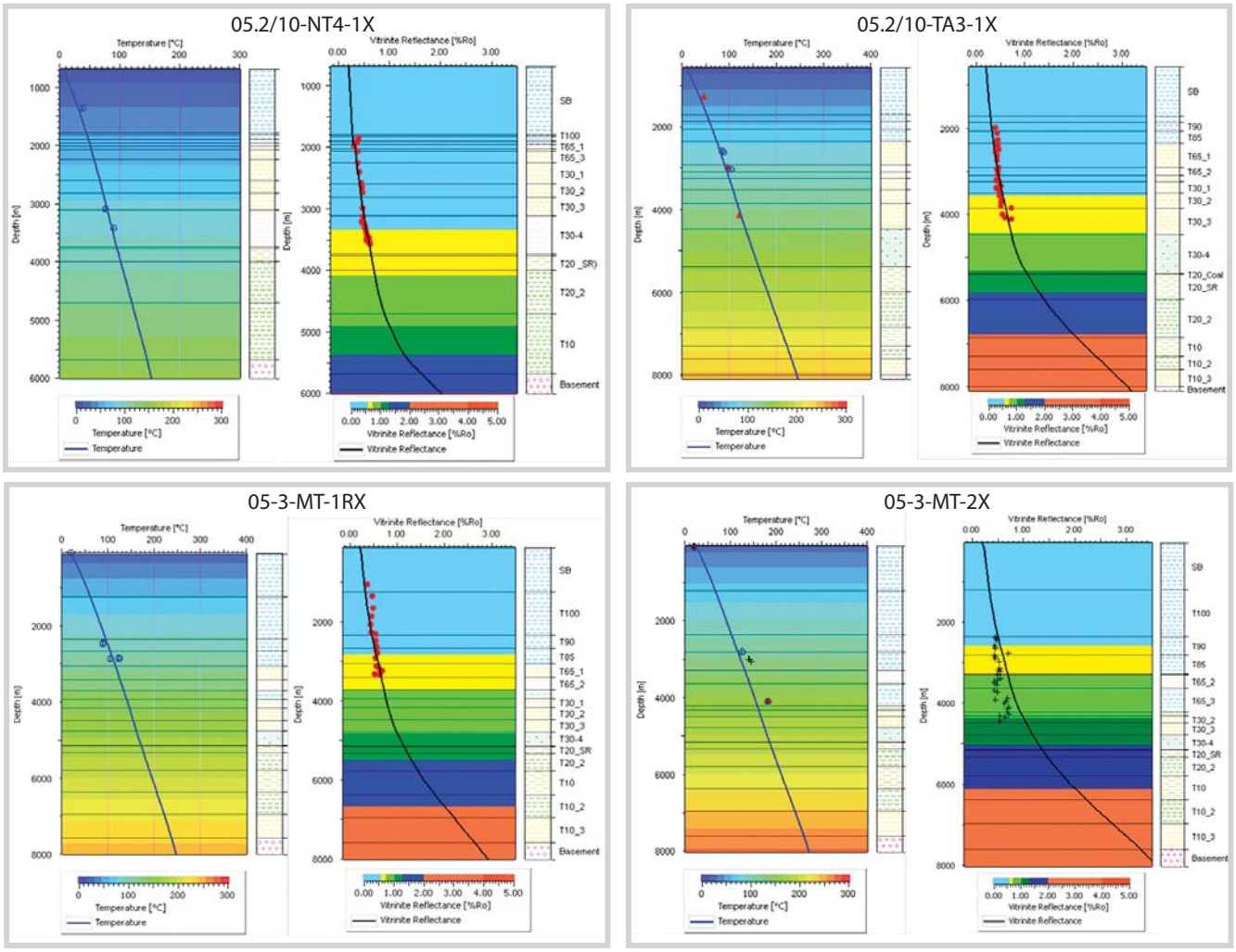



***Figure 8.*** *Vitrinite calibration of key wells in Blocks 05-2 & 05-3*

flow model is a modification of the classic McKenzie model (McKenzie, 1978) [1]. The heat flow profiles have been well calibrated with measured vitrinite reflectance and temperature values from wells (Figure 7, 8). It can be observed that heat flow exhibit profiles 2 peaks at 30Ma and 10.5Ma which are consistent with reliable rifting phases in the Nam Con Son basin (Figure 9). The recent uprising in heat flow observed from the 1D modelling is consistent for all modelled wells in the Nam Con Son basin.

The heat flow trends of 1D models were used to interpolate the heat flow maps in 3D models.

### *2.4. Kerogen type and source rock kinetic*

For 3D models, main source rocks are swamping shale in the Oligocene - Lower Miocene sequences, and some lacustrine source was assumed existing in deep grabens. The input TOC and in 2D models were determined from the highest frequency of analysed samples for each source rock formation. Oligocene swamping deposit is the primary source rock for Nam Con Son basin with most-likely TOC of 2% and HI of 400mgHC/gTOC.

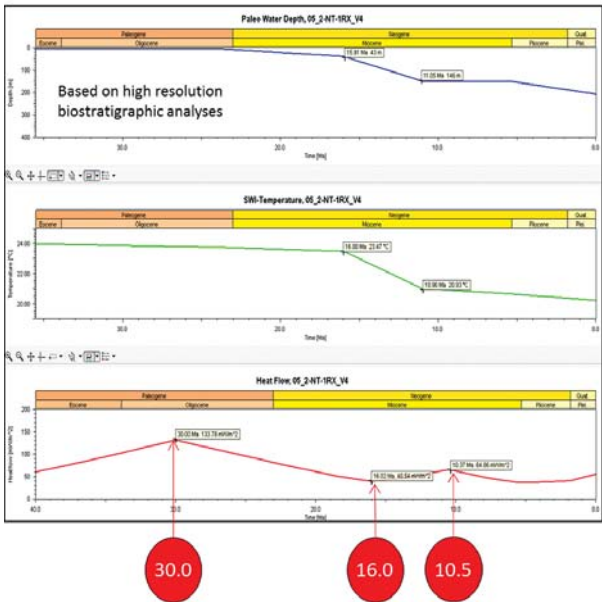



***Figure 9.*** *Boundary conditions used to calibrate temperature and vitrinite*

Based on the study of the depositional environment, the lacustrine source rock may be limited. In addition, coal was encountered at near top T20 sequence such

as in LD-1X, NT4-1X wells with the total thickness up to 20m. The averaged TOC (av. 53.84%) and HI (av. 224) were used for the coal layers. The organic richness of T30 shale seems to be poor with most-likely TOC of about 1% and HI of 300mgHC/g TOC.

With the organofacies concept of Oligocene and Early Miocene mentioned above, it can be seen that the source rocks in the study area mainly consist of type III kerogen and minor type II/III deposited in the swamping environment. For that reason, compositional kinetic models named Handil_Mahakam Delta; IES_TIII_Tertiary_Coal_4C were selected for Oligocene - Lower Miocene shale and coal.

## 3. Modelling results

### *3.1. Maturity of source rock*

In basin analysis studies, vitrinite is used to calibrate the burial and thermal history models as well as hydrocarbon generation. The approach to determination of vitrinite-reflectance value is using temperature and measured Ro of key wells to calibrate modelled maturity.

The 3D modelling results show the detailed maturity level of all potential source rocks in Block 05-3. Modelled Ro maps indicate that the Oligocene (T20 sequence) section is mature for generation and expulsion of wet to dry gas in the study areas (Figure 10). In fact, the maturity maps point out the T20 source rock located at the central area completely entered the dry gas phase (red colour), while due to burial depth source rock at Moc Tinh and Tho Tinh well is now wet gas (blue colour) in top T20.

At shallower stratigraphy levels T30 - Lower Miocene source rocks entered the oil window to the dry gas phase over most of Block 05-3. The T30 sequence was split into 4 subzones named T30-4; T30-3; T30-2 and T30-1 (Top T30) in the 3D Petromod models. Due to the influence of the depositional environment (shore - face sand and shallow marine) in upper parts T30, the lowermost part of the sequence T30-4 was considered as Lower Miocene source rock (Figure 11).

### *3.2. Timing of hydrocarbon generation and expulsion*

Based on extracted 1D models combined with the cumulative generation curve (Figure 12), it can be clearly seen that T30 source rock has generated HC since 12Ma in the central area while T20 SR has generated HC since 24Ma in the central area and migration phase was widespread from 15Ma to 8Ma. In fact, the increase in maturity level of Oligocene source rock is not stable; it is commonly

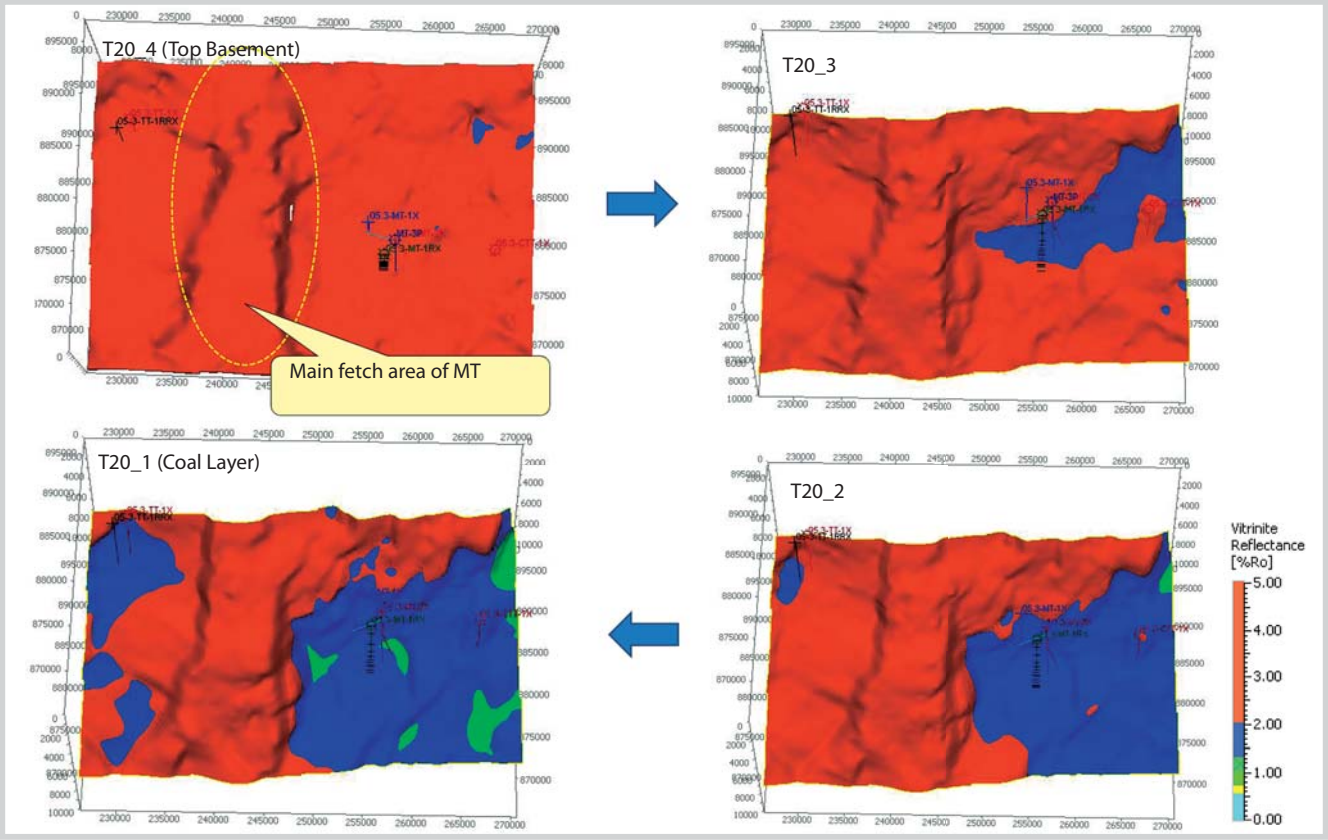



***Figure 10.*** *Modelled vitrinite reflectance for T20 source rock*

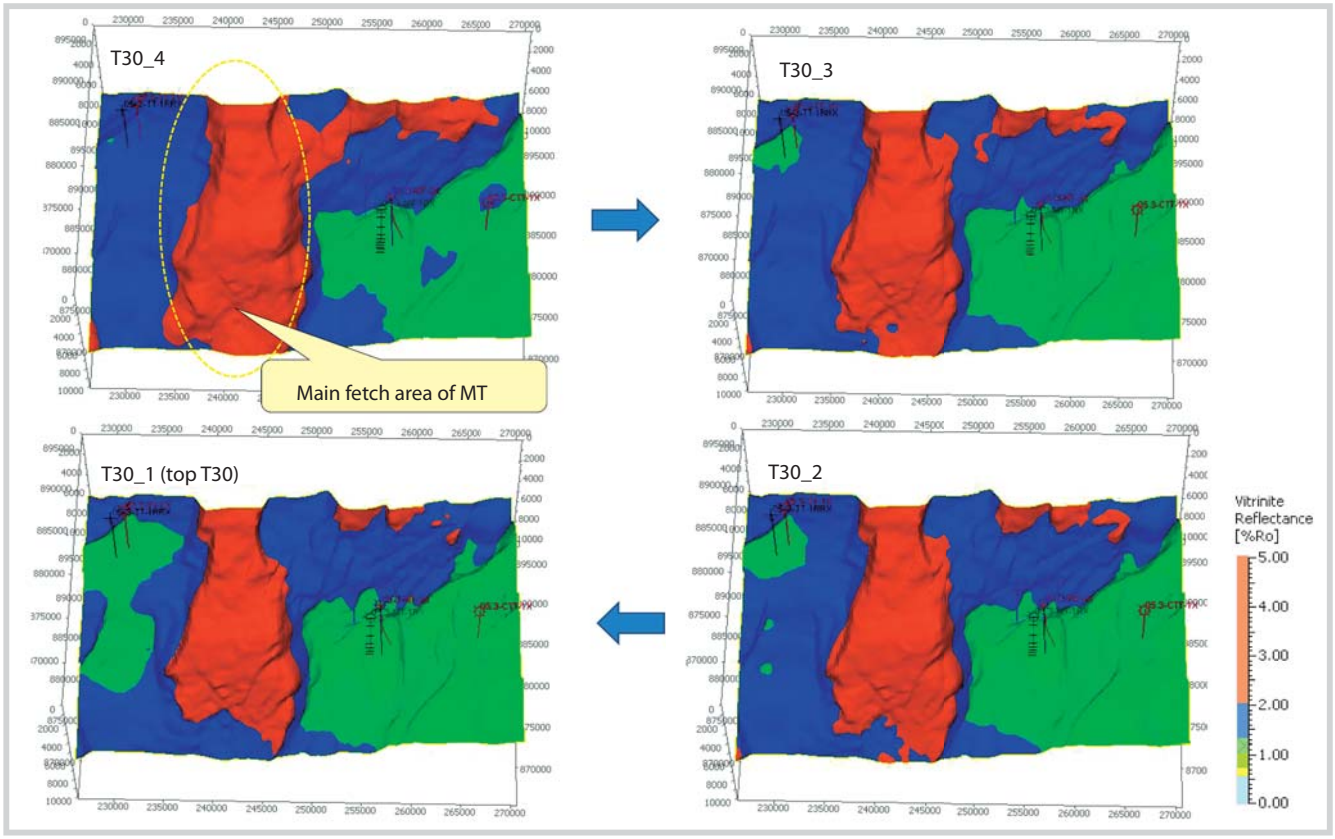



***Figure 11.*** *Modelled vitrinite reflectance for T30 source rock*

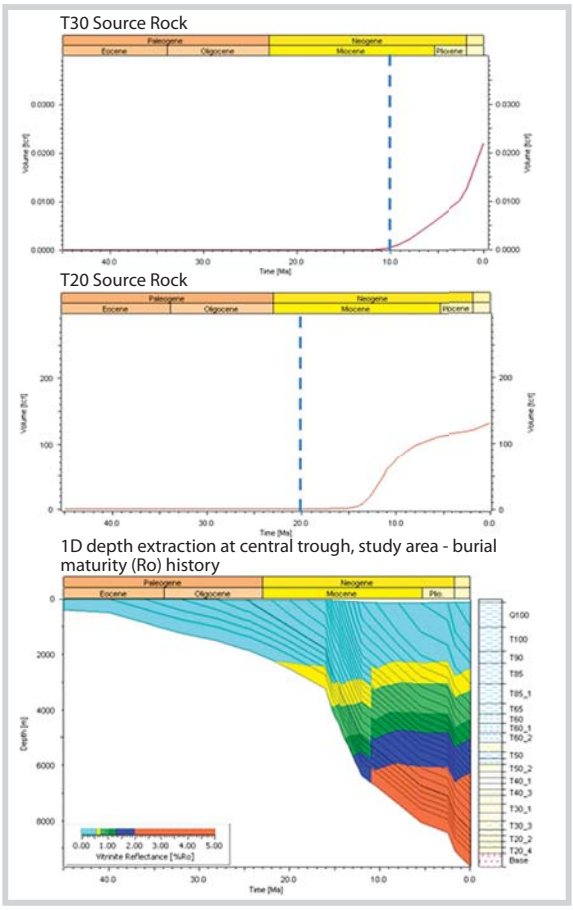



***Figure 12.*** *Cumulative generation and expulsion of source rock layers in Block 05-3*

speeded up during rifting phases or high heat flow phases. This explains why during the Early Miocene the generation was not much changed, but it significantly increased during the Middle Miocene (16 - 10.5Ma).

Moreover, Lower Miocene source rock started to generate hydrocarbon since 12Ma. At that time, this source rock was in the early mature stage. The main oil generation time of this source rock is from 5.5Ma to present.

### *3.3. Hydrocarbon migration and accumulation*

Together with the source rock potential and maturity, the effectiveness of migration is a key factor deciding the exploratory success or failure [5].

3D Model accumulation volume or fluid composition outputs can be compared with the information at discovery wells of Block 05-3 and the model can be adjusted to improve the match. Figure 13 shows that flow path lines for all levels, all accumulations, with Oligocene TR map underneath; fault (gray colour) provides a preferential migration pathway.

Firstly, the accuracy of simulation was proven by matching at discovery wells (the wells in Moc Tinh fields). Most Oligocene source rock is in gas prone at present, so it is reasonable to explain why the accumulations in Moc Tinh discovery are condensate and dry gas ($CH_4$).

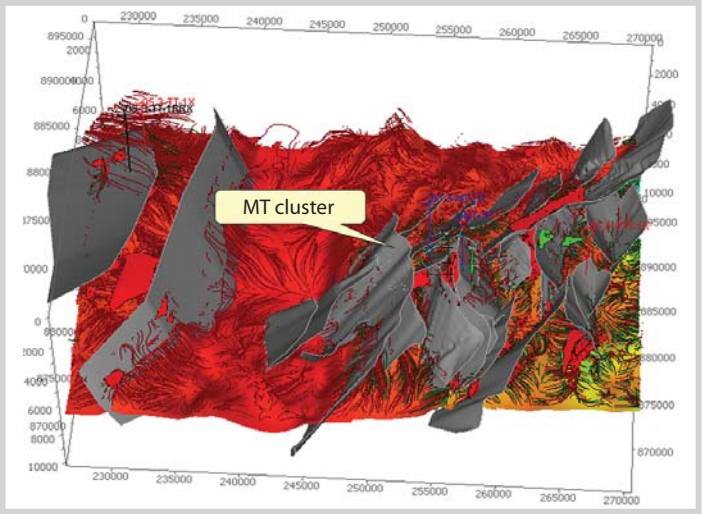



***Figure 13.*** *Flow path lines for all levels, all accumulation in study area*

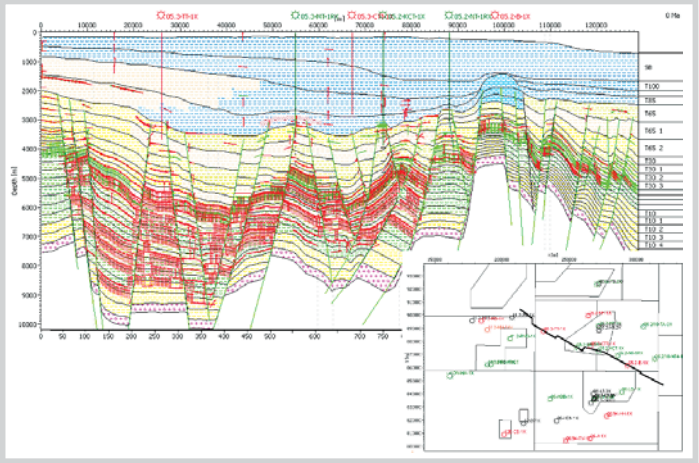


***Figure 14.*** *Hydrocarbon migration and accumulation in Moc Tinh and Tho Tinh prospect-2D basin modelling*

To increase the accuracy of basin modelling, the 2D migration and accumulation model is simulated. Based on 2D modelling results, the charge system in the central part of the Nam Con Son basin is dominated by vertical migration through faults and imperfect intra formation seals. Moreover, Moc Tinh and Moc Tinh Tay structures can be charged with higher column height of gas and condensate (Figure 14).

The modelling results of 3D petroleum system modelling show possible significant accumulations in T50, and T85 reservoir levels in the Moc Tinh Tay structure. Besides, it is predicted that the parts of T30 sequence on the Moc Tinh Tay structure have been charged by minor amount of oil and gas.

## 4. Conclusions and recommendations

In this study, detailed 1D, 2D, and 3D modelling of petroleum system in Block 05-3 has been carried out. The inputs for the modelling have been integrated from various investigations on structural development, paleo-depositional environment, heat-flow calibration, top seal calibration, source rock properties and the aspects of in-fault migration. The results show that:

- The Oligocene, Lower Miocene sedimentary layer contains mainly kerogen type III and a mix of kerogen type III and I. The Oligocene, Lower Miocene source rocks have got enough organic matter richness for HC generating.

- Hydrocarbon generation potential: Main source rock (Oligocene & Lower Miocene) is mainly located in the centre trough and in gas prone at present.

- Migration and charge: Hydrocarbon was expelled since 24Ma from Oligocene T20 SR which widely migrated from 15 to 8Ma.

- Main accumulation in prospect Moc Tinh Tay is in T50 and T30 layers. No accumulation in Oligocene sandstones due to low porosity.

- Uncertainties of model: the presence and amount of HC accumulations depend on time-depth conversion; sample grid; and fault properties.

In general, the findings from basin modelling reveal that Moc Tinh Tay prospect can be charged from source rock in surrounding areas with significant amount. To reduce investment risk in oil and gas exploration in Block 05-3, further studies including verification of facies and lithology distribution at Moc Tinh Tay prospect by seismic inversion are recommended.

## References

1. Thomas Hantschel, A.I. Kauerauf. *Fundamentals of basin and petroleum systems modeling*. Springer Berlin Heidelberg. 2009.

2. Talisman Joint Study. *The tectonic and stratigraphic development of the Nam Con Son and Vung May basins*. Final report. 2011.

3. BP sub-Surface team. *Block 05-3 Moc Tinh reserves report*. 2006.

4. J.J.Sweeney, A.K.Burnham. *Evaluation of a simple model of vitrinite reflectance based on chemical kinetics*. AAPG Bulletin. 1990; 74: p. 1559 - 1570.

5. G.R.Beardsmore, J.P.Cull. *Crustal heat flow: A guide to measurement and modelling*. Cambridge University Press. 2001.

6. R. L. Folk. *Petrology of Sedimentary Rock*. Hemphill Publishing Company, Austin, Texas. 1974.

# PETROPHYSICAL CHARACTERISATION OF PORE SYSTEM FOR A CARBONATE RESERVOIR IN THE HR STRUCTURE

Pham Huy Giao[1], Nguyen Hoai Chung[1, 2]
[1]Geo-exploration & Petroleum Geoengineering Program, Asian Institute of Technology (AIT)
[2]Vietnam Petroleum Institute (VPI)
Email: hgiao@ait.asia, chungnh@vpi.pvn.vn

**Summary**

*The purpose of reservoir characterisation is to figure out the spatial distribution of petrophysical properties such as porosity, permeability and water saturation that are key parameters for construction of the geological model. Characterisation of a carbonate reservoir is often difficult mainly due to the complexity of its pore system. This study presents an integrated approach to using well log and micro-geological data to characterise rock fabrics and their pore system for a carbonate reservoir in the HR structure. Based on well log data such as GR, PE, PHIN and RHOB, two major rock types of dolostone and limestone were identified. A further combination with thin section and SEM analysis results indicated four types of carbonate rock fabric, namely limestone with grain-dominated grainstone, limestone with grain-dominated packstone, dolostone with grain-dominated grainstone and dolostone with grain-dominated packstone. For each identified carbonate fabric, two types of pore were found, including interparticle and vuggy pores. The latter can be further subdivided into separate-vug pores and touching-vug pores. For the HR structure, the touching vug porosity and the interparticle porosity were estimated to be in the range of 1 - 3% and 1 - 8%, respectively. The inter-crystalline porosity, which might be considered as a subset of the interparticle porosity and could be estimated by SEM analysis, was found in the range from 1,5% to 3%. It is expected that the integrated analysis approach using well log and micro-geological data employed in this study can be applied to evaluate the characteristics of carbonate reservoirs at other well sites in Song Hong basin.*

***Key words:*** *Petrophysics, pore system, carbonate reservoir, Ham Rong structure, Song Hong basin.*

## 1. Introduction

Carbonate reservoir has been studied over many years. Characterisation of a carbonate reservoir is often difficult mainly due to the complexity of its pore system [2, 3, 4]. Carbonate pore types are considered the key factor affecting permeability and water saturation. This study presents an integrated approach to using well log and micro-geological data to characterise rock fabrics and their pore system for a carbonate reservoir in the HR structure and develop the appropriate workflows that can be probably used in log analyses and petrophysical interpretation.

Well log and samples were collected from well 106-HR-A belonging to the HR structure in Song Hong basin, offshore Vietnam, about 75km SE of Hai Phong city (Figure 1). In the late 1990s Nielsen et al. [5] conducted a comprehensive study on hydrocarbon generation for this area and suggested that the huge and still underexplored Song Hong basin provides attractive areas for further exploration. Al-Atroshi et al. [6] reported that a Pre-Tertiary carbonate reservoir was proven with the discovery of HR-1X ST4 and HR-2X in this structure.

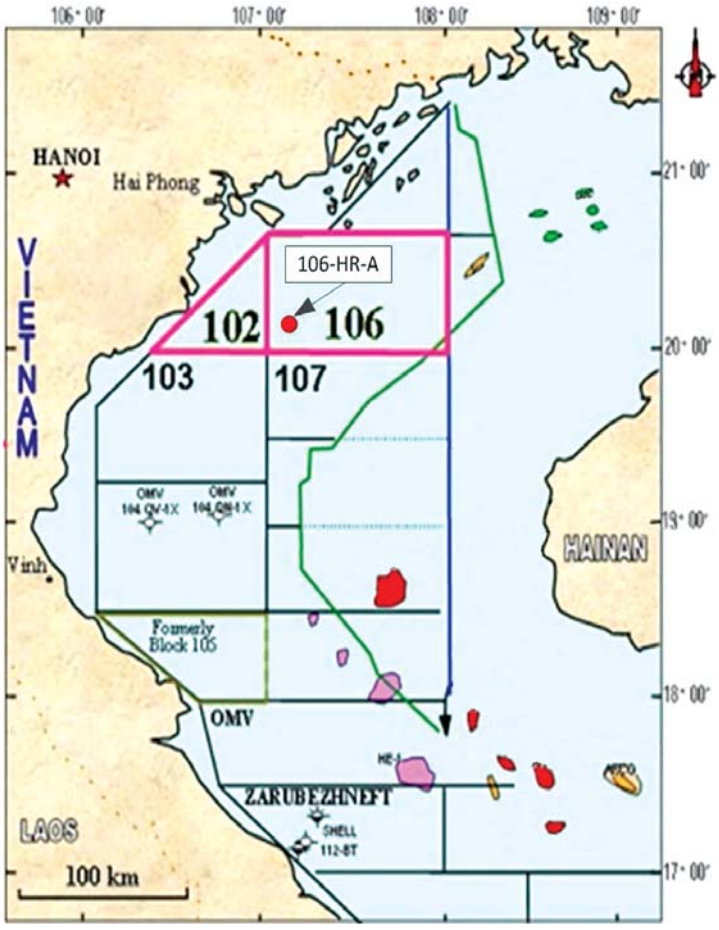



***Figure 1.*** *Location of study area [1]*

## 2. Methodology of study

Characterisation of pore system was done over a carbonate reservoir interval of several hundred metres thick. The methodology is explained by the flow chart shown in Figure 2 with the main steps being explained in the following:

### *2.1. Lithological identification using well log data*

The first step is lithological identification, in which one tried to separate major types of rocks, i.e. limestone and dolostone. This could be done using well log data such as density (RHOB), neutron (PHIN), Gamma ray (GR) and photoelectric number (PE). The zoning criteria proposed by Crain [7], as shown in Table 1, were applied in this study. The cross-plot value between neutron and density porosity (N-D) as well as the photoelectric number are quite stable parameters to help the zonation. Some minor adjustments in PE values proposed by Lucia [3] are also mentioned in Table 1.

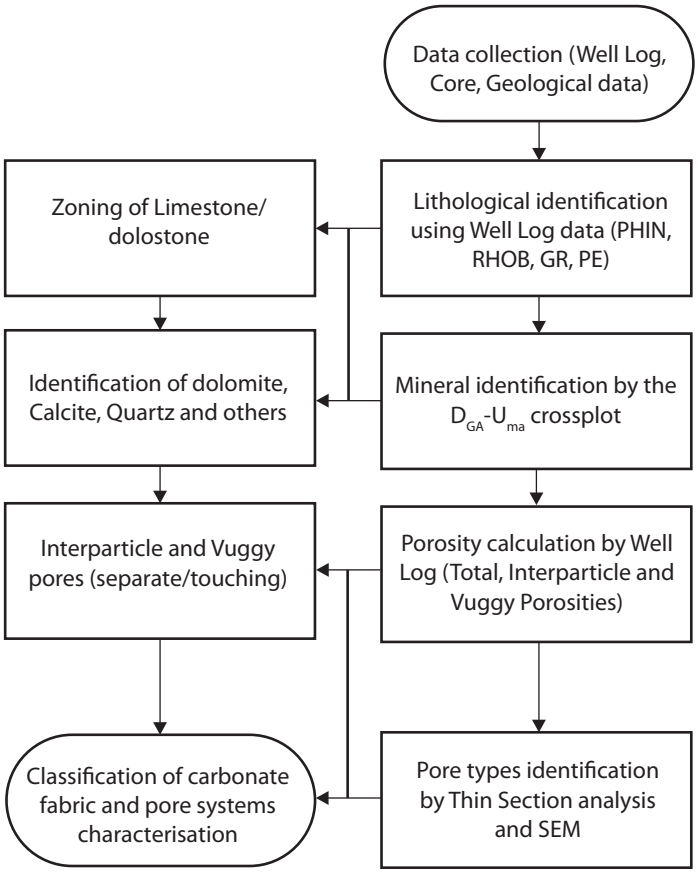



***Figure 2.*** *The flowchart of petrophysical characterisation of carbonate pore system used in this study*

***Table 1.*** *Lithological zoning criteria by well log data [7]*

| Rock | N-D (LS scale) | PE | | GR |
|---|---|---|---|---|
| | | Crain (2014) | Lucia (2007) | |
| Sandstone | -7 | 2 | 1.81 | Low |
| Limestone | 0 | 5 | 5.08 | Low |
| Dolostone | 8+ | 3 | 3.14 | Low |
| Anhydrite | 15+ | 5 | 5.05 | Low |
| Salt | -45 | 4.5 | 3.99 | Low |
| Shale | 13+ | 3.5 | | High |

### *2.2. Mineral indication by the $D_{GA}$-$U_{ma}$ cross-plots*

After zonation, the next step is mineral identification using the $D_{GA}$-$U_{ma}$ lithology cross plots as suggested by Burke et al. [8], where $D_{GA}$ and $U_{ma}$ stand for apparent dry density and apparent volumetric factor, respectively as explained below:

$$U = \frac{PEF \times (RHOB + 0.1883)}{1.07} \quad (1a)$$

$$D_{GA} = \frac{RHOB - RHOB_f \times \phi_t}{1 - \phi_t} \quad (1b)$$

$$U_{ma} = \frac{U - U_f \times \phi_t}{1 - \phi_t} \quad (1c)$$

Where:

U: Volumetric cross section (barns/cm$^3$);

$U_f$: Pore fluid volumetric factor = 0.398barns/cc (assumed water in the pores);

$RHOB_f$: Pore fluid density, equal to 1.0g/cc (assuming water in the pores);

$\phi_t$: Total porosity;

$U_{ma}$: The apparent volumetric factor (barns/cm$^3$);

$D_{GA}$: The apparent dry grain density (g/cc).

1barn = $10^{-28}$m$^2$ (barn is a unit of area which is used to describe the physical properties of nuclear, expressing the cross sectional area of nuclear reactions).

Eq. (1a) shows a conversion of photoelectric absorption factor (PE) and density (RHOB) to U, a parameter called volumetric cross section [9, 10]. The proximity of the data to the mineral endpoints of the triangle will help indicate the mineral composition.

### *2.3. Porosity calculation using well log data*

Lucia [4] proposed the interparticle porosity be calculated based on the travelling time of acoustic log. Hence, vuggy porosity can be calculated by subtracting interparticle porosity from total porosity as follows:

$$\emptyset_t = \frac{\phi_D + \phi_N}{2} \quad (2a)$$

$$\emptyset_{intp} = \frac{DT - DT_{ma}}{DT_f - DT_{ma}} \quad (2b)$$

$$\emptyset_{vug} = \emptyset_t - \emptyset_{intp} \quad (2c)$$

Where:

$\phi_{intp}$: Interparticle porosity;

$\phi_{vug}$: Vuggy porosity;

$\phi_t$: Total porosity based on $\phi_D$ and $\phi_N$;

$DT_{ma}$: Slowness of formation rocks (dolostone, limestone) µs/ft;

$DT_f$: Slowness of fluid µs/ft.

### 2.4. Pore type identification by thin section and SEM analyses

*2.4.1. Thin section analysis by modal counting method*

The thin section preparation involved vacuum impregnation with blue resin in order to distinguish and count visible porosity of the rocks. All thin sections have been described in terms of mineral composition, texture, and rock classification. Mineral composition and visible porosity have been performed by modal analysis which was applied for quantitative mineral volume on thin section since 1956 [11]. The percentage of mineral species can be calculated as follows:

$$\%\ mineral = \frac{\sum counting\ points}{total\ number\ of\ counts} x\ 100\% \quad (3)$$

The modal analysis was done by counting 300 points at 20X magnifications in each thin section as shown in Figure 3. The basic data records for modal analysis include mineral species, grain size, fracturing and pore observations, based on which the percentage of porosity per total number of points can be calculated.

*2.4.2. SEM analysis*

Pore system can be assessed from SEM images by using ImageJ (IJ 1.48v), which was developed by Wayne Rasband (1997) at the United States National Institute of Health [12]. Creating a histogram for each image and establishing a threshold in the histogram, SEM images are first converted into binary images to be analysed by ImageJ software. The procedure is shown in Figure 4. The SEM analysis results included a summary table containing total number of pores, percentage of pores, pore size, and the area of the binary image of each individual pore.

### 2.5. Carbonate fabric classification and pore type characterisation

There are many classification systems proposed for carbonate rocks, but in this study the classification proposed by Lucia [3, 13] was selected due to its advantage in allowing the linkage between carbonate pore-size distribution and pore type. Choquette and Pray [14] had earlier indicated that pore-size distribution is controlled by pore type. Lucia [3, 13] pointed out further that the different types of pore have effects on petrophysical properties. In Lucia's classification [3] two main types of porosity are interparticle porosity and vuggy porosity. Interparticle porosity is defined as the pore space located between grains, allochems and crystals, while vuggy porosity is defined as the pore space within grains/crystals, fossil chambers, fractures and large irregular cavities. Furthermore, vuggy pore space can be subdivided into separate-vug pores which are interconnected only through interparticle pore network, i.e. leached grains

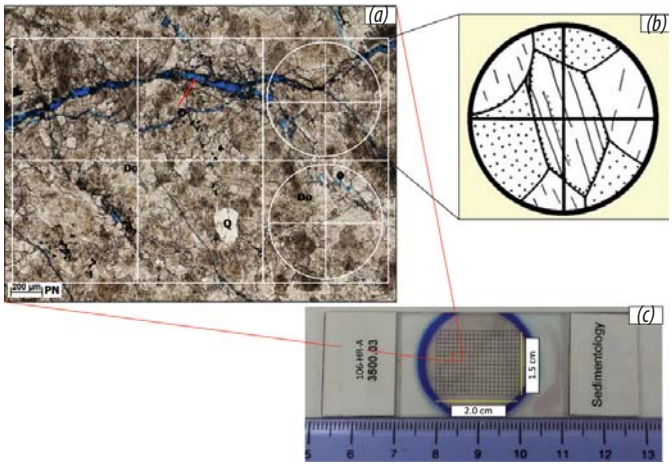



***Figure 3.*** *Counting point framework: Field numbers (a); Field of view (b); Grid system (c)*

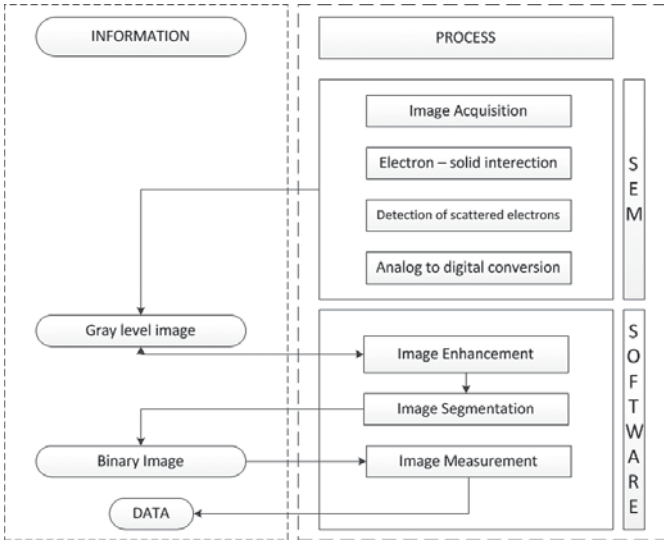



***Figure 4.*** *The flowchart of the acquisition and processing of SEM image [15]*

*Table 2. Lucia's carbonate classification [3, 13]*

| Petrophysical class occupied with the range of crystal size | Dolostone | Limestone |
|---|---|---|
| Class 3: < 20μm | • Fine crystalline mud-dominated dolostones | • Mud-dominated (e.g. packstone, wackestone and mudstone |
| Class 2: 20 - 100μm | • Grain-dominated packstones<br>• Medium crystalline mud-dominated dolostones | • Grain-dominated packstone |
| Class 1: 100 - 500μm | • Grainstone<br>• Large crystalline grain-dominated dolopackstones<br>• Mud-supported dolostone | • Grainstone |

*Table 3. Classification of carbonate rock fabrics by thin section analysis*

| Zone | Lithology | Contained mud | Rock fabric classification (Lucia's classification, 1995) | | | |
|---|---|---|---|---|---|---|
| | | | Type of fabric | Petrophysical class | Range of grain size (μm) | Fracture |
| 1 | Dolostone (Grainstone) | | Grain-dominated | Class 1 | 100 - 200 | ✓ |
| 2 | Limestone (Grainstone) | | Grain-dominated | Class 1 | 20 - 100 | ✓ |
| 3 | Dolostone (Grainstone) | | Grain-dominated | Class 1 | 100 - 150 | ✓ |
| 4 | Dolostone (Packstone) | ✓ | Grain-dominated | Class 2 | 20 - 100 | ✓ |
| 5 | Limestone (Grainstone/Packstone) | ✓ | Grain-dominated | Class 1/Class 2 | 20 - 100 | ✓ |
| 6 | Dolostone (Grainstone) | | Grain-dominated | Class 1 | 200 - 350 | ✓ |

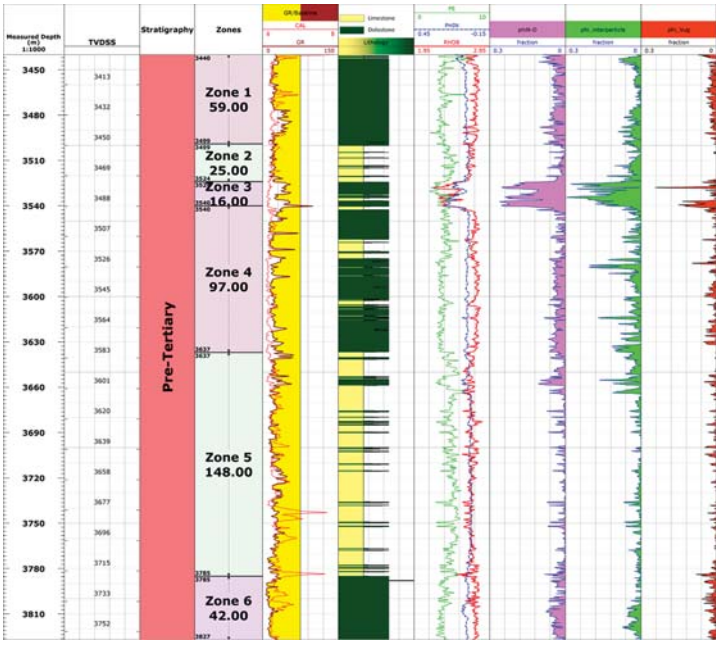



*Figure 5. Porosity and type of rock distribution at well 106-HR-A*

and fossil chambers and touching-vug pores that form an interconnected pore system of significant extent, i.e. solution-enlarged fractures, and irregular cavities. Lucia's classification [3, 13] divides carbonate rocks into three classes based on crystal size and groundmass components as shown in Table 2.

## 3. Results and discussion

### *3.1. Zonation*

Neutron (PHIN), density (RHOB), Gamma ray (GR) and photoelectric factor (PE) were successfully used in lithological identification. As seen in Figure 5 and Table 3, a total of 6 carbonate reservoir zones with two main facies were identified, i.e. limestone facies with PE of about 5.08 and dolostone facies with PE of about 3.14.

### *3.2. Mineral identification using the $D_{GA}$-$U_{ma}$ cross-plot*

The $D_{GA}$-$U_{ma}$ cross-plots were plotted for 6 reservoir zones as shown in Figure 6. The main clusters are grouped either at the calcite or dolomite vertex. There is a good agreement between the $D_{GA}$-$U_{ma}$ cross-plot and thin section analysis results in mineral identification.

### *3.3. Results of carbonate fabrics characterisation using thin section and SEM analyses*

Four types of carbonate rock fabric were found as shown in Table 3, i.e. i) limestone as grain-dominated grainstone; ii) limestone as grain-dominated packstone; iii) dolostone as grain-dominated grainstone; and iv) dolostone as grain-dominated packstone.

Based on Lucia's [3] classification two petrophysical classes were identified, i.e. 1) Class 1: for limestone or dolostone as grain-dominated grainstone, which has inter-crystalline pores space; and 2) Class 2: for limestone or dolostone as grain-dominated packstone, which has some interparticle pores (including the pores between allochems and clastic grains) filled with mud. These

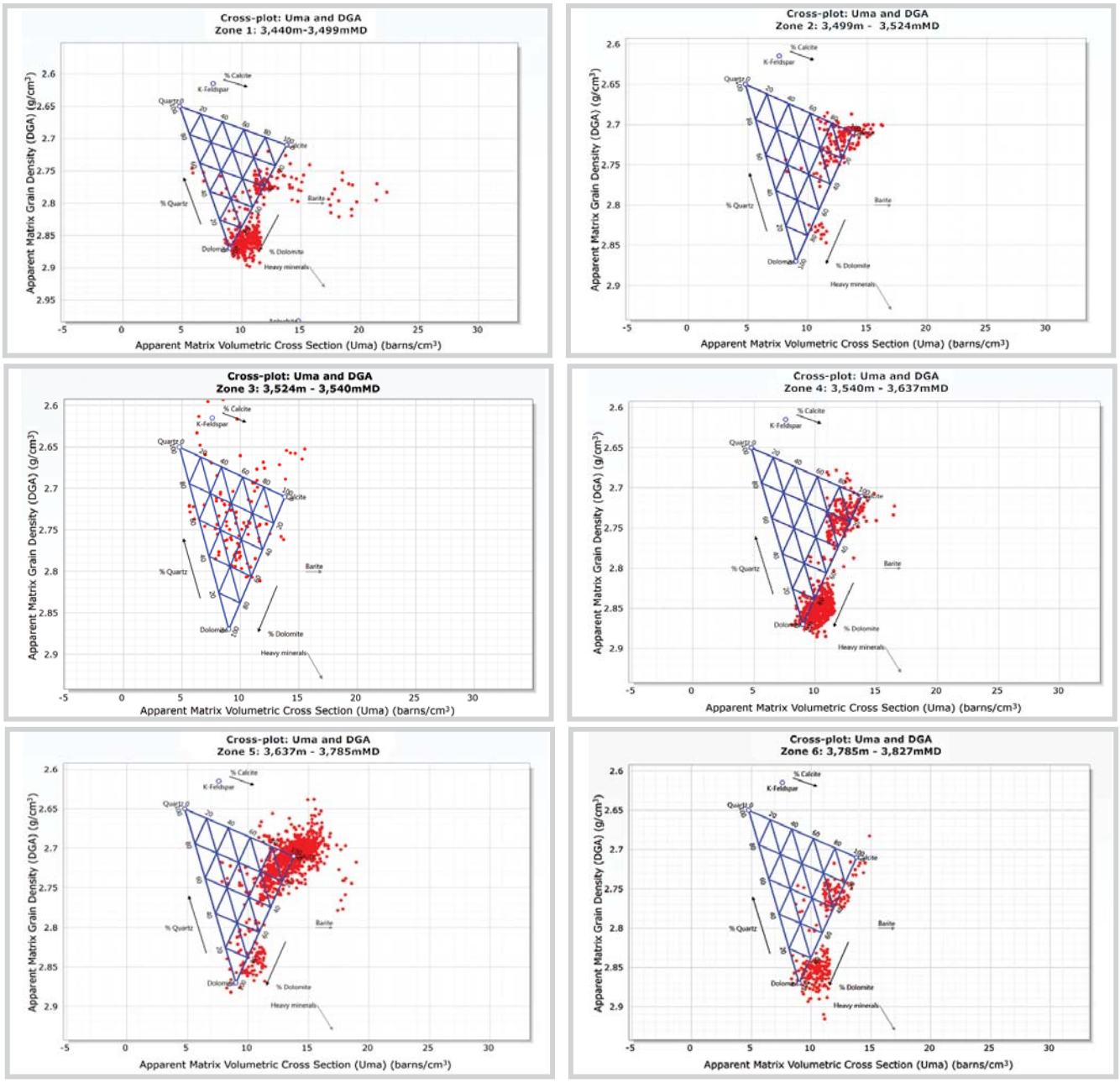
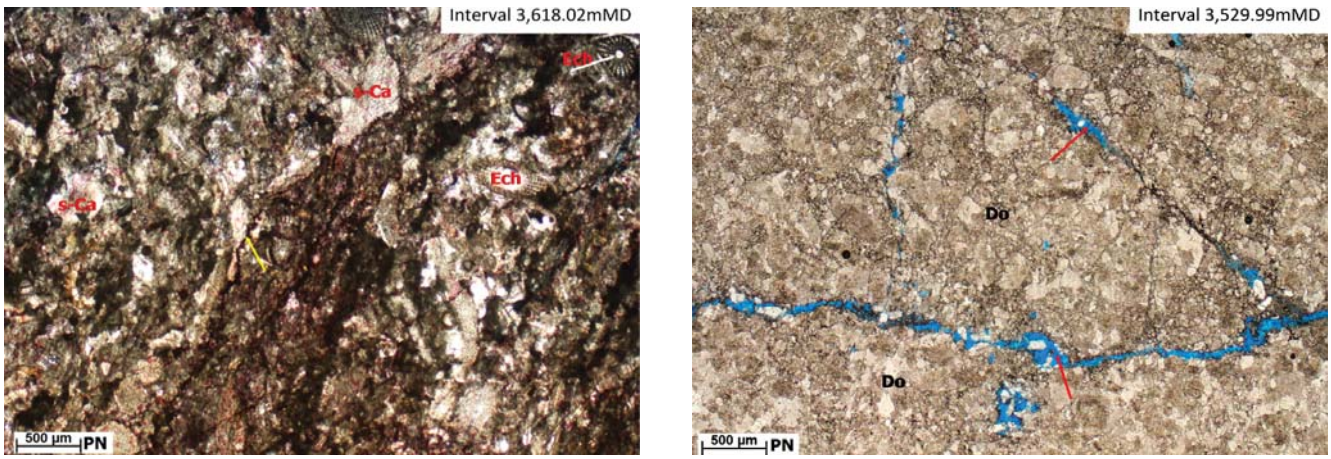
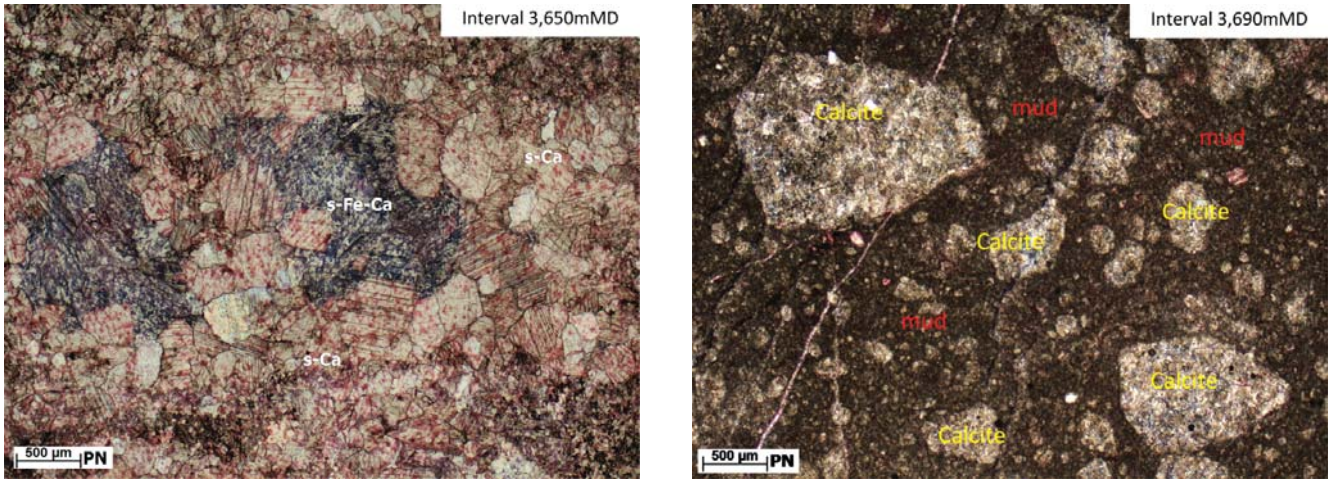



***Figure 6.*** *Mineral identified based on $U_{ma}$-$D_{GA}$ cross-plot at different zones*



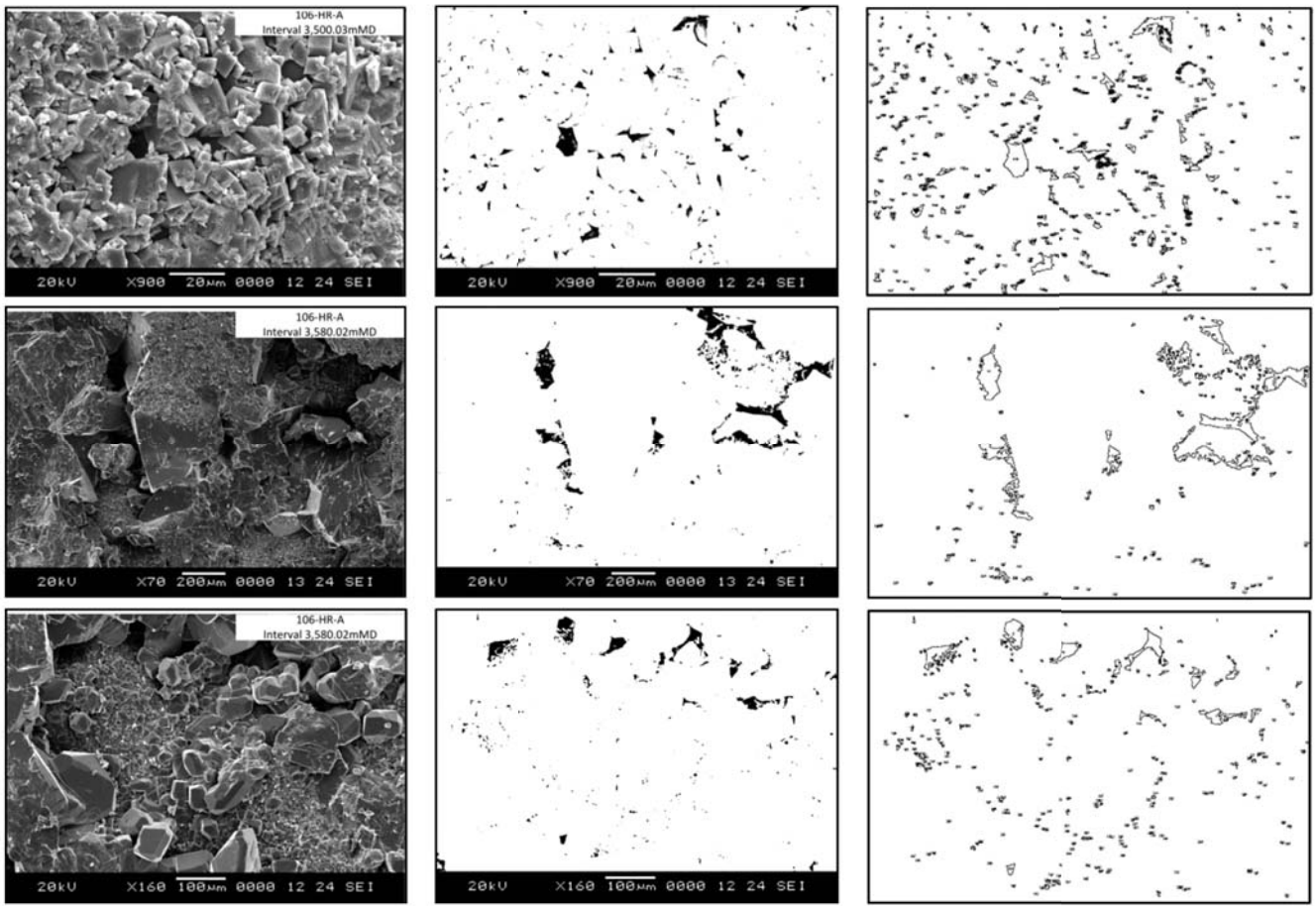

*(a)* *(b)*

***Figure 7.*** *The photomicrograph of the dolostone fabrics: Grain-dominated packstone with sparry calcite filled up fractures in zone 4 (a); Grain-dominated grainstone in zone 3 (b)*




(a) (b)

***Figure 8.*** *The photomicrograph of the limestone fabrics in zone 5: Grain-dominated grainstone (a); Grain-dominated packstone (b)*




(a) (b) (c)

***Figure 9.*** *Segmentation of microspore: Original SEM image (a); Binary image, on which the micro-pore network can be identified by the darkest spots (b); Pore geometry (c)*

rocks are strongly fractured and filled up with sparry calcite and silicic mineral.

The thin section photomicrographs as illustrations for dolostone and limestone fabrics for zone 3, 4 and 5 are shown in Figures 7 and 8, indicating two main types of grain-dominated grainstone and grain-dominated packstone.

The original SEM images (Figure 9a) were first converted into binary images (Figure 9b) that will be analysed by the ImageJ software, i.e. the pores could be identified as the darkest spots. As a result, one could obtain the percentage of different pore types, and the inter-crystalline porosity of grain-dominated grainstone was found to be in the range from 1% to 3% of the whole

*Table 4. Carbonate rock fabrics and pore system characterisation*

| Zone | Lithology | Type of fabric | Calculated Porosity (%) | | | | | | |
|---|---|---|---|---|---|---|---|---|---|
| | | | By thin sections | | | By SEM | By well log data | | |
| | | | Total | Inter-particle | Touching vug | Inter-crystalline | Total | Inter-particle | Vug |
| 1 | Dolostone | Grainstone | 4 | | 4 | 1.73 | 5.04 | 3.47 | 1.79 |
| 2 | Limestone | Grainstone | 4 | 2.3 | 1.7 | 3.02 | 3.47 | 2.01 | 0.20 |
| 3 | Dolostone | Grainstone | 9.6 | 2.3 | 7.3 | | 17.99 | 14.45 | 4.21 |
| 4 | Dolostone | Packstone | 0 | | | 2.92 | 4.23 | 4.21 | 0.06 |
| 5 | Limestone | Grainstone/ Packstone | 3 | 1.25 | 1.75 | 1.5 | 0.95 | 0.55 | 0.41 |
| 6 | Dolostone | Grainstone | 0 | | | | 4.52 | 2.93 | 1.59 |

image. The range of inter-crystalline porosity is quite similar to that of interparticle porosity estimated by thin section analysis, which indicated that the pores between the carbonate mineral crystals play a main role in the interparticle porosity. In addition, the pore geometry could be visualised as seen in Figure 9c and the pore sizes were found in the range from 0.1µm to 30.8µm in diameter.

The final results of an integrated petrophysical analysis using both well log and micro-geological data of thin section and SEM analyses in this study are summarised in Table 4.

## 4. Conclusions and recommendations

More than 400m thick carbonate rock interval was analysed at the study well site in the HR structure. Six lithological zones were identified as limestone and dolostone having main fabrics as grainstone with grain-dominated fabric and packstone with grain-dominated fabric. Different pore types were identified such as interparticle, vuggy and inter-crystalline. It is worth noting that the $D_{GA}$-$U_{ma}$ cross-plots proved to be useful for identification of predominant minerals. It could be plotted for each zone identified and could help to indicate the predominant mineral.

As a result, the analysis interval at the study well was divided into six zones. Zones 1, 3 and 6 were classified as dolostone of grain-dominated grainstone with total porosity of about 2 - 17% in which interparticle porosity varies from 2% to 14% and touching vug from 1% to 4%. Zones 2 and 5 were classified as limestone of grain-dominated grainstone and packstone with total porosity from 1 to 4% in which interparticle porosity varies from 0.5% to 2% and touching vug from 0.2% to 0.4%. Zone 4 is dolostone which was classified as grain-dominated packstone with total porosity from 2% to 4% in which interparticle porosity varies from 2% to 4%.

It is noted that zone 3 of grain-dominated grainstone dolostone (Tables 3 and 4) is somewhat special comparing with the other zones as all of the porosity components are significantly higher. It is suspected that the solution-enhanced pores might be the reason for the high porosity in this zone. Further detailed analysis is recommended for pore characterisation of this dolostone zone.

The use of Lucia's [3, 13] classification in carbonate fabric characterisation and linkage with the pore system is very helpful. The integrated analysis proposed and applied in this study for petrophysical characterisation of carbonate rock pore system can be applied for other well sites in the HR structure in the Song Hong basin.

## Acknowledgements

Thanks are due to the Analysis Laboratory Centre, Vietnam Petroleum Institute (VPI), Petrovietnam Exploration Production Corporation (PVEP) colleagues, and in particular to Mrs. Bui Thi Ngoc Phuong, Manager of Sedimentary Laboratory, for their kind support on part of the input data as well as valuable discussions.

## References

1. Petrovietnam. Investment opportunity in Block 102/10 & 106/10. www.pvn.vn.

2. L.A.Lubis, Zuhar Zahir Harith. *Pore type classification on carbonate reservoir in off shore sarawak using rock physics model and rock digital images*. IOP Conference Series Earth and Environmental Science. 2013.

3. F.J.Lucia. *Rock fabric/petrophysical classifi cation of carbonate pore space for reservoir characterization*. AAPG Bulletin. 1995; 79(9): p. 1275 - 1300.

4. F.J.Lucia. *Carbonate reservoir characterization: An integrated approach* (2nd edition). New York: Springer. 2007.

5. L.H.Nielsen, A.Mathiesen, T.Bidstrup, O.V.Vejbæk, P.T.Dien, P.V.Tiem. *Modelling of hydrocarbon generation in the Cenozoic Song Hong basin, Vietnam: A highly prospective basin*. Journal of Asian Earth Sciences. 1999; 17(1 - 2): p.269 - 294.

6. K.Al-Atroshi, Tan Ching Kiang, Armi Amdan. *Analytical review of Ham Rong geology and geophysics data*. First EAGE South-East Asia Regional Geology Workshop -Workshop on Palaeozoic Limestones of South-East Asia and South China. 5 December, 2011.

7. E.R.Crain. *Crain's petrophysical handbook*. 2014.

8. J.A.Burke, R.L.Campell Jr, A.W.Schmidt. *The litho porosity cross plot: A new concept for determining porosity and lithology from logging methods*. SPWLA 10th Annual Logging Symposium, Houston, Texas, US. 25 - 28 May, 1969.

9. John H.Doveton. *Principle of mathematical petrophysics*. Oxford University Press. 2014.

10. Schlumberger. *Log interpretation principles/ applications*. 1989

11. Felix Chayes. *Petrographic modal analysis: An elementary statistical appraisal*. John Wiley & Sons Inc.1956.

12. The National Institute of Health (NIH). *ImageJ manual press*. 2015.

13. F.J.Lucia. *Petrophysical parameters estimated from visual descriptions of carbonate rocks: A field classification of carbonate pore space*. Journal of Petroleum Technology.1983; 35(3): p. 629 - 637.

14. Philip W.Choquette, Lloyd C.Pray. *Geologic nomenclature and classifi cation of porosity in sedimentary carbonates*. AAPG Bulletin. 1970; 54(2): p. 207 - 250.

15. Volodymyr Kindratenko. *Development and application of image analysis techniques for identification and classification of microscopic particles*. Illinois University. 1997.

# THE PROBLEM OF HIGH WAX CRUDE OIL TRANSPORTATION THROUGH SUBSEA PIPELINES FROM A MARGINAL OFFSHORE OIL FIELD

Tong Canh Son, Le Dinh Hoe, Nguyen Quang Vinh
*Vietsovpetro*
*Email: sontc.rd@vietsov.com.vn*

**Summary**

*In the last few years, Petrovietnam has discovered some marginal oil fields such as Nam Rong, Doi Moi, Ca Ngu Vang, Hai Su Den, Hai Su Trang, and Gau Trang, etc. Most of the oil and gas will be produced from the basement reservoir, but the oil and gas reserves from these fields are modest. The test results of wells during drilling showed that the maximum production rate from the wells of these fields is expected to be about 20,000 barrels/day (3,000 tons/day). The efficient development of these offshore oil fields will be problematic for the engineers. Oil production practices around the world show that, if the production of an offshore oilfield is not more than 20,000 barrels/day, then the tie-in of the marginal fields to the nearest larger oil field will be a more effective way to produce the oil and gas.*

*In some cases, it will be a larger challenge because of the high pour point (~36°C) and high wax content (19 - 25%) of the crude oil produced from these fields. In addition, the wellhead temperature may be lower than the wax appearance temperature (WAT), which is in the range of 45 - 50°C. The offshore transportation of this oil and gas through long distance pipelines together with conditions of relatively low seabed temperatures (~21°C) will pose serious problems due to the deposition of paraffin wax.*

*The decision to tie-in smaller, marginal fields with high pour point and waxy crude to adjacent oil production platforms through subsea pipelines is very important for future oil production in Vietnam. This paper will describe the complexities and problems associated with oil and gas transportation from Nam Rong - Doi Moi oil field to the Rong oil field of Vietsovpetro.*

***Key words:*** *Wax deposition, pour point temperature, viscosity, Nam Rong - Doi Moi oil fields.*

## 1. Introduction

Doi Moi oil field is located in the Nam Rong area, about 18km from the fixed platform RP-1 and 21.5km from platform RP-2. The operators of Doi Moi and Nam Rong oil fields will be the "Vietnam - Russia - Japan" JV and Vietsovpetro. The results of well testing showed that the maximum production from Doi Moi oil field should reach 2,000m$^3$/day and the minimum production may be only 300 - 570m$^3$/day. Hence, the maximum production of crude oil from both Nam Rong and Doi Moi oil fields will be about 3,600m$^3$/day and the minimum daily production is expected to be about 500m$^3$.

The practice of oil and gas gathering and transportation with low flow rates through subsea pipelines often poses a serious problem due to the deposit of wax on the walls of pipeline [1]. Transportation of crude oil from Doi Moi and Nam Rong oil fields through the subsea pipeline will have a low flow rate and is therefore expected to experience problems of wax deposition on the pipeline walls. The problem will be worse in offshore conditions with a minimum seabed temperature of ~21°C.

## 2. Rheological properties of the crude oil

The crude oil produced from Nam Rong - Doi Moi oil fields has a high paraffin wax and asphaltene resin content. The pour points of these crudes range from 29 - 36°C and their viscosity at 50°C range from 9 - 17.4mm$^2$/s. Table 1 shows some of the main physical and chemical properties of Nam Rong - Doi Moi crude oil.

The pressure - volume - temperature (PVT) studies in the laboratory demonstrated that the influence of solvent gas on the viscosity of Doi Moi oil is a little effective at temperatures higher than 32°C, however at temperatures lower than 32°C, quantities of solvent gas injected into the oil will reduce the viscosity of Doi Moi crude oil.

***Table 1.*** *Selected physical and chemical properties of Nam Rong - Doi Moi crude oil*

| Parameter | Oil field | |
|---|---|---|
| | Doi Moi | Nam Rong |
| Specific gravity, at 20°C, kg/m$^3$ | 869.7 - 876.4 | 865 - 870 |
| GOR, m$^3$/m$^3$ | 45 | 35 |
| Water content, % V | 3.2 - 0.1 | 0 |
| Solid content, % mass. | 0.046 - 0.19 | 0.02 - 0.04 |
| Viscosity at 50°C, mm$^2$/s | 13.54 - 17.42 | 9.6 -14.1 |
| Pour point, °C | 35 - 36 | 32 - 33 |
| Sulfur content, % mass. | 0.102 - 0.1058 | 0.1169 - 0.084 |
| Paraffin content, % mass. | 17.20 - 17.55 | 19.56 - 21.8 |
| WAT, °C | 58.6 - 59.2 | 57 - 55 |
| Asphaltene resin content, % mass. | 13.3 -14.45 | 10.56 - 12.41 |
| Boiling temperature, °C | 84 - 116 | 76 - 95 |

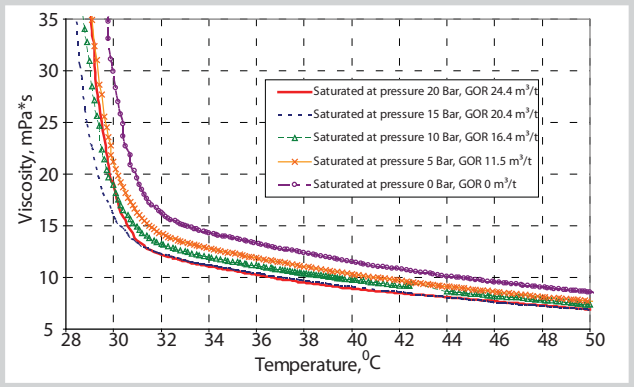
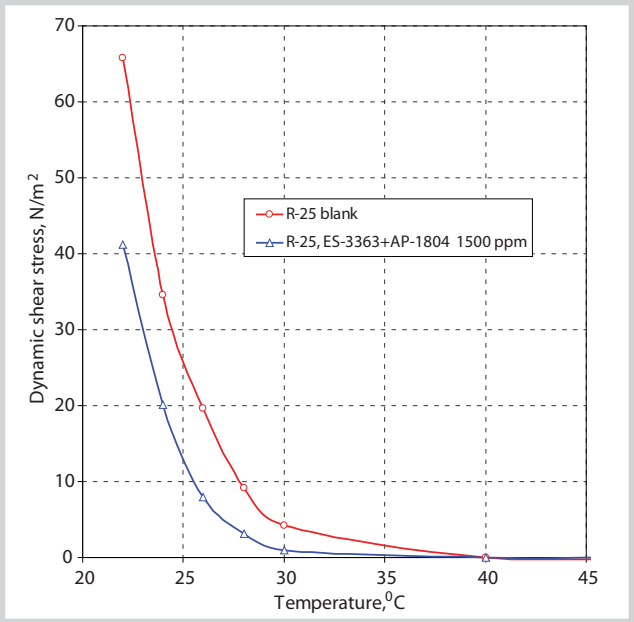



***Figure 1.*** *Viscosity of crude oil from well DM-3X at different gas-oil ratio and temperatures*

Figure 1 shows the influence of solvent at different pressures on the viscosity of a crude oil sample taken from well DM-3X of Doi Moi oil field.

In order to fully understand the crude oil characteristics and rheological properties of Nam Rong - Doi Moi crude oil, with and without pour point depressant, tests were conducted at different temperatures using specialised laboratory equipment - "ROTOVISCO-RV-20". The results are presented in Figures 2 and 3.

As presented in Figures 2 and 3, the laboratory results showed that:



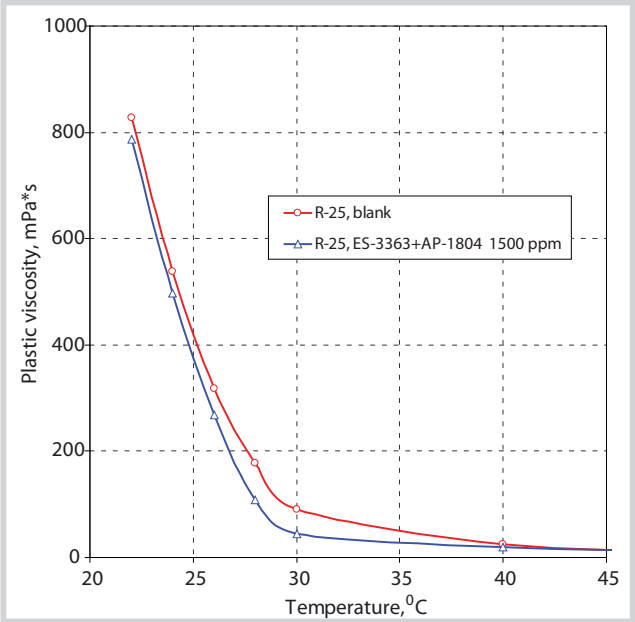
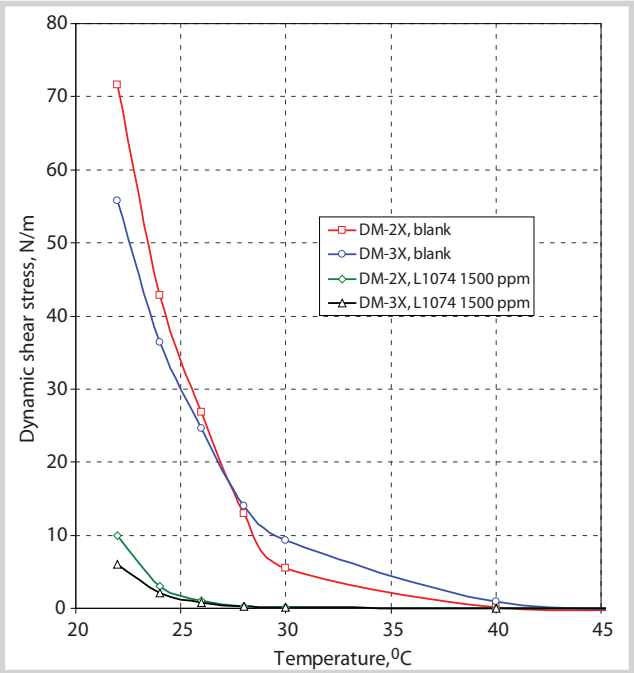




***Figure 2.*** *The influence of pour point depressant on the viscosity and shear stress of Nam Rong crude oil*



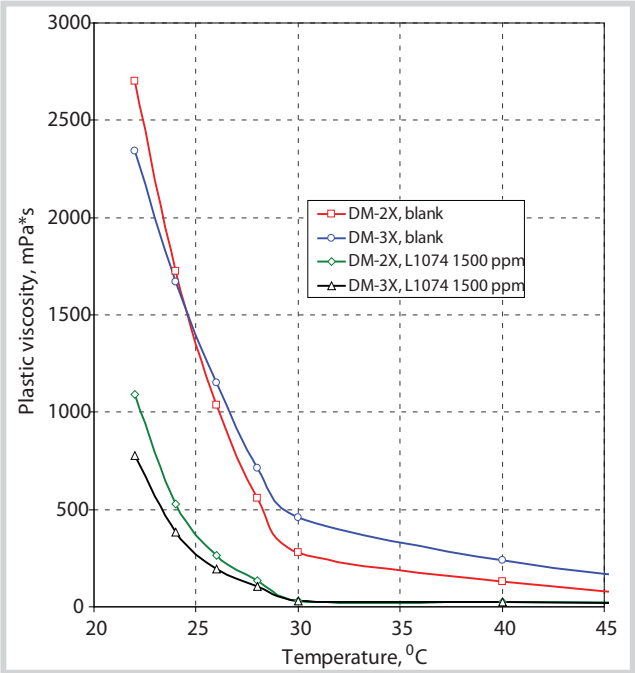




***Figure 3.*** *The influence of pour point depressant on the viscosity and shear stress of crude oil from DM-3X well*

***Table 2.*** *Results of wax deposit studies from Doi Moi crude oil using the "cold finger" method*

| "Cold finger" temperature, °C | Oil temperature, °C | The wax deposit tendency g/(m²·h), at shear rate (20s⁻¹) and chemical (PPD) dose of 1,500ppm | |
|---|---|---|---|
| | | Well # DM-2X | Well # DM-3X |
| 25 | 30 | 15.00 | 15.12 |
| 30 | 35 | 4.03 | 5.41 |
| 35 | 40 | 2.02 | 1.64 |
| 40 | 45 | 0.55 | 0.80 |
| 45 | 50 | 0.35 | 0.65 |

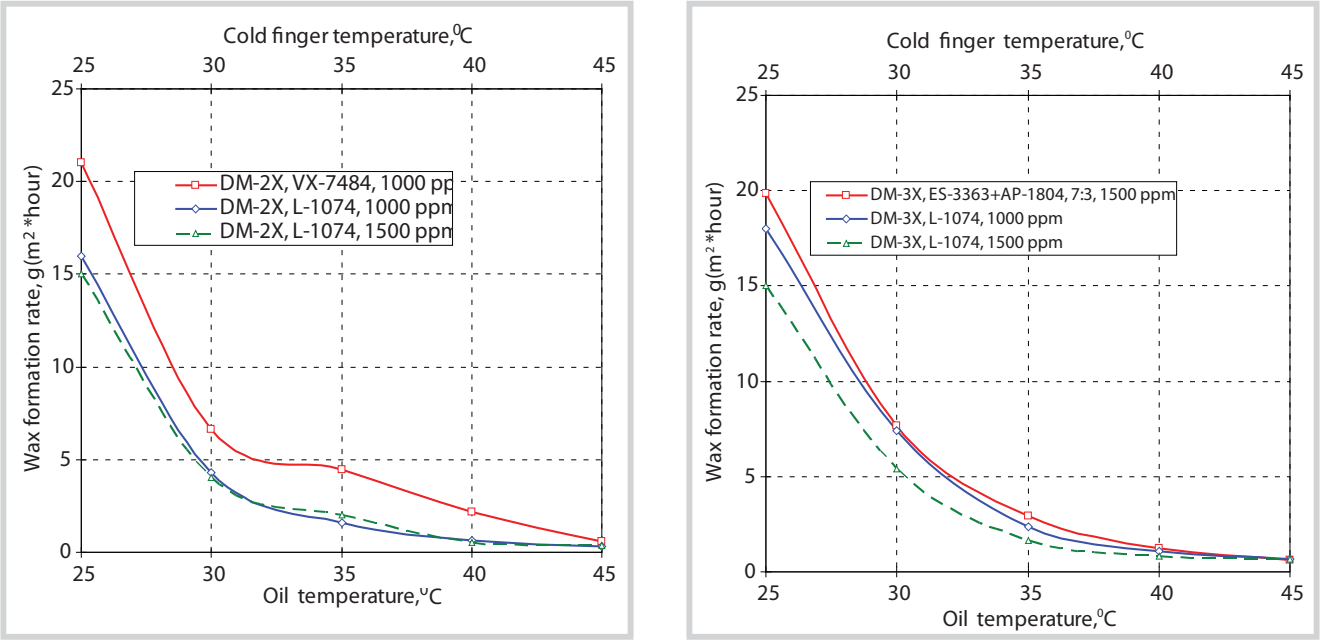



***Figure 4.*** *Wax deposit tendency of Doi Moi crude oil with the addition of pour point depressant*

- The viscosity and dynamic shear stress of crude oil samples from Nam Rong oil field (Figure 2) could be improved a little with pour point depressant;

- Rheological properties of crude oil samples from Doi Moi oil field injected with pour point depressant were strongly improved. The pour point of crude oil could be decreased from 35°C to 24°C with a dosage of 1,500ppm of pour point depressant.

To study the wax deposit tendency of crude oil samples from Doi Moi oil field, the "cold finger" apparatus was used. The results of the studies are presented in Table 2 and Figure 4. The laboratory studies were carried out at different temperatures from 35°C to 50°C. The subsea pipeline, planned to be used in Doi Moi oil field for oil and gas transportation, will be insulated with composite. Therefore, the difference in oil temperatures between the centre and the walls of pipeline will be small. Hence, in the laboratory tests, the temperature difference between the oil and the "cold finger" was kept at approximately 5°C.

The results presented in Table 2 and Figure 4 show that during a decrease of the oil temperature, the wax deposit tendency of the crude oil increased and it was higher when the shear rate was decreased. The pour point depressants used for treatment of Doi Moi crude oil do not help to solve the problem of wax deposition during transportation.

Experience in the Vietsovpetro's Rong oil field of the subsea pipeline RP-3 → PLEM-UBN-3 production [2] demonstrates that when the flow rate is low (not more than 2,000 - 3,000m³/day), serious problems of wax deposition occur on the walls of the subsea pipeline. To solve this problem, increased flow rates through the pipeline are achieved by adding sea water to the transportation pipeline.

It can, therefore, be concluded that the transportation of crude oil from Nam Rong - Doi Moi oil fields with low flow rates through the subsea pipeline to the Vietsovpetro FSO will be associated with problems of wax deposition.

### 3. The transportation of Nam Rong - Doi Moi crude oil through a pipeline with low flow rate

As described above, at present, Vietsovpetro operates some offshore oil fields in the Southern part of offshore Vietnam. The Nam Rong - Doi Moi oil fields are the nearest to Rong oil field and the tie-in of Nam Rong - Doi Moi oil fields to the Rong oil field will allow the gathering and processing of all production coming from these oil fields on the Vietsovpetro fixed platforms. The only problem to consider is to which fixed platform to transport the crude. A lot of variants had to be considered, but the route from Nam Rong - Doi Moi to RP-1 fixed platform is considered as preferable.

Two satellite platforms (RC) RC-DM and RC-4 are planned to be constructed for oil production in Nam Rong - Doi Moi oil fields. On the RC platforms only wellhead equipment without processing was considered. The production from Nam Rong oil field will be transported to RP-1 for processing. For the transportation of crude oil from Nam Rong - Doi Moi oil fields to RP-1, a thermal insulated subsea pipeline RC-DM-RC-4 → RP-1 from RC-DM to RP-1 will be built with a length of 17km.

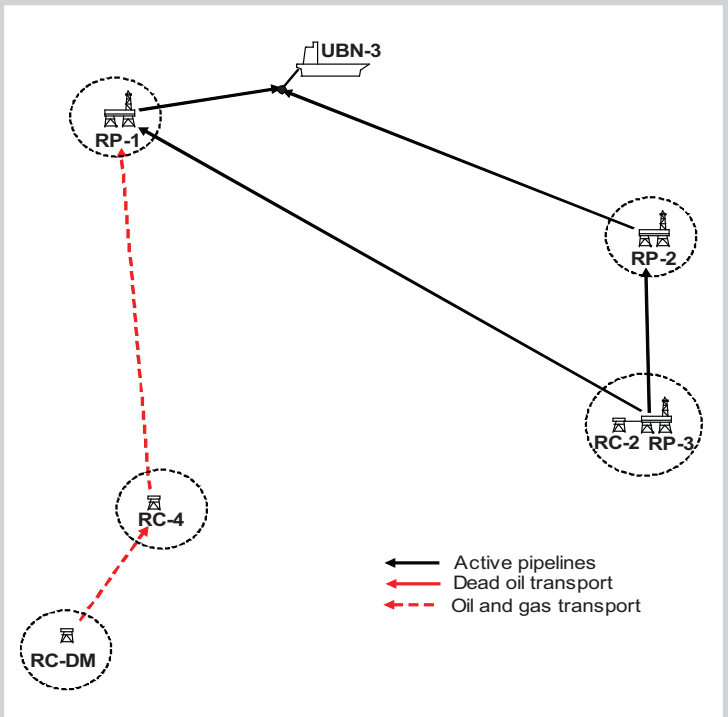



***Figure 5.*** *Schematic of oil and gas transportation from Nam Rong - Doi Moi to RP-1 of Rong oil field*

***Table 3.*** *Maximum production will be through the pipeline RC-DM → RC-4 → RP-1*

| Parameter | Transportation value | Production on RC | |
|---|---|---|---|
| | | RC-DM | RC-DM + RC-4 |
| Maximum liquid | $Q_{liquid}$, $m^3$/day | 2,254 | 3,655 |
| | Water content, % mass. | 0.0 | 0.0 |
| Maximum water content | $Q_{liqiud}$, $m^3$/day | 914 | 1619 |
| | Water content, % mass. | 66.7 | 67.8 |

Figure 5 shows the schematic of the interconnecting platforms in Nam Rong - Doi Moi and Rong oil fields.

To determine the required diameter of the pipelines RC-DM → RC-4 → RP-1, the hydraulic calculation for the maximum flow rate through the pipeline was considered. The maximum production rates that could be expected from Nam Rong - Doi Moi oil fields are presented in Table 3.

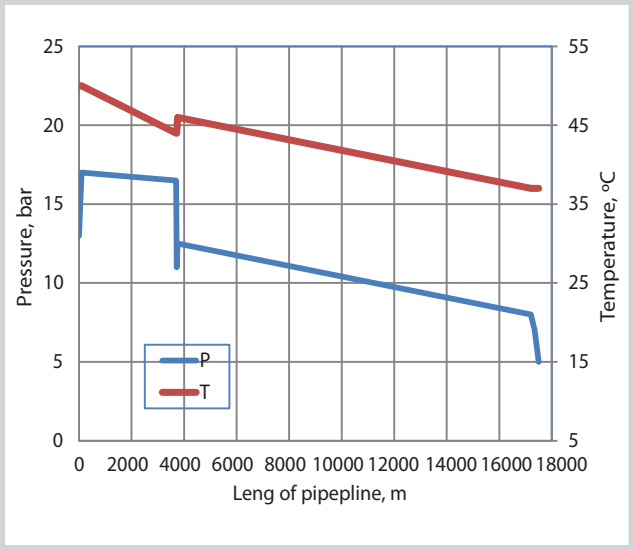
The results of hydraulic calculations for oil and gas transportation from Nam Rong to RP-1 through the subsea pipeline with a diameter of 325 x 16mm, plus composite insulation of 35mm with a head transfer coefficient of 0.1w/(m*K) showed that:

- In the case of maximum liquid flow rate, the drop in pressure for transportation from RC-DM to RP-1 is about 9bars (oil pressure on the RC-DM will be 14bars and on RP-1 5bars). If the temperature on RC-DM is ~50°C, the temperature of oil arriving at RP-1 is expected to be about 36°C.

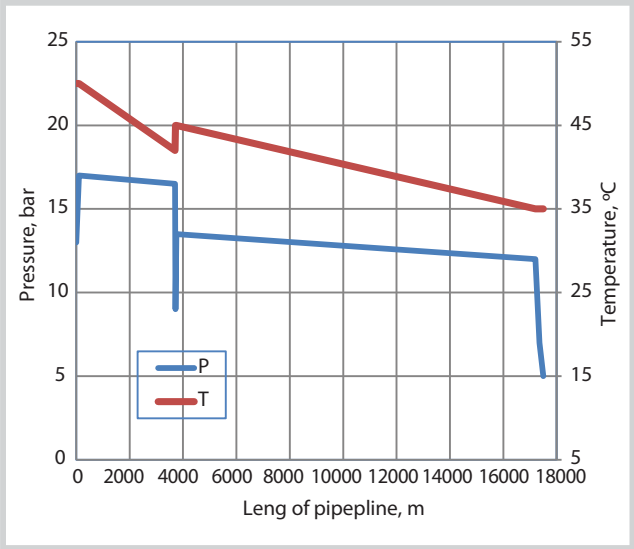
- In the case of maximum water content, the pressure drop for fluid transportation from RC-DM to RP-1 is expected to be about 7bars (oil pressure on RC-DM is 12bars and on RP-1 is 5bars). The temperature on RC-DM is expected to be about 50°C and the oil coming to RP-1 is expected to have a temperature of about 34°C.

Therefore, if the wellhead pressure is about 20bars and the pressure drop for liquid transportation through the pipeline is 9bars, the diameter of the oil transportation pipeline is calculated to be 325 x 16mm. Figure 6 presents the profiles of the pressure and temperature along the length of pipeline RC-DM → RP-1 with a diameter of 325 x 16mm. This line will be used to transport crude oil fluids from Nam Rong and Doi Moi oil fields to RP-1.

During the first year of production from Nam Rong and Doi Moi oil fields, production was be low and expected to be ~930$m^3$/day. In this scenario, oil production from Doi Moi oil field will be 570$m^3$/day. Transportation of crude oil from Doi Moi and Nam Rong oil fields through the subsea pipeline will have a low flow rate and be expected




*In case of maximum liquid flow in the pipeline*




*In case of maximum water content in production*

***Figure 6.*** *The profiles of pressure and temperature in pipeline RC-DM → RC-4 → RP-1*

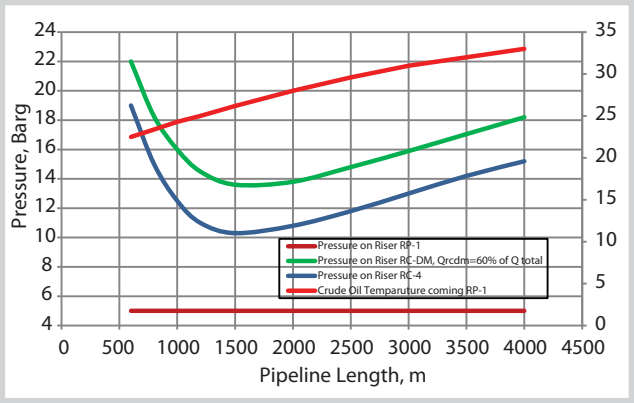



***Figure 7.*** *The effect of pressure and temperature on the flow rate of pipeline liquids coming from RP-1*

to experience problems of wax deposition on the walls of pipeline. The problem will be worse in offshore conditions with a minimum seabed temperature of ~21°C.

To predict the transportation problems of oil and gas from RC-DM to RP-1 via subsea pipeline (diameter of 325 x 16mm and length of 17km), hydraulic calculations for determining the influence between pressure drop and liquid flow rate in the pipeline from RC-DM → RC-4 → RP-1 were carried out.

Figure 7 demonstrates the influence of pressure and temperature on oil coming from RC-DM, RC-4 and oil coming from RP-1 on the liquid flow rate through the pipeline RC-DM → RP-1. The liquid flow rate of Doi Moi crude oil will be about 60% of the total flow rate through the pipeline from RC-4 → RP-1. Hydraulic pressure calculation results showed that if the oil pressure on RP-1 is 5bars and the local pressure drop in the pipeline on RC is about 2bars, then it should be safe to transport crude oil from Doi Moi and Nam Rong fields to RP-1. However, the flow rate through the pipeline from RC-DM → RC-4 → RP-1 should not be lower than 1,500m³/day. In another scenario, the oil temperature in the pipeline during transportation is taken to be lower than the wax appearance temperature (WAT). In this case, the transportation of crude oil from Nam Rong and Doi Moi oil field to RP-1 will pose serious problems of wax deposition on the walls of the pipeline.

To solve the problems highlighted above, the pipeline system will require either a pigging or a hot water pump system on RC-DM to remove wax from the pipe walls.

The hydraulic calculation results shown in Figure 7 highlighted that:

- In the case of a flow rate through the pipeline of 1,500m³/day, the oil pressure in the riser block of RC-DM will be at a minimum and oil coming from RP-1 will be at a temperature of 26 - 27°C;

- In the case of a flow rate higher than 1,500m³/day, the operating pressure on RC-DM will be increased and the oil temperature coming to RP-1 will also be increased to more than 26 - 27°C. In this case, oil and gas transportation through pipeline from RC-DM → RP-1 will be improved;

- In the case of a liquid flow rate less than 1,500m³/day, the oil pressure on RC-DM will be increased and expected to be 18bars when the liquid flow rate is about 800m³/day, the oil temperature coming to RP-1 will be

24°C. In this scenario, the problem of wax deposition in the pipeline will be more serious;

- In the case of a flow rate less than 800m$^3$/day, the oil pressure in the riser block of RC-DM will be higher than 18 - 20bars and it will not allow the transportation of oil and gas from RC-DM to RP-1 using subsea pipeline with a diameter of 325 x 16mm, because maximum wellhead pressure is only 20bars.

**4. Conclusions**

Newly discovered marginal oil fields, such as Nam Rong and Doi Moi oil fields, can be connected to the nearest operating platform (e.g. Rong oil field) for oil processing on the fixed platform RP-1 and then for continuous transport to an FSO for processing;

To safely transport crude oil from Nam Rong and Doi Moi oil fields to RP-1 platform in Rong oil field, the liquid flow rate through the pipeline (diameter 325 x 16mm) should not be less than 1,500m$^3$/day;

The minimum flow rate through the pipeline RC-DM → RC-4 → RP-1 for crude oil transportation from RC-DM to RP-1 could be higher than 800m$^3$/day. In this case, there will be a serious problem with wax deposits on the wall of the pipeline and the oil pressure in the riser block of RC-DM will increase up to ~20bars. To remove the wax deposits from the pipeline, it will be necessary to add sea water to the pipeline to increase the flow rate in the pipeline, which should not be less than 1m/s [3, 4].

**References**

1. Phung Dinh Thuc, Ha Van Bich, Tong Canh Son, V.P.Vygovskoy, Le Dinh Hoe. *A new approach to study on thixotropic properties of waxy crude oil from Dragon and White Tiger fields offshore Vietnam*. SPE Asia Pacific Oil and Gas Conference and Exhibition, Jakarta, Indonesia, 20 - 22 April, 1999.

2. Phung Dinh Thuc, Ha Van Bich, Tong Canh Son, Le Dinh Hoe, V.P.Vygovskoy. *The problem in transportation of high waxy crude oils through submarine pipelines at JV Vietsovpetro oil fields, offshore Vietnam*. Journal of Canadian Petroleum Technology. 2003; 42(6): p. 15 - 18.

3. Nguyen Thuc Khang, Ha Van Bich, Tong Canh Son, Le Dinh Hoe. *Transporting oil and gas mixture in gathering system at White Tiger oil field*. SPE Asia Pacific Oil and Gas Conference and Exhibition, Jakarta, Indonesia. 9 - 11 September, 2003.

4. Nguyen Thuc Khang, Ha Van Bich, Tong Canh Son, Le Dinh Hoe, Phung Dinh Thuc. *A new approach for regime optimization of oil and gas mixture pipeline transportation*. SPE Asia Pacific Oil and Gas Conference and Exhibition, Perth, Australia. 18 - 20 October, 2004.

# INDUSTRIAL SCALE EXPERIENCE ON STEAM REFORMING OF $CO_2$-RICH GAS

Peter Mølgaard Mortensen, Ib Dybkjær, Gabriel Antberg
*Haldor Topsøe A/S, Denmark*
*Email: PMOR@topsøe.dk*

**Summary**

*This paper summarises experiences on industrial scale reforming of $CO_2$-rich natural gas. Methane can react in a direct route with $CO_2$ to form a synthesis gas consisting of CO and $H_2$, so called dry reforming (DMR). This reaction is closely related to steam methane reforming (SMR). DMR has received much attention as it in theory offers a way of using $CO_2$, which is considered in many industries as a waste product and environmentally as a polluting greenhouse gas. In an industrial scale with realistic feedstock, water cannot be completely omitted from the reaction, as this specifically will be needed for removal of higher hydrocarbons. Instead, high severity $CO_2$-reforming can be done, which have been proven in several industrial plants. Sulfur passivated reforming (SPARG) has demonstrated that $CO_2$-reforming can be achieved without use of expensive noble metals. In addition to thermodynamic consideration, mass balance constrains must be considered. Mass balance dictates that high severity $CO_2$-rich gas will result in a synthesis gas with low $H_2$/CO ratio. Thus, the commercial feasibility of $CO_2$-reforming is highly dependent on the desired product. $CO_2$ reforming may be an attractive solution for product requiring lower $H_2$/CO ratio, such as higher alcohols, reducing gas, and acetic acid, etc.*

***Key words:*** *$CO_2$-reforming, Dry reforming, DMR, SPARG, Methanol synthesis.*

## 1. Introduction

The last 40 years have seen significant developments in the petrochemical industry. In 1975, the world was facing an oil crisis when the cost of a barrel exceeded the record price of USD 13. This resulted in the search for many alternative technologies to most efficiently utilise energy and rapidly expanded searches for new energy sources. It was also the time that Petrovietnam was founded and for Haldor Topsøe a time of new technologies including further development of its reforming technology and the start of its formaldehyde technology.

Fast forward 40 years and today we think that oil is cheap at less than USD 50/barrel. We also have a wide array of new technologies available which are optimised for various applications. Today, Petrovietnam is reviewing utilisation of a $CO_2$-rich natural gas and the solution to such utilisation is part of the developments in reforming technology which was initiated 40 years ago.

The utilisation of $CO_2$-rich gas requires extra considerations compared to traditional high methane containing natural gas feed. The primary challenge in reforming $CO_2$-rich gas is carbon formation, as the low H/C ratio of the feed implies that a high potential for carbon formation exists.

Synthesis gas production is one of the largest industries in the world with its development stemming back from 1930 [1]. Important bulk chemicals such as hydrogen, ammonia, and methanol are produced on the basis of this. Among the reforming reactions, steam reforming of methane-rich natural gas (SMR) must be considered as the principal reaction for production of synthesis gas and hydrogen. Steam reforming of $CO_2$-rich gas (in the following referred to as "$CO_2$-reforming") or reforming of methane-rich feedstock with carbon dioxide alone ("dry methane reforming", in the following referred to as DMR) are receiving much attention as they in theory offer ways of using $CO_2$, which is considered in many industries as a waste product and environmentally as a polluting greenhouse gas.

One of the primary tasks in the development of $CO_2$-reforming or DMR is to find operating conditions in combination with a suitable catalyst to avoid carbon formation. Nickel (Ni), cobalt, and noble metal catalysts have been tested as catalyst for $CO_2$-reforming, with nickel being the most investigated system, as this is the conventional choice in SMR and a relatively cheap catalyst in comparison to noble metals [2].

Haldor Topsøe A/S has many years of experience in reforming. The first start-up of a steam reformer designed by Haldor Topsøe dates back to 1956. In the current work, our experience within the field of $CO_2$-reforming and DMR is summarised, starting with a short review on the science behind the $CO_2$-reforming process in industrial scale.

## 2. Thermodynamic considerations

Traditional SMR is the endothermic reaction between steam and methane at elevated temperatures to produce synthesis gas:

$$CH_4\,(g) + H_2O\,(g) \leftrightarrows CO\,(g) + 3H_2\,(g) \quad (1)$$

DMR takes place in a similar way, but with $CO_2$:

$$CH_4\,(g) + CO_2\,(g) \leftrightarrows 2CO\,(g) + 2H_2\,(g) \quad (2)$$

The stoichiometric DMR reaction yields a synthesis gas with a $H_2$/CO ratio of 1, compared to 3 for SMR.

Besides the reforming reactions, also water gas shift (WGS) takes place during reforming; specifically reverse water gas shift (RWGS) is relevant for DMR:

$$CO_2\,(g) + H_2\,(g) \leftrightarrows CO\,(g) + H_2O\,(g) \quad (3)$$

The reforming reactions and the RWGS are all endothermic reactions, and temperatures in the order of 750°C are required for an effective conversion of methane and carbon dioxide [3 - 4].

Besides the endothermic reforming reactions, the choice of operating conditions is additionally influenced by the Boudouard reaction (also called CO disproportionation), the CO reduction reaction, and the methane decomposition reaction:

$$2CO\,(g) \leftrightarrows C\,(s) + CO_2\,(g) \quad (4)$$

$$CO\,(g) + H_2\,(g) \leftrightarrows C\,(s) + H_2O\,(g) \quad (5)$$

$$CH_4\,(g) \leftrightarrows C\,(s) + 2H_2\,(g) \quad (6)$$

As these may be responsible for carbon formation during the reaction, it should be emphasised that carbon formation is a non-linear phenomenon and prediction of the risk for carbon formation will require a thermodynamic evaluation for a given feed composition.

### 3. Carbon deposition

The low H/C ratio in DMR makes carbon formation a major challenge [5]. For practical application of the reforming reactions, it is a mandatory to ensure that carbon formation does not take place [6]. The methane decomposition reaction (6) and the Boudouard reaction (4) are the primary sources of carbon on the catalysts during DMR and these reactions can to some extent be predicted on the basis of thermodynamic calculations.

Noble metals are more resistant toward carbon formation than nickel, and have a low tendency for formation of whisker carbon [7]. The potential for carbon formation is significantly decreased by lowering the nickel particle size. Even lower potential for carbon formation was achieved by Rostrup Nielsen and Bak Hansen [8] by passivating the nickel catalysts with sulfur giving an equilibrium constant for methane decomposition comparable to Ru and Rh catalysts. Overall, it is apparent that the potential for carbon formation is dictated by thermodynamics, but it can be markedly influenced by the choice of active material on the catalyst and the particle size of this, as this determines the stability of the formed carbon. Besides carbon formation on catalysts, also carbon formation on/in metal surfaces (as the reactor wall and equipment downstream the primary reformer) can be a problem during reforming, a phenomenon known as metal dusting. This causes disintegration of metal alloys of Fe, Ni, and Co, observed as loss of surface material as a metal dust due to carbon formation in the metal [9]. This is usually a problem on reactor walls of plants operating with aggressive carbonaceous gases with high CO partial pressure and low water partial pressure. CO and $CH_4$ are usually reported as the source of metal dusting by reactions (4) and (6) [9 - 11].

### 4. Industrial experience with large scale reforming of $CO_2$-rich gas

A typical layout for an industrial scale reforming plant is illustrated in Figure 1. The feedstock, which may range from lean natural gas to heavy naphtha, is heated to around 400°C and then cleaned for sulfur species in a desulfurisation section [12]. Subsequently, any higher hydrocarbons in the feedstock are reformed to a mixture of $H_2$, $CO_2$, $CH_4$, and traces of CO in a pre-reformer. This is done at relatively low temperatures of 400 - 550°C to avoid carbon formation from the higher hydrocarbons [13]. The actual reforming takes place in a tubular reformer (primary reformer) for the conversion of the $CH_4/H_2O/CO_2$ mixture to synthesis gas. In this configuration, many tubes are placed in a row (or parallel rows) in a furnace box where heat is delivered to the endothermic reaction by combustion of fuel. Typically, the inlet temperature is adjusted to 400 - 600°C prior to the primary reformer and then heated to an exit temperature up to 950°C in the reformer tubes. The high exit temperature is required for sufficient conversion of the methane when the process gas flows through the reformer tubes in plug flow it will be close to equilibrium. Thus, carbon formation can be expected if the principle of equilibrated gas predicts carbon formation at any temperature between 400 - 1,000°C for a given feed gas composition.

It is essential to design a reforming plant to completely avoid carbon formation. If a potential for carbon formation exists, it will only be a matter of time before a shutdown will be forced due to too high pressure drop. In industrial context this will be expensive due to lost time on stream and loading of a new batch of catalyst. It is emphasised that carbon formation at reforming conditions is as whisker carbon. This is destructive in nature toward the catalyst pellet and regeneration is therefore not an option.

Thus, the possible operating range for a tubular reformer will be defined by the conditions which will not have a potential for carbon formation. When sufficient knowledge about the thermodynamics of carbon formation for a specific catalyst is known, the exact limit for carbon formation can be calculated and this can be illustrated by the carbon limit curve depicted in Figure 2 [14 - 15]. The curves are derived from the principle of equilibrated gas and show the most severe conditions (as a function of initial $H_2O/CH_4$ and $CO_2/CH_4$ ratio or O/C and H/C ratio) which can be tolerated in the entire temperature range from 400 - 1,000°C at a pressure of 25.5bar. Carbon formation will be expected on the left of the curves and "safe" operation on the right. This shows that the tendency for carbon formation increases with decreasing $CO_2/CH_4$ and $H_2O/CH_4$ ratios. The severity of operation can be defined relative to the placement compared to the carbon limit curves; operation far beyond the carbon limit curve is considered very severe.

The limit for carbon formation can be pushed by the choice of catalyst. Thus, more severe conditions can be tolerated with a Ni catalyst compared to formation of graphitic carbon (Figure 2). However, performing "traditional" DMR, without $H_2O$ in the feed, over a Ni catalyst in a tubular reformer, will result in carbon formation as this is placed far beyond the carbon limit curve for Ni catalysts in Figure 2. Instead, $CO_2$-reforming is possible as long as the $H_2O/CH_4$ ratio is balanced accordingly.

The cases in Table 1 cover operation at full scale plants (referred to on the basis of the nations where the plants were constructed) and tests in a pilot plant placed in Houston, Texas, United States (referred to as HOU). The industrial references in Table 1 are all examples of plants which have been designed around the principle flow sheet in Figure 1, but adapted to the specific needs of the site and the downstream requirements for the synthesis gas utilisation. The sizes of these plants range from production of 2,400$Nm^3$/hour up to 133,000$Nm^3$/hour of dry synthesis gas. A differentiation is made between plants operated with a natural gas feed (natural gas in Table 1) or a naphtha feed. Natural gas is considered as a gaseous feed consisting mainly of methane, but can also contain $CO_2$, higher hydrocarbon ($C_2$ - $C_6$), among other gas species. Naphtha is a heavier liquid feedstock which will consist mainly of $C_6$ to $C_{12}$ hydrocarbons. For naphtha based plants the pre-reforming section is an important and integrated part of the plant as the very reactive higher hydrocarbons should be converted prior to the primary reformer to avoid carbon formation from these. Several of the plants addition-

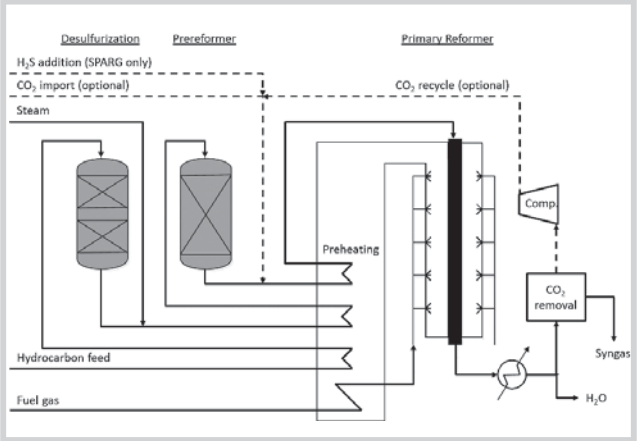



***Figure 1.*** *General flow sheet of a reforming process. Dotted lines indicate optional configurations. $CO_2$ can be added to adjust the feed gas composition or recycle from the $CO_2$ removal unit. $H_2S$ import is only used for the SPARG process*

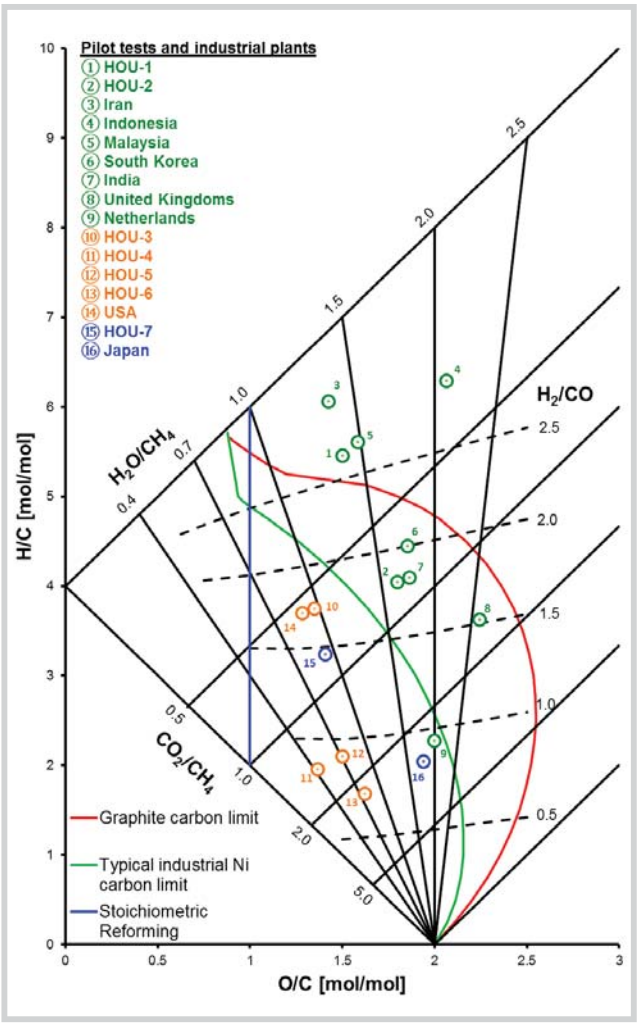



***Figure 2.*** *Carbon limit diagram at different $H_2O/CH_4$ and $CO_2/CH_4$ feed ratios. The curves are the carbon limits at 25.5bar for graphite and a typical industrial Ni catalyst. The left-hand sides of the curves are the areas where carbon formation is expected for temperatures between 400°C and 1,000°C. The product $H_2/CO$ ratio is evaluated at TExit = 950°C. The stoichiometric reforming region is shown for reference. The points refer to specific large scale tests with Ni catalysts (green), SPARG (orange), and noble metal catalysts (blue), further information on these is found in Table 1*

***Table 1.*** *Comparison of full size monotube pilot experiments (HOU) and industrial plants (referenced with countries where they are constructed) of $CO_2$ rich reforming with different catalysts and under different conditions. SPARG: Sulfur-passivated reforming, NG: Natural gas, TOS: Time on stream*

| | | Operating conditions | | | |
|---|---|---|---|---|---|
| | | Catalyst | Feed | P (barg) | $T_{Exit}$ (°C) |
| Ni catalyst | HOU-1 | $Ni/MgAl_2O_4$ | Natural gas | 23 | 945 |
| | HOU-2 | $Ni/MgAl_2O_4$ | Natural gas | 24 | 945 |
| | Iran | $Ni/MgAl_2O_4$ | Natural gas | 20 | 960 |
| | Indonesia | $Ni/MgAl_2O_4$ | Natural gas | 12 | 960 |
| | Malaysia | $Ni/MgAl_2O_4$ | Natural gas | 25 | 950 |
| | South Korea | $Ni/MgAl_2O_4$ | Naphtha | 25 | 900 |
| | India | $Ni/MgAl_2O_4$ | Naphtha | 22 | 920 |
| | United Kingdom | $Ni/MgAl_2O_4$ | Naphtha | 20 | 900 |
| | Netherlands | $Ni/MgAl_2O_4$ | Natural gas | 15 | 815 |
| Sulfur-passivated reforming (SPARG) | HOU-3 | $Ni/MgAl_2O_4$ | Natural gas | 6 | 890 |
| | HOU-4 | $Ni/MgAl_2O_4$ | Natural gas | 6 | 930 |
| | HOU-5 | $Ni/MgAl_2O_4$ | Natural gas | 14 | 930 |
| | HOU-6 | $Ni/MgAl_2O_4$ | Natural gas | 15 | 945 |
| | USA | $Ni/MgAl_2O_4$ | Natural gas | 7 | 900 |
| Noble catalyst | HOU-7 | $Ru/MgAl_2O_4$ | Natural gas | 23 | 940 |
| | Japan | $Ru/MgAl_2O_4$ | Natural gas | 2 | 850 |

ally operated with a $CO_2$ import or recycle stream to give a high $CO_2/CH_4$ ratio in the feed gas to the primary reformer.

### *4.1. Ni catalysts for $CO_2$-reforming*

As already discussed, Ni based catalysts are industrially preferred. Table 1 lists several examples of how Ni based catalysts have been used for $CO_2$-reforming. A few references were made at the full size monotube reforming reactor in Houston in the beginning of the 1990s (tests denoted HOU1-2), but several full scale plants have been designed and constructed relative to the principle of equilibrated gas and the carbon limit curve shown in Figure 2. Common for all of these references is that they were operated over long periods (several years) without problems with carbon formation. As long as the plant is operated as intended and not poisoned by external sources, lifetimes of more than a decade can be obtained for industrial reforming catalysts [16]. Large fractions of $CO_2$ in the feed were demonstrated in the Houston pilot plant demonstration run 2 and the plants in India, South Korea, and the United Kingdom. However, as seen from both Figure 2 and Table 1, significant amounts of water were needed in the feed to comply with the limitations of the carbon limit curve and additionally to adjust the composition so the synthesis gas is produced with the desired $H_2/CO$ ratio. The plant in the Netherlands was operated under very severe conditions for a Ni based catalyst with 71 dry mole % of $CO_2$ in the feed, producing a synthesis gas with a $H_2/CO$ ratio of 1.2. As seen from Figure 2, this plant was operated slightly beyond the conventional border for carbon formation for Ni catalysts. After two years of operation at these conditions, analysis of the spent catalyst revealed insignificant carbon formation, varying between 500 - 1,100$ppm_w$ along the length of the reactor tube. Analysis of the spent catalyst showed that operation under the quite severe conditions was only possible because the Ni particles were stabilised at a significantly lower particle size than what is usually seen during steam reforming at industrial conditions, which was helped by the relatively low exit temperature of 815°C used for the current plant. However, it should still be noted that a $H_2O/CH_4$ ratio of 2 was used at the given operating conditions. Operation at the same conditions with a Ni catalyst with larger Ni particles later proved to cause carbon formation, supporting the fundamentals on carbon formation. All the examples presented for Ni based $CO_2$-reforming show how important it is to know where the limit for carbon formation is, as this confines the freedom for designing reforming processes.

### *4.2. SPARG process*

In the SPARG (Sulfur passivated reforming) process, sulfur is used to selectively poison the most active sites and in this way prevent formation of carbon while maintaining some activity for reforming. Rostrup-Nielsen [17] described that coke formation requires a larger ensemble of Ni atoms compared to SMR and that one sulfur atom quenches the four neighbouring Ni atoms. Thus, sulfur will more effectively inhibit carbon formation than SMR/DMR activity. Ideally, the sulfur coverage should be larger than 0.7 to prevent carbon formation [17]. On the basis of the observations of the beneficial effect of sulfur passivation, the SPARG process was developed. Here, a small co-feed of $H_2S$ was added to prevent carbon formation on Ni-based catalysts. This should be accompanied by a small co-feed of hydrogen ($H_2S/H_2 < 0.9$) to avoid formation of bulk Ni sulfides. The SPARG approach offers a route to circumvent the carbon limit curve in Figure 2. The first large scale test of this concept was made in the full size monotube pilot plant in Houston at a $CO_2$/Natural gas feed ratio of 0.65 and $H_2O$/Natural gas ratio of 1.0, and an outlet temperature of 890°C. These conditions would result in carbon formation on a conventional Ni catalystas illustrated by point 10 (HOU-3) in Figure 2. However, with the sulfur-passivated Ni catalyst no carbon was observed after 500 hours of operation at the conditions. Building on the success of HOU-3, "dry" DMR tests were

made in the pilot plant with the sulfur-passivated Ni catalyst, a $CO_2$/Natural gas feed ratio of 2.5, and 890°C as outlet temperature. However, at these conditions, carbon deposition was observed in the first part of the reactor tube after a short period of operation. This was concluded to be due to cracking of the larger hydrocarbons in the natural gas on the sulfur passivated catalyst, which now had insufficient activity for higher hydrocarbon reforming. To avoid the severe carbon deposition observed from higher hydrocarbons, it was realised that a pre-reformer was essential prior to the tubular reformer to remove the higher hydrocarbons in the natural gas. On the basis of this experience, a general flow-sheet for $CO_2$-reforming using the SPARG technology should therefore be as illustrated in Figure 1. Initially, sulfur is removed from the natural gas to enable pre-reforming of the higher hydrocarbons over a Ni based catalyst, which is intolerant to sulfur. A controlled amount of $H_2S$ is then added to the gas mixture of $H_2O/CO_2/CH_4$ prior to the primary reformer.

The SPARG technology was demonstrated in industrial scale by revamping the reforming plant in the United States (Figure 2 and Table 1) from SMR to $CO_2$-reforming. Originally, the plant operated at a S/C of 1.9 and a $CO_2$/C of 0.4 with an exit temperature of 900°C, but to increase the production of CO the plant was modified with the SPARG technology to operate at a S/C of 0.9 and a $CO_2$/C of 0.5 instead. Table 2 shows a comparison between the synthesis gas composition out of the primary reformer of the plant prior to the revamp and at SPARG conditions. A significant increase in the CO concentration was achieved by implementing the SPARG conditions. The only major difference between the original operation and the SPARG operation was that a pre-reformer had to be installed to remove the higher hydrocarbons prior to the primary reformer, as also observed in the pilot experiments. The primary reformer and the surrounding equipment could all be used directly for the SPARG process.

***Table 2.*** *Comparison of the synthesis gas composition from the plant in USA pre-SPARG and during SPARG*

| | Pre-SPARG | SPARG |
|---|---|---|
| $H_2$ (dry mole%) | 65 | 60 |
| CO (dry mole%) | 24 | 33 |
| $CO_2$ (dry mole%) | 8 | 5 |
| $CH_4$ (dry mole%) | 3 | 3 |
| $N_2$ (dry mole%) | 0.1 | 0.1 |
| $H_2$/CO | 2.7 | 1.8 |

Carbon free-operation was demonstrated throughout four years of continuous operation on one batch of catalyst on the SPARG conditions. The revamp of the plant from SMR to SPARG was calculated to give 23% savings in production costs at that time [18].

### *4.3. Noble metal catalysts for $CO_2$-reforming*

As already discussed in Section 0, noble metals generally have a lower tendency for carbon formation compared to Ni catalysts. This group of catalysts therefore offers a route for operation at severe conditions without carbon formation. This was demonstrated in large scale with the HOU-7 pilot test where a ruthenium catalyst was used to operate at a $H_2O/CH_4$ of 0.9 and a $CO_2/CH_4$ of 0.8. These conditions are far beyond the carbon limit curve of the Ni catalyst, as shown in Figure 2. The experience from HOU-7 was used to demonstrate the durability of the catalyst prior to installation in a convection reformer in Japan. The plant should produce CO from a mixture of natural gas, a $CO_2$ import stream, and a recycle stream, which ultimately meant that high amounts of $CO_2$ should be processed. Use of the noble metal catalyst enabled operation at quite severe conditions while maintaining a syngas $H_2$/CO product ratio of 1. This plant operated for several years without any catalytic problems.

## 5. Mass balance constraints

DMR and SMR result in synthesis gases with different stoichiometric composition; DMR a $H_2$/CO ratio of 1, compared to 3 for SMR. The suitability of the synthesis gas depends on the downstream utilisation. For instance, methanol synthesis requires a gas module, $M = (H_2 - CO_2)/(CO + CO_2)$ of 2 for optimal performance in order to avoid excess $H_2$, CO or $CO_2$. Reaction (7) visualizes the stoichiometric ideal reaction for syngas production for methanol synthesis.

$$3CH_4\,(g) + CO_2 + 2H_2O\,(g) \leftrightarrows 4CO\,(g) + 8H_2\,(g) \quad (M = 2) \qquad (7)$$

Reaction (7) is a net result of reactions (1 - 3) and can closest be categorised as being SMR with addition of $CO_2$ to achieve an ideal syngas module, M, for methanol production. Higher concentration of $CO_2$ than suggested in reaction (7), hence $M < 2$, will cause a shortage of $H_2$ in the methanol synthesis and excess $CO_2$ which will cause costly operation of the methanol synthesis. This means that an ideal feed gas for methanol production contains 1 $CO_2$ for each 3 $CH_4$ available (on mole basis) in the feed gas.

$CO_2$ reforming may be an attractive solution for product requiring lower $H_2$/CO ratio, such as higher alcohols, reducing gas, and acetic acid, etc.

## 6. Conclusions

The DMR reaction is closely related to the SMR reaction.

Despite having origin in different reactants, the fast equilibration of the WGS results in similar reaction conditions in the two processes at an early stage in a reactor. Carbon deposition must be considered as the biggest challenge of DMR, as the stoichiometric DMR reaction implies severe conditions for carbon formation. This phenomenon is to a large extent controlled by thermodynamics and the principle of equilibrated gas is an important method to determine suitable operating conditions. Water cannot be completely omitted from the reaction, as this specifically will be needed for removal of higher hydrocarbons. Thus, "dry" DMR is difficult to realise in large scale with realistic feedstocks, but high severity $CO_2$-reforming can be done. Pushing the potential for carbon formation can be aided by approaches such as the SPARG process. Several $CO_2$-reforming plants have been designed using Ni based catalysts, SPARG or noble metals, where the latter two allow for more severe operating conditions. In addition to thermodynamic consideration, mass balance constrains must be considered. DMR produces a synthesis gas with a $H_2$/CO ratio of 1 and SMR a $H_2$/CO ratio of 3. To what extent $CO_2$ reforming is attractive depends on the downstream utilization of the synthesis gas. For instance, methanol requires a gas module, $M = (H_2 - CO_2)/(CO + CO_2)$ of 2. The net reaction to produce such synthesis gas can closest be categorised as being SMR with addition of $CO_2$. The net reaction also reveals that the ideal feed gas for synthesis production to methanol should contain 1 $CO_2$ for each 3 $CH_4$ available (on mole basis). $CO_2$ reforming may be an attractive solution for product requiring lower $H_2$/CO ratio, such as higher alcohols, reducing gas, and acetic acid, etc.

**References**


1. J.R.Rostrup-Nielsen. *Steam reforming of hydrocarbons: A historical perspective*. Studies in Surface Science and Catalysis. 2004; 147: p. 121 - 126.

2. J.R.Rostrup-Nielsen, L.J.Christiansen. *Routes to syngas*. Concepts in Syngas Manufacture. Imperial College Press. 2011; 10: p. 3 - 72.

3. Mun-sing Fan, Ahmad Zuhairi Abdullah, Subhash Bhatia. *Catalytic technology for carbon dioxide reforming of methane to synthesis gas*. ChemCatChem. 2009; 1(2): p. 192 - 208.

4. M.K.Nikoo, N.A.S.Amin. *Thermodynamic analysis of carbon dioxide reforming of methane in view of solid carbon formation*. Fuel Processing Technology. 2011; 92(3): p. 678 - 691.

5. C.Papadopoulou, H.Matralis, X.Verykios. *Utilization of biogas as a renewable carbon source: Dry reforming of methane*. Catalysis for Alternative Energy Generation. Springer. 2012: p. 57 - 127.

6. Jens Rostrup-Nielsen, Lars J.Christiansen. *Concepts in syngas manufacture*. Catalytic Science Series. Imperial College Press. 2011; 10: p. 233 - 294.

7. S.E.L.W.Madsen, J.H.Bak Hansen, J.R.Rostrup-Nielsen. *Industrial aspects of $CO_2$-reforming*. AIChE Spring Meeting. 1997.

8. J.R.Rostrup-Nielsen, J.H.B.Hansen. *$CO_2$-reforming of methane over transition metals*. Journal of Catalysis.1993; 144(1): p. 38 - 49.

9. A.Agüero, M.Gutiérrez, L.Korcakova, T.T.M.Nguyen, B.Hinnemann, S.Saadi. Oxidation of Metals. 2011: p. 1 - 20.

10. H.J.Grabke. *Metal dusting*. Material and Corrosion. 2003; 54(10): p. 736 - 746.

11. P.V.Daham S.Gunawardana, Thoa Thi Minh Nguyen, John C.Walmsley, Hide J.Venvik. *Initiation of metal dusting corrosion in conversion of natural gas to syngas studied under industrially relevant conditions*. Industrial and Engineering Chemistry Research. 2014; 53(5): p. 1794 - 1803.

12. K.Aasberg-Petersen, T.S.Christensen, I.Dybkjær, J.Sehested, M.Østberg, R.M.Coertzen, M.J.Keyser, A.P.Steynberg. *Synthesis gas production for FT synthesis*. Fischer-Tropsch Technology. Amsterdam: Elsevier. 2004; 4: p. 258 - 405.

13. T.S.Christensen. *Adiabatic prereforming of hydrocarbons - an important step in syngas production*. Applied Catalysis A: General. 1996; 138(2): p. 285 - 309.

14. H.C.Dibbern, P.Olesen, J.R.Rostrup-Nielsen, P.B.Tøttrup, N.R.Udengaard. *Make low $H_2$/CO syngas using sulfur passivated reforming*. Hydrocarbon Processing. 1986; 65(1): p. 71 - 74.

15. J.R. Rostrup-Nielsen. *40 years in catalysis*. Catalysis Today. 2006; 111(1-2): p. 4 - 11.

16. L.Storgaard, H.C.Nielsen. *Catalysts for cost effective hydrogen production*. Digital Refining. 1999: p. 1 - 8.

17. J.R.Rostrup-Nielsen. *Sulfur-passivated nickel catalysts for carbon-free steam reforming of methane*. Journal of Catalysis. 1984; 85(1): p. 31 - 43.

18. N.R.Udengaard, J.H.B.Hansen, D.C.Hanson, J.A.Stal, *Sulfur passivated reforming process lowers syngas $H_2$/CO ratio*. Oil and Gas Journal. 1992; 90(10): p. 62 - 67 .

# WSA TECHNOLOGY TURNS YOUR OFF-GAS INTO MONEY

Amrul Atiqi
*Haldor Topsøe A/S*
*Email: aasa@topsoe.dk*

**Summary**

*When oil and gas is being processed the generated $H_2S$ needs to be removed and converted, due to environmental legislation. Traditionally, acid gas is converted in a Claus plant forming elemental sulfur; however this is an inefficient approach both out of an economic and operational context.*

*Today the most optimal solution for treating acid gases from Acid Gas Removal Units (AGRUs) is with the innovative WSA (Wet gas sulfuric acid) technology that converts acid gases into sulfuric acid.*

*The WSA technology is a superior solution for treatment and conversion of acid gases, and this paper will describe both the potential economic benefits and the unique process principles of the technology.*

***Key words:*** *$H_2S$, $SO_2$, WSA , Claus, emission, refineries, gas processing, sulfur, off-gas, steam, sulfuric acid, environmental, flue gas, acid gas, desulfurisation, sour gas, SOx, NOx.*

## 1. Introduction

The reason why the WSA process today is the most optimal technology for converting acid gases is due to the following facts:

- A Topsøe WSA plant has lower investment costs than a plant producing elemental sulfur with the same emission requirements.
- A Topsøe WSA plant can meet the most stringent environmental regulations, even without tail gas treatment. Neither chemicals nor other additives are consumed in the process, and there will not be any solid or liquid effluents requiring additional treatment.
- A Topsøe WSA plant is much simpler than a plant producing elemental sulfur. This simplicity of the process also makes it easy to operate and thereby contributes to a higher availability and less unintended shutdowns.
- When producing sulfuric acid, a lot more energy is released than when producing elemental sulfur. The steam production is as much as 4 times higher when producing sulfuric acid as compared to producing sulfur. Why not utilise this energy yourself rather than "exporting" it with the sulfur?
- A Topsøe WSA plant requires neither tail gas treatment nor sulfur degassing. Pelletising is not relevant. There is no risk of sulfur dust being spread over the local community. Sulfuric acid just requires a simple carbon steel tank.
- In a Topsøe WSA plant, the first process step is a complete combustion of the feed gas with excess air. Therefore, ammonia and hydrocarbons in the feed gas will not cause problems and a higher feed-flexibility is possible.

The WSA and SNO™ processes are efficient for recovering sulfur from various sulfur containing processes and flue gases originating in the refinery in the form of commercial grade sulfuric acid. Today, more than 130 plants have been licensed worldwide for treatment of process gases in a wide range of process industries and oil refineries.

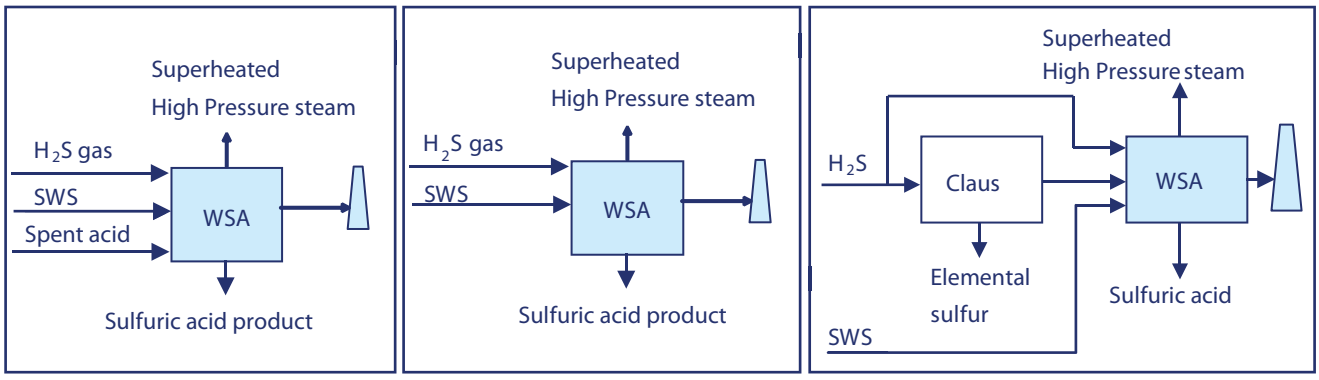
This paper shows various configurations of WSA and SNOX™ handling the following streams in the refinery: $H_2S$ gas, Sour Water Stripper off-gas (SWS gas), Claus plant tail gas, Spent alkylation acid, Flue gas from combustion of sulfurous fuels.

## 2. WSA - Tailored to every need

The WSA plant is engineered based on very individual refinery requirements to maximise energy recovery and to eliminate any waste production. Over the past 30 years we have continuously improved the design so that the current generation of WSA is the best available technology on the market for treatment of sulfur containing streams.

In this section, three possible refinery configurations using WSA technology are presented. It should be mentioned that the most suitable solution for the refinery needs to be evaluated on a case-to-case basis.

The first configuration shows the handling of regeneration of spent sulfuric acid from an alkylation unit,




(a) (b) (c)

***Figure 1.*** *WSA plant treating all acid gases and regenerating spent acid (a); WSA plant treating all acid gases (b); Integrated WSA with Claus (c)*

$H_2S$ and SWS gases in one WSA plant. A block diagram of this configuration is shown in Figure 1a. The second configuration shown in Figure 1b is the same as the first, except no spent acid is being regenerated.

In this layout all sulfur removed from the oil fractions ends up as commercial-grade sulfuric acid. Moreover, in addition to the produced sulfuric acid there will be a large amount of superheated high pressure steam available for export. If this configuration is applied, the refinery can be designed completely without Claus plants, hence no handling of elemental sulfur is needed.

It is also possible to combine the WSA process with a Claus unit. A schematic of this configuration is shown in Figure 1c. A simple Claus plant handles most of the $H_2S$ gas, and the Claus plant tail gas is treated together with SWS gas in a WSA plant, producing sulfuric acid. This layout makes it possible to design the Claus plant much simpler and cheaper as the tail gas treatment will be performed in the WSA unit and no $NH_3$ and hydrocarbons will cause problems in the more sensitive Claus plant. In addition to the above, co-generation of sulfuric acid and elemental sulfur will also add some flexibility to the product pool.

### 3. The WSA process principles

Contrary to conventional sulfuric acid processes, the WSA process treats the process gas with all of its water content. This means that no cooling/condensation prior to the $SO_2$ conversion stage is required. Consequently, there will be no liquid waste

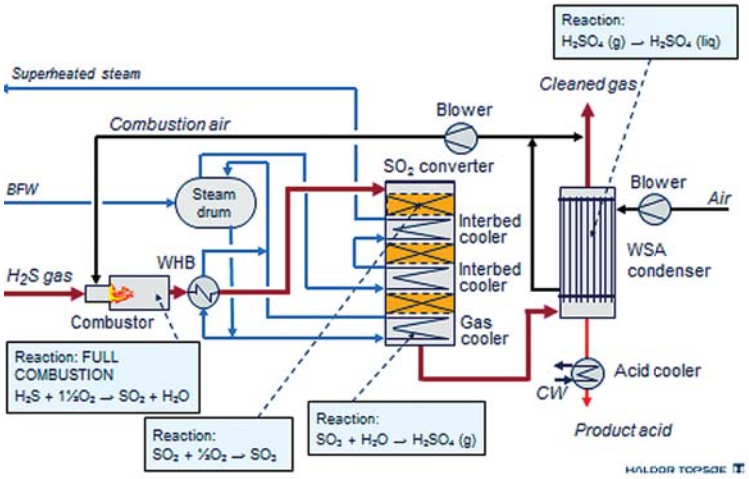



***Figure 2.*** *Flow diagram of a WSA plant treating $H_2S$ gas*

effluent, no loss of acid, no use of cooling water for this part, and no loss of heat.

Because of the initial combustion process, the WSA has the ability to accept any stream from a refinery including streams containing $NH_3$ (sour water stripper gas).

A typical WSA plant treating a $H_2S$ gas is shown in Figure 2. The process comprises the following major steps:

- The first step involves the combustion of the $H_2S$ gas containing stream, typically at around 1,000°C. This thermally oxidises the $H_2S$ to produce $SO_2$.
- The converted $SO_2$ stream exits the combustor and is then cooled to roughly 400°C through a waste heat boiler.
- Upon exiting the waste heat boiler, the $SO_2$ stream enters the $SO_2$ converter which converts the $SO_2$ to $SO_3$. The gas passes through three stages of catalyst to achieve maximum conversion. The process of converting $SO_2$ to $SO_3$ is exothermic and the heat recovered is used to superheat the process steam.
- After the last stage of the $SO_2$ converter, the process gas is cooled to 290°C, and the hydration of $SO_3$ takes place to produce sulfuric acid in vapour phase.

• The gas containing sulfuric acid vapour is then passing to the WSA condenser where it is cooled using atmospheric air and a sulfuric acid liquid of 98% concentration is produced. The acid is subsequently cooled to 40°C and pumped to storage tanks.

• The heated atmospheric air that exits the condenser is then routed to the incinerator to improve the overall energy efficiency. The cleaned process gas exits the condenser and is emitted through the stack.

**4. What makes the WSA technology superior**

The WSA process converts the $H_2S$ into sulfuric acid whereas the conventional Claus process produces elemental sulfur, and when selecting which route to go, a number of parameters must be considered, many of which are not subject to discussion in this paper. However, there are some inherent advantages in the WSA concept when compared with the Claus technology, where the major ones are:

***4.1. Higher energy efficiency***

Going from $H_2S$ to $H_2SO_4$ instead of stopping at elemental S is much more favourable because of thermodynamics. This means that due to the number of exothermic reactions occurring in the WSA process, about four times the amount of steam, of higher quality, is produced when compared to the Claus process.

When converting hydrogen sulfide to elemental sulfur, the sulfur goes from oxidation state -2 to oxidation state 0. This is an exothermal process, yielding approx. 222kJ/mole of hydrogen sulfide processed (equal to 95,500Btu per lbmole).

When converting hydrogen sulfide to sulfuric acid, the sulfur goes in two steps from oxidation state -2 first to oxidation state +4 and finally to oxidation state +6. The reactions involved are also exothermal, but with an almost four times higher enthalpy jump, in total yielding approx. 804kJ/mole of hydrogen sulfide processed (equal to 346,000Btu/lbmole).

This difference in reaction enthalpies between Claus and WSA, illustrated in Figure 3, means that

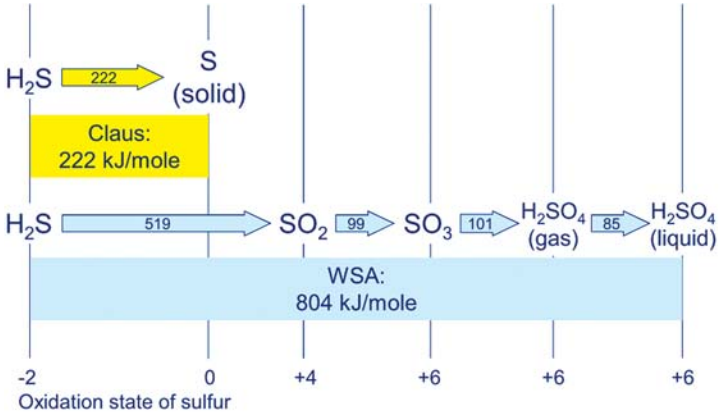



***Figure 3.*** *Enthalpies of sulfur conversion*

a WSA plant exports much more energy than a Claus plant. The export of energy from a WSA plant is in the form of superheated high-pressure steam.

***4.2. Feed flexibility***

In the feed streams to a Claus plant most other compounds than hydrogen sulfides are potential troublemakers. Other combustibles than hydrogen sulfide make it more difficult to hit the desired ratio of usually 2.0 between hydrogen sulfide and sulfur dioxide after the partial combustion. Additionally, ammonia may form polluting NOx, and hydrocarbons may form COS and $CS_2$ that makes it difficult to achieve the desired high sulfur recovery rate or carbon that blocks the Claus catalyst as the content of hydrocarbons fluctuating over the time, making the process more complicated to operate.

The WSA process is sensitive neither to hydrocarbons nor to nitrogen containing compounds such as $NH_3$ in the feed gas, and it is also able to accommodate significant changes in feed gas flow and composition. This is mainly due to the fact that in the WSA process there is complete combustion of the feed gases as initial step, whereas the Claus process has a somewhat more complex combustion which controls the $H_2S$ to $SO_2$ ratio to the optimum 2:1. It should be noted that if significant amounts of nitrogen containing compounds are present in the feed gas, a Selective Catalytic Reduction (SCR) reactor has to be installed in order to reduce NOx formed in combustion.

***4.3. Meeting the environmental regulations***

Treatment of the gas exiting the Claus plant is always required, since the Claus plant itself rarely achieves more than 98% sulfur recovery. Even in the rare cases where 98% sulfur recovery is sufficient to fulfil emission regulations, it is required to incinerate the tail gas, because emission of hydrogen sulfide is not allowed.

In a WSA plant, all sulfur compounds must be oxidised to sulfur dioxide, so the feed streams are combusted with sufficient

air to oxidise also any ammonia, hydrocarbon and other combustibles. Even the simplest process lay-out of a WSA plant allows more than 99% removal of the sulfur compounds, and an advanced WSA plant can be designed for up to 99.99% sulfur removal. This is higher than any environmental standard requires today.

### *4.4. End-product*

Sulfuric acid can in many aspects be a beneficial product when compared to elemental sulfur, but this should be evaluated on a case-to-case basis taking local conditions into consideration. However, one basic fact is that approximately 90% of all the elemental sulfur produced worldwide will be further processed into sulfuric acid. One could therefore argue that going from $H_2S$ to sulfuric acid in one step compared to a multi-step approach where elemental sulfur is produced as an intermediate is more efficient in many aspects. Moreover, sulfuric acid also has a broader market segment with users such as the fertiliser industry, steel industry, water treatment, polymer industry, oil refining, and chemical industry, etc. In addition, sulfur can also liberate $H_2S$ which makes product handling troublesome.

### *4.5. Cost*

A WSA plant will typically have lower investment cost when compared with a Claus plant equipped with downstream tail gas treatment unit (TGTU). This is mainly due to the simple WSA design consisting of relatively few pieces of equipment. When considering operating costs, the WSA technology also has some important benefits. The large amount of high pressure steam produced in the WSA process, see section above, will have a positive impact on the operating income. Finally, the relatively simple design and operation of a WSA plant results in lower O&M cost compared to the more complex Claus plant.

If more than 99.6% conversion of the sulfur is required, WSA-DC, which is a double condensation version of the WSA technology, can be applied. In this way the $SO_2$ conversion can reach a level of 99.99%, which is much higher than required by any legislation today. Alternatively, a tail gas treatment can be applied, where the tail gas is scrubbed with hydrogen peroxide. Neither of the two methods produces any by-products.

Table 1 shows an economical comparison between Claus and WSA for a specific anonymous case. Of course, the unit prices and other particulars differ from one location to another, but it is clearly seen that the WSA comes out very favourably compared to the Claus plant. The investment in a Claus unit plus tail gas treatment is comparable to the investment in a WSA unit. Usually the WSA unit is a little cheaper,

***Table 1.*** *Economical comparison between Claus and WSA*

| **Basics** | **Unit** | |
|---|---|---|
| Feed stream/acid gas | $Nm^3/h$ | 2,700 |
| Content of $H_2S$ | Vol-% | 30 |
| Total sulfur amount | tons/day | 28 |
| Sulfuric acid amount equivalent | tons/day | 85 |
| Sulfur recovery | % | 99.5 |

| **Consumption figures** | USD/ton | **Claus + TGTU** | | **WSA** | |
|---|---|---|---|---|---|
| | | Cons. tons/hour | USD/year | Cons. tons/hour | USD/year |
| Fuel gas | 130 | 0.23 | 257,152 | - | - |
| Oxygen | 47 | 0.56 | 226,363 | - | - |
| HP steam | 17 | 1.33 | 194,455 | - | - |
| Boiler feed water | 0.34 | 3.70 | 10,819 | 11.2 | 32,750 |
| Cooling water | 0.03 | - | - | 30.8 | 7,947 |
| Electric power | USD 0.08/kWh | 400kWh | 275,213 | 205.0 | 141,047 |
| **Total consumption cost** | **USD** | | **964,002** | | **181,744** |

| **Production figures** | USD/ton | **Claus + TGTU** | | **WSA** | |
|---|---|---|---|---|---|
| | | Prod. tons/hour | USD/year | Prod. tons/hour | USD/year |
| Sulfuric acid | 32 | | | 3.56 | 978,939 |
| Sulfur | 80 | 1.16 | 799,980 | | |
| HP steam | 17 | | | 9.5 | 1,388,965 |
| LP steam | 12 | 2.7 | 278,653 | | |
| **Total production value** | **USD** | | **1,078,633** | | **2,367,904** |
| **Net production income** | **USD** | | **114,631** | | **2,186,160** |

| **Financial figures** | **Claus + TGTU** | **WSA** |
|---|---|---|
| Investment (USD) | 10,000,000 | 10,000,000 |
| Net present value (USD) | -7,000,000 | 18,500,000 |
| **Comparative advantage of WSA over 20 years** | | **USD 25,500,000** |

**Plant life time 20 years, inflation 4% p.a., discount rate 7% p.a.*

but for easy comparison the investments are assumed to be equal.

## 5. Case Story - WSA Technology for lean $H_2S$ gas from a gas sweetening plant

JOB Pertamina - Medco Tomori Gas Sweetening site generates additional 5.5MW power using WSA technology for treating lean acid gases from AGRU.

Using the WSA technology, JOB Tomori manages to comply with the local environmental regulation while producing huge amounts of HP superheated steam and saleable sulfuric acid.

### *5.1. Background*

The project is named Senoro Upstream Gas Project and is located in Central Sulawesi Province, Indonesia for upstream production of feed gas pipelined for Donggi-Senoro LNG production. Senoro Upstream Gas Production facility has a total production capacity of 310MMSCFD of gas and 8,500 barrels/day of condensate. It is jointly owned by MedcoEnergi, Pertamina and Tomori EP.

The WSA technology has been chosen to treat acid gases, originating from the gas sweetening process at the gas production facility. The $H_2S$ in the gases coming from both acid gas removal unit (AGRU) and the LP fuel gas treatment are converted into sulfuric acid of commercial grade with the WSA process.

### *5.2. Challenges*

- Meet local emission regulations;

- Low $H_2S$ concentration of only 1.78 - 2.33vol-% and a gas flow of 2,200lbmole/h;

- High reliability and availability are needed for this kind of project.

### *5.3. Evaluation model*

JOB TOMORI has created the evaluation model based on several criteria, namely:

- Availability/Reliability factor - it needs to be a proven technology with many references;

- Technical feasible solution for very lean $H_2S$ gases without concentrating;

- Simplicity of the process will bring down the cost for maintenance and overall OPEX;

- Investment cost - concentrating of the acid gas would be too expensive;

- The energy recovery needs to be sufficient to justify a steam turbine;

- The market potential for sulfuric acid is more diverse compared to sulfur.

Based on the above criteria, JOB Tomori´s internal and a 3rd party evaluation done by Worley Parsons, Topsøe's WSA technology emerged as the optimal solution for their gas sweetening project.

### *5.4. Topsøe´s WSA solution*

- A WSA plant that produces 45tons/day of sulfuric acid;

- Production of 780tons/day of steam (433°C, 28.5bar g) allowing production of 5.5MW power;

- Minimum $SO_2$ conversion of 97% has been guaranteed.

The WSA plant will, in this single catalytic bed layout, convert minimum 97% of the sulfur and produce 45tons/day of commercial grade sulfuric acid, which is sold on the local market. In addition, about 780tons/day of superheated steam will be produced and the steam will be routed to a turbine to produce power. In order to maximise steam production in the WSA plant, energy from the condensation of sulfuric acid is recovered in the form of hot air, most of which is supplied to the combustor. The rest of the hot air is used for preheating the incoming boiler feed water. This design makes the plant extremely energy efficient due to the fact that most of the heat is recovered back into the process.

## 6. SNOX - Efficient and cost-effective removal of SOx and NOx

As sweet crude oil reserves diminish, energy companies are forced to turn to heavy crude oil with high content of sulfur in order to satisfy the demand for petroleum.

At the same time, these companies have to strive for high energy efficiency and low emission levels.

Refineries using petcoke and/or heavy residue as a fuel for generation of steam and electrical power are finding that conventional methods of flue gas desulfurisation (FGD) using limestone wet scrubbing are becoming significantly more expensive and troublesome to operate as fuel sulfur content increases.

The SNOX™ process combines removal of NOx, SOx, Hg and particulates into a process that is not only less expensive to operate at high fuel sulfur levels, but also

produces commercial-grade sulfuric acid as a revenue source while avoiding purchase of absorbents and eliminating waste treatment and disposal costs.

Recycling of hot combustion air back to the boilers ensures a high degree of fuel burn-out and high thermal efficiency, keeping energy costs at a minimum and reducing specific $CO_2$ emission.

Finally, the SNOX™ process demonstrates a higher level of sustainability than conventional processes because it consumes hardly any water and produces no waste requiring expensive handling, treatment and disposal.

SNOX™ plants (e.g. at OMV - Austria, Agip - Italy and Vattenfall - Denmark) have demonstrated consistently high availabilities and efficiencies over many years. All new SNOX™ plants, at for instance Petrobras (Brazil), are designed for the same proven availabilities and reliabilities.

## 7. Refinery configurations with Topsøe SNOX™ technology

When the flue gas from combustion of high-sulfur heavy residues shall be cleaned, a SNOX™ plant is the ideal solution, since it neither requires absorption materials nor produces waste materials.

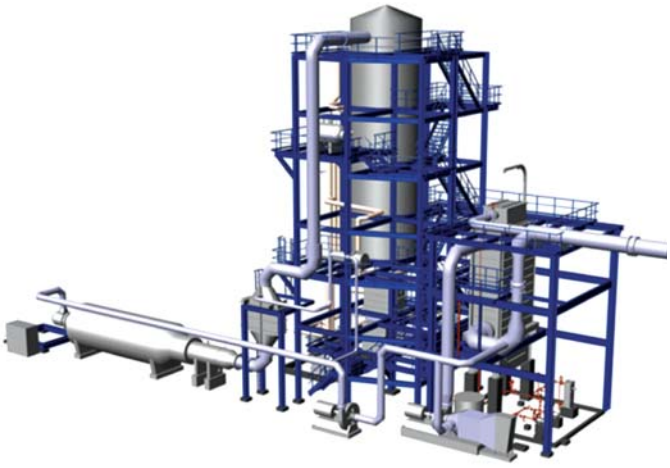


***Figure 4.*** *3D computer model of a WSA plant treating $H_2S$ gas*

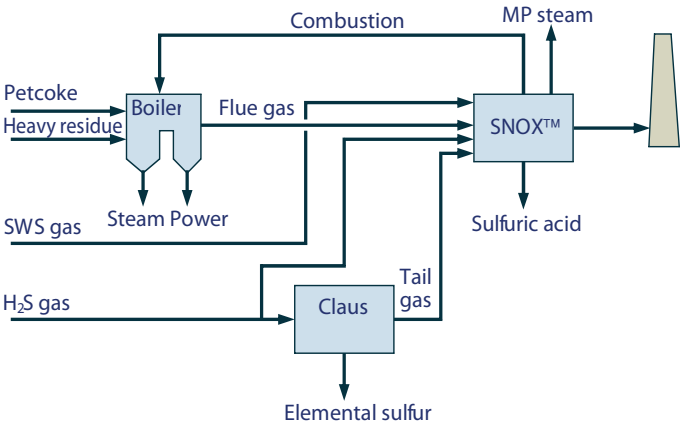



***Figure 5.*** *SNOX™ plant treating $H_2S$, SWS, Claus tail and boiler flue gases*

***Table 2.*** *Comparison of a SNOX™ plant equipped pulverised coal boiler with a CFB boiler with SCR DeNOx and tail-end FGD producing 300MW electricity from petcoke with 6% sulfur content and an LHV of 32MJ/kg*

| | Unit | SNOX™ with pulverized coal boiler | Limestone FGD + SCR with CFB boiler |
|---|---|---|---|
| **Comparison SNOX™ versus limestone FGD + SCR** | | | |
| Net electric output | MW | 300 | 300 |
| Net electric efficiency (on LHV basis) | % | 39 | 38 |
| Petcoke consumption | tons/hour | 88.3 | 89.7 |
| SOx removal efficiency | % | 98 | 98 |
| NOx content in stack gas | ppm | < 20 | 30 |
| $H_2SO_4$ production | tons/hour | 15.6 | 0 |
| Total Ca/S ratio in SOx absorption | | 0 | 2.8 |
| $CaCO_3$ consumption | tons/hour | 0 | 47* |
| Waste production | tons/hour | 0 | 75** |
| $NH_3$ consumption | tons/hour | 0.25 | 0.1 |
| **Financial impact in USD/year at 8,000 full-load hours** | | | |
| $H_2SO_4$ sold at USD 15/ton | USD/year | 1,800,000 | 0 |
| $CaCO_3$ supplied at USD 20/ton | USD/year | 0 | -7,500,000 |
| $NH_3$ supplied at USD 300/ton | USD/year | -600 | -240,000 |
| Waste disposal cost at USD 20/ton | USD/year | 0 | -12,000,000 |
| Cost of difference in fuel consumption at USD 40/ton petcoke | USD/year | 0 | -400,000 |
| **Total** | **USD/year** | **1,200,000** | **-20,140,000** |
| Cost impact per MWh | USD | -0.50 | 8.40 |

** Use of $CaCO_3$ containing CFB waste for tail gas FGD in assumed.*
*** Mixture of $CaSO_4$, CaO, $CaCO_3$ and ash.*
*Weight depends on $H_2O$ content. Figure varies considerably with the location.*

The product is sulfuric acid of 94 - 97wt.% concentration. A very special advantage of the SNOX™ technology is that it becomes more economical the more sulfur is contained in the feed streams, hence, it is also beneficial to treat $H_2S$ and SWS gases in the SNOX™ plant. Figure 5 shows a configuration where $H_2S$ gas is primarily handled in a Claus plant producing elemental sulfur, while the flue gas from combustion of heavy residues is cleaned in a SNOX™ plant together with SWS gas and Claus plant tail gas.

**8. Competitive cost profile of SNOX™**

Table 2 compares the economics of a pulverised coal boiler using the SNOX™ process and a CFB boiler using SCR and tail-end FGD with limestone-based scrubbing.

Table 2 also shows that the much lower operating costs of a pulverised coal boiler using the SNOX™ process results in a 8.90USD reduction per MWh, compared with CFB boiler power generation using SCR DeNOx and tail-end FGD with limestone scrubbing.

**9. Conclusions**

The WSA and SNOX™ processes are simple and efficient sulfur recovery processes which meet the demands of the industry for environmental compliance, low energy usage, and low overall operating costs. Sulfur in any form is recovered as concentrated sulfuric acid of commercial quality. The WSA and SNOX™ technologies can be applied for a variety of process streams in various industries.

**The WSA technology** can meet the most stringent environmental regulations, even without tail gas treatment. One of the main advantages over a traditional Claus plant is that the steam production is as much as 4 times higher when producing sulfuric acid as compared to producing sulfur. Moreover, the WSA technology is a simple and reliable process that contributes to a higher availability and less shutdowns.

**The SNOX™ process** enables trouble-free burning of petcoke and heavy residue. Essentially, all $SO_3$ and heavy metal oxides are removed from the flue gas without corrosion problems.

The SNOX™ process is particularly suited for treatment of flue gas from combustion of up to 100% petcoke and heavy residue in pulverised coal boilers. The high combustion temperatures and 3 - 4% excess $O_2$ required for high burn-out of petcoke and the high content of vanadium in the fly ash result in a high flue gas content of NOx and $SO_3$, which can both be removed without corrosion or other problems in a SNOX™ plant. The higher air preheat temperature of the SNOX™ process also improves petcoke burn-out.

The main attraction of the SNOX™ process is that it requires much lower operating costs compared to traditional FGD technology and that it enables the combustion of cheap, high-sulfur petcoke and heavy residue for generation of steam and power without any significant water consumption or formation of waste products. Neither does it pose emission and operating problems other than those normally associated with burning coal and oil.

The SNOX™ process demonstrates high energy efficiency by recycling hot, preheated air to the boilers. In addition, the SNOX™ process can be used for handling of other sulfur waste streams such as $H_2S$, SWS gas and Claus tail gas.

# POST-SYNTHESIS DESIGN OF HIERARCHICAL ZSM-5 MATERIALS FOR OPTIMAL CATALYTIC PERFORMANCE IN THE CRACKING OF PETROLEUM FEEDSTOCK

Vu Xuan Hoan[1], Dang Thanh Tung[1], Phan Minh Quoc Binh[1], Nguyen Anh Duc[1], Udo Armbruster[2], Andreas Martin[2]
[1]*Vietnam Petroleum Institute*
[2]*Leibniz Institute for Catalysis*
*Email: hoanvx.ctat@vpi.pvn.vn*

**Summary**

*ZSM-5 zeolites are widely used as catalysts in the oil refining and petrochemical industry due to their outstanding catalytic performance. Despite their undisputed applications, the relative small pore size of ZSM-5 zeolites often imposes intra-crystalline diffusion limitations for reactant molecules, provoking the lower catalyst utilisation. To alleviate such limitations, in this work, an additional network of mesopores has been introduced by the post-synthesis modification. It was found that a hierarchical ZSM-5 material with the large fraction of mesopores (297$m^2$/g) coupled to the preservation of microporous characteristics (strong Brønsted) can be optimally prepared by base treatment in 0.5M NaOH and subsequent acid washing in 0.5M HCl. The gas phase cracking of cumene, carried out at 250$^oC$ as a model reaction to test the spacious properties, revealed that the introduction of mesoporosity enhanced the utilisation of active acid sites mostly located inside the micropores of ZSM-5, consequently the superior cumene cracking activity. Thus, the advantages of ZSM-5 zeolites (strong acidity) and mesostructured materials (high accessibility) can be combined to create advanced hierarchical ZSM-5 catalysts for petroleum processing.*

***Key words:*** *Hierarchical ZSM-5, post-synthesis, acidity, catalytic cracking.*

## 1. Introduction

Zeolites are a unique class of crystalline aluminosilicates which are widely used as catalysts in the oil refining and petrochemical industry. Medium pore zeolite ZSM-5 (Zeolite Socony Mobil-5) belonging to MFI topology, patented by Mobil Oil Company in 1975, is one of the most important zeolites that has been applied in a number of industrial-scale catalysed reactions such as cracking, isomerisation, alkylation, dewaxing or methanol-to-gasoline or methanol-to-olefins (MTG, MTO) etc. [1, 2]. The exceptional performance of ZSM-5 in catalysis primarily results from its strong Brønsted acidity, hydrothermal stability and uniform micropores of molecular dimensions. A typical example among others is the application of ZSM-5 additive in the industrial FCC (fluid catalytic cracking) process. Admixture of a second catalyst containing ZSM-5 to a FCC unit significantly increases the yield of light olefins (propene and butenes) with a gain in gasoline octane number by selective cracking of linear gasoline range olefins [3]. However, ZSM-5 as well as other zeolites to be considered for such applications has a major drawback. As one side effect of their micropores, zeolite catalysts often suffer from diffusion limitations for reactant molecules. The restricted access and slow molecular transport to and from active acid sites inside the micropores provoke lower catalyst utilisation. Obviously this limited mass-transfer negatively impacts on activity, and sometimes on selectivity and lifetime of the zeolite based catalyst [3 - 5].

In order to alleviate the internal diffusion limitations, facilitating the utilisation of the active volume in conventional ZSM-5, much effort has focused on increasing the access to zeolites' active sites by shortening the diffusion path length which leads to the so-called hierarchical zeolites [4, 5]. In such hierarchical zeolites, a large fraction of mesoporosity is introduced in combination with genuine microporosity. More importantly, the various domains of porosity should be interconnected to fulfil a distinct function: the micropores provide a high active surface area, the access to which is enhanced by the newly introduced mesopores [6]. Over the past decades, a wealth of synthesis approaches have been proposed and proved to be effective in introducing additional pores with other dimensions in ZSM-5 and related materials. Top-down routes normally involve the post-synthesis treatment of previously grown zeolites by means of selective leaching of framework atoms, e.g. dealumination by steaming or acid leaching [7] and desilication by base leaching [8], thereby generating the voids inside zeolite crystals. Bottom-up routes can create intercrystalline mesopores by assembling nanosized zeolites or by dispersing them on a porous matrix such as alumina or mesoporous aluminosilicates, etc. [9]. Among them, the introduction of mesoporosity by post-synthesis

design is perhaps the most promising route due to the combination of experimental simplicity and efficiency.

Recently, we have successfully developed hierarchical ZSM-5 materials by post synthesis modification of commercial ZSM-5 zeolites [11]. The resulting hierarchical ZSM-5 showed significantly enhanced conversion and selectivity toward gasoline-range hydrocarbons and light olefins in the cracking of triglyceride feedstock. In this study, we explored the application of such hierarchical ZSM-5 materials as advanced catalysts for the cracking of petroleum feedstock. The gas phase cracking of cumene was used as a model reaction to evidence the improved performance of the hierarchical ZSM-5 compared to commercial ZSM-5.

## 2. Experiment

### *2.1. Catalyst preparation*

The post-synthesis design of hierarchical ZSM-5 materials from commercial ZSM-5 (Zeocat PZ-2/25, ZeoChem AG) involved a two-step process, being similar to the previous work [11]. Various samples of the commercial ZSM-5 were first treated in the base solution with increasing NaOH concentrations to generate mesopores by desilication. Then the resulting alkaline treated samples were exposed to a strong acid solution (0.5M HCl) for the complete removal of amorphous debris in order to improve the textural and acidic properties.

In a typical experiment, 3.0g of parent Na-ZSM-5, denoted as ZSM-5-P, was submitted to 100ml of NaOH solutions with different concentrations (0.3, 0.5 and 0.8M) at 65°C under stirring for 30 minutes. In a subsequent acid washing step, 1.0g of the alkaline treated samples was dispersed in 0.5M HCl at 65°C for 2 hours. The resulting sample upon alkaline and subsequent acid treatment is denoted as HZ-xAAT, where AAT means alkaline-acid treatment; HZ and x represent the hierarchical ZSM-5 and the NaOH concentration in the first step, respectively. Prior to characterisation and catalytic study, ZSM-5-P, HZ-xAAT materials were transformed into protonated form by ion-exchanging twice in 0.5M $NH_4NO_3$ solution at 80°C for 4 hours.

### *2.2. Catalyst characterisation*

The nitrogen physisorption studies were conducted at -196°C with an ASAP 2010 apparatus (Micromeritics). The temperature-programmed desorption of ammonia ($NH_3$-TPD) measurements was carried out in a home-made set-up using a quartz tube reactor in the range of 100 - 550°C. The Fourier transform infrared spectroscopy measurements for acidity study were performed on a Tensor 27 spectrometer (Bruker) using self-supporting wafers and pyridine as probe molecule (py-IR). The Al and Si contents were determined by inductively coupled plasma atomic emission spectroscopy (ICP-AES; 715-ES, Varian) and atomic absorption spectroscopy (AAS; Analyst 300, Perkin Elmer), respectively. More details of these characterisation methods and experiment parameters were described elsewhere [12].

### *2.3. Catalytic evaluation*

The gas phase cracking of cumene was carried out in a fixed-bed down-flow stainless steel reactor (10mm internal diameter) equipped with mass flow controllers for reactant metering (Figure 1).

Typically, a fixed amount of the sieved catalyst (0.2g, particle size 300 - 700µm, diluted with 2.0g of quartz beads of the same size) was placed in the reactor. Prior to the reaction, the sample was activated in $N_2$ flow at 300°C for 2 hours to remove physically adsorbed water. Liquid cumene was fed at a rate of 0.6g/hour by a liquid flow mass controller (Liquid Flow, Bronkhorst) coupled to a controlled evaporator mixer (CEM, Bronkhorst) using $N_2$ flow (90ml/minute) as a carrier gas. By this way, the reactant was mixed with $N_2$ and then evaporated before entering the reactor. The catalytic cracking was conducted at 25°C under atmospheric pressure.

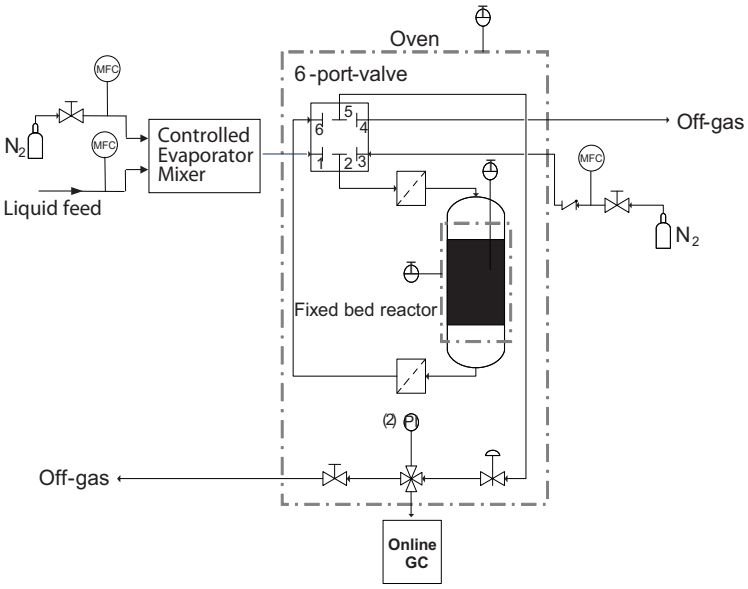



***Figure 1.*** *Experimental setup for catalytic evaluation of ZSM-5-P and HZ-xAAT materials in the gas phase cracking of cumene*

Feed and product samples were analysed with an online gas chromatograph (HP 5890, equipped with a sampling valve, a fused silica capillary column (HP5, 50m x 0.32mm x 0.52µm) and a flame ionisation detector. The temperature of the column was held at 50°C for 2 minutes, then increased to 280°C at a rate of 15K/minute and held for 4 minutes.

## 3. Results and discussion

### *3.1. Physico-chemical properties of commercial ZSM-5 (ZSM-5-P) and hierarchical ZSM-5 materials (HZ-xAAT)*

As reported previously [11], ZSM-5-P consists of small crystals (ca. 250nm) and their aggregates (ca. 800nm), forming inter-crystalline voids. No intra-crystalline mesopores were evidenced by TEM (not shown) or by analysis of BJH pore size distribution (Figure 2b).

The newly generated mesopores upon base-acid treatment are clearly revealed by $N_2$-sorption from the transformation of the type I isotherm (ZSM-5-P) into the type I+IV isotherms (HZ-xAAT) with enhanced uptake at high relative pressures (Figure 2a). Moreover, the direct evidence of generated mesopores can also be seen from the corresponding pore size distribution (Figure 2b). The changes in the recovery yield, composition, textural and acidic properties are summarised in Table 1. The post synthesis modification leads to a maximum external surface ($S_{meso}$ = 297m²/g) which is about 3 times greater than that of ZSM-5-P ($S_{meso}$ = 11m²/g) at a base concentration of 0.5M and a subsequent acid washing of 0.5M. The severe base treatment (0.8M NaOH) of ZSM-5-P lowers the $S_{meso}$ and $V_{micro}$ of the resulting sample (HZ-0.8AAT) due to the extensive dissolution of the zeolite crystals. Thus, the treatment conditions, i.e. 0.5 NaOH and 0.5 HCl at which the maximum $S_{meso}$ is reached, are defined as "turn point". In addition, the alkaline and subsequent acid treatment decreases the recovery yield and total acidity, but increases the Si/Al ratio (Table 1).

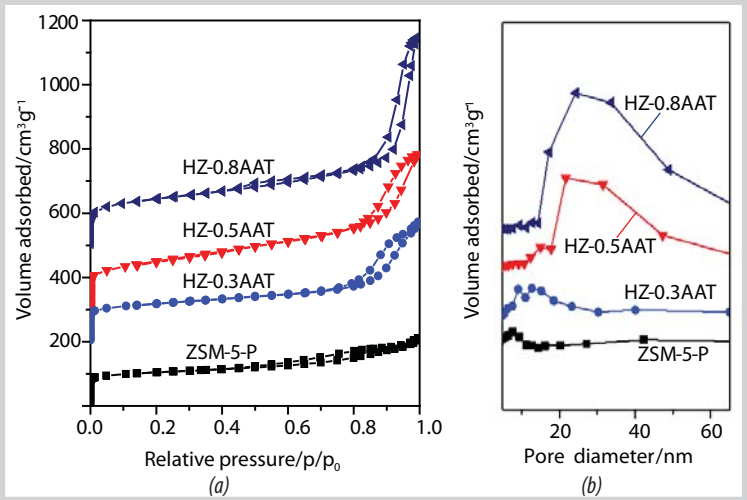



***Figure 2.*** *Nitrogen sorption isotherms (a) and the corresponding pore size distribution curves (b) of commercial ZSM-5-P and hierarchical ZSM-5 materials (HZ-xAAT)*

Figure 3a depicts the IR spectra of pyridine adsorbed on the parent and treated ZSM-5 samples after the adsorption procedure and evacuation at 400°C. All samples show two bands responsible for adsorbed pyridine on strong acid sites. The band at ca. 1543cm$^{-1}$ can be attributed to the pyridinium cation and indicates strong Brønsted acid sites (PyH+, BS), while the band at ca. 1455cm$^{-1}$ is characteristic of pyridine coordinated to strong Lewis acid sites (PyL, LS)]. The quantitative estimation of BS and LS was obtained by normalising the integral intensity of the corresponding bands to the BET surface area (Figure 3b). In good agreement with the $NH_3$-TPD data, the surface density of strong BS and LS undergoes a gradual decline upon the base and subsequent acid treatment. This can be explained by the occurrence of dealumination process during the post-synthesis modifications [13]. Compared to commercial ZSM-5-P, nevertheless, about 74% surface density of strong BS was retained on hierarchical HZ-0.5AAT upon the optimal treatment.

### *3.2. Gas phase cracking of cumene*

The catalytic performance of hierarchical ZSM-5 (HZ-xAAT) compared to commercial ZSM-5 (ZSM-5-P) was evaluated in the gas phase cracking of cumene. Cumene cracking is a well-established test reaction to assess

***Table 1.*** *Physico-chemical properties of commercial ZSM-5 (ZSM-5-P) and hierarchical ZSM-5 materials (HZ-xAAT)*

| Sample | Yield[a] (%) | Si/Al[b] | $S^c_{meso}$ (m²/g) | $S_{BET}$ (m²/g) | $V^c_{micro}$ (cm³/g) | $V_t$ (cm³/g) | Total acidity[d] (mmol $NH_3$/g) |
|---|---|---|---|---|---|---|---|
| ZSM-5-P | 100 | 11 | 110 | 373 | 0.113 | 0.22 | 1.24 |
| HZ-0.3AAT | 67 | 16 | 124 | 445 | 0.144 | 0.49 | 0.85 |
| HZ-0.5AAT | 62 | 20 | 297 | 456 | 0.130 | 0.71 | 0.71 |
| MZ-0.8AAT | 33 | 38 | 253 | 436 | 0.116 | 0.82 | 0.42 |

*[a]recovery yield (defined as grams of solid received after treatment per gram of parent sample; [b]analysed by AAS and ICP; [c]t-plot method; [d]$NH_3$-TPD*

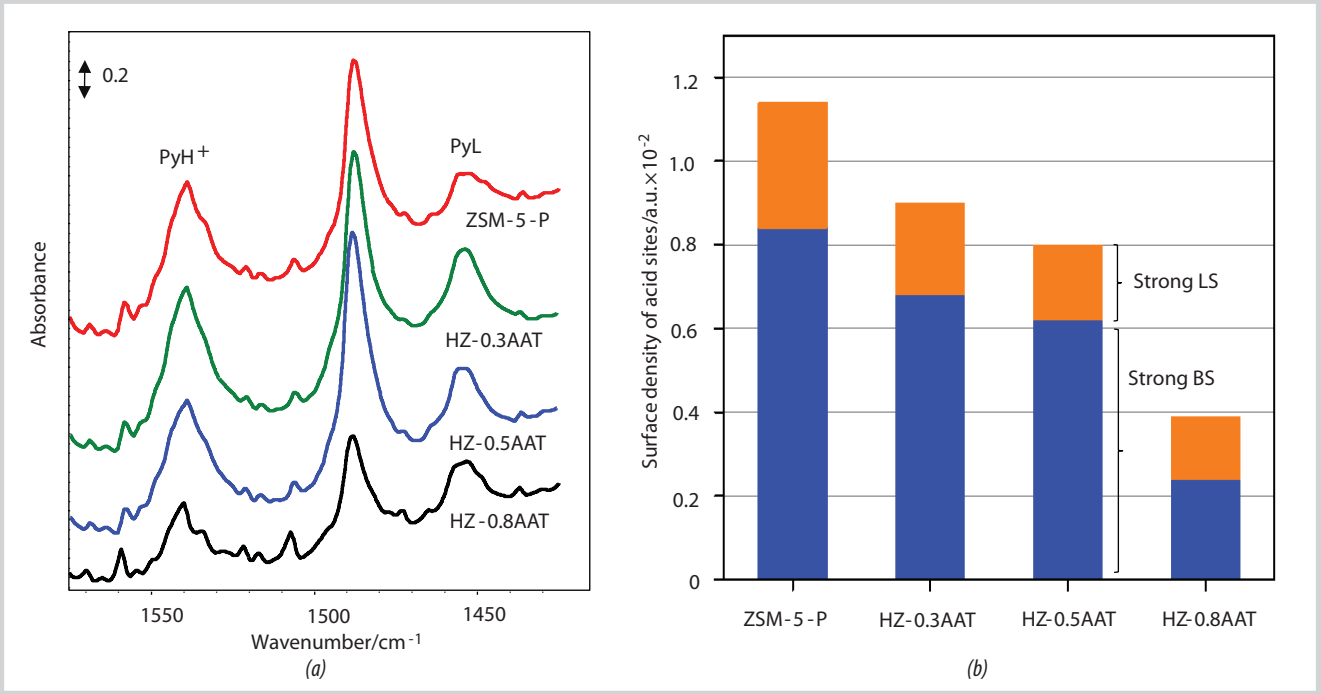



***Figure 3.*** *IR spectra (a) of pyridine adsorbed on the commercial ZSM-5 (ZSM-5-P) and hierarchical ZSM-5 materials (HZ-xAAT) and their corresponding surface density of strong BS (b)*

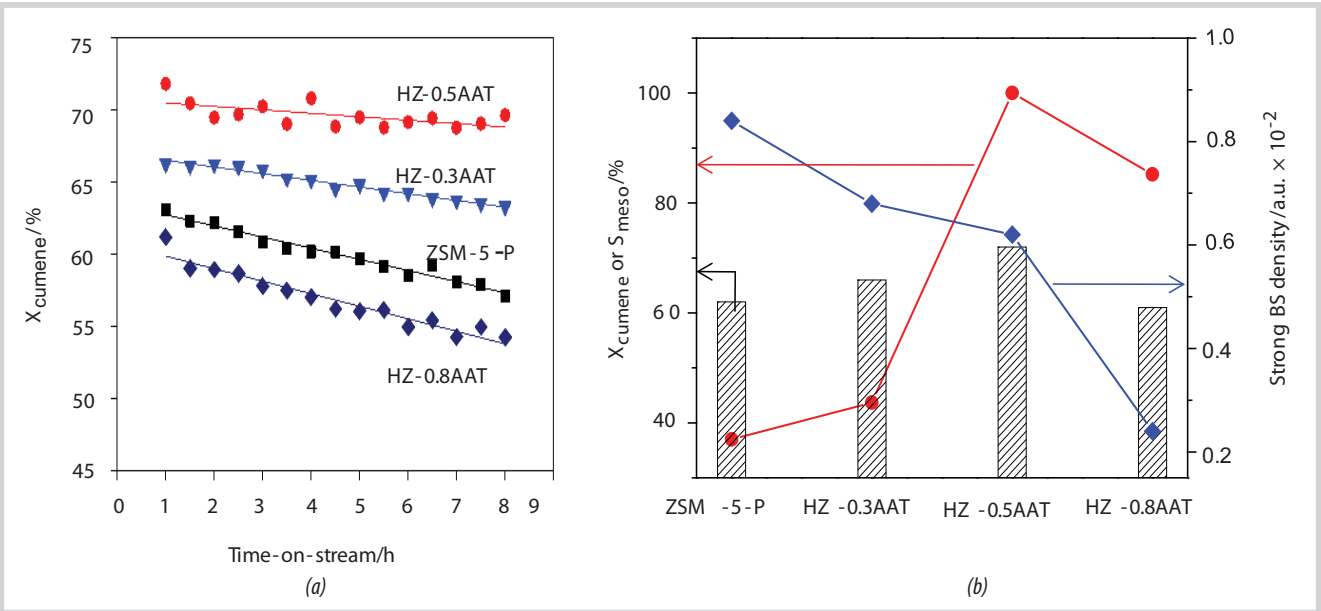



***Figure 4.*** *The cumene conversion (Xcumene) over ZSM-5-P and HZ-xAAT with time-on-stream (a) and Xcumene after 1h on-stream in the relation with the external surface (Smeso) and density of strong BS (b)*

hydrocarbon cracking activities of zeolite catalysts [14]. With its molecular cross-section of 0.5nm, cumene can penetrate the micropores of ZSM-5 (pore opening size of 0.52 - 0.54nm) wherein most active strong BS are located. However, even when cumene molecules have readily entered ZSM-5 crystals, the pore diffusion might be relatively slow, which reduces the catalyst utilisation, and thereby consequent catalytic activity [15, 16]. Thus, in this study, the cumene cracking over ZSM-5-P and HZ-xAAT catalysts was run at 250°C to evaluate the influence of both the acidic properties and porosity on their catalytic performance because the overall cracking reaction rate of cracking is likely to be determined by the diffusion rate at such low temperature [15]. The effect of thermal cracking was checked with an inert material (glass beads). No cumene conversion was detected with glass beads under the investigated reaction conditions. With the presence of the catalysts, cumene was mostly dealkylated on BS to form benzene and propylene as main products, suggesting that BS are at play in this reaction [14].

Figure 4a presents the cumene conversion over the various catalysts with time-on-stream. As expected, hierarchical HZ-xAAT catalysts show higher cracking activities than commercial parent ZSM-5-P, except HZ-0.8AAT. Remarkably, HZ-0.5AAT displays the highest cumene conversion which looks almost stable within the initial 8 hours on-stream. Figure 4b shows the cumene conversion over ZSM-5-P and MZ-xAAT after 1 hour on-stream with respect to their strong BS density and $S_{meso}$. No reasonable relationship between the cumene conversion and the strong BS density can be found, suggesting that there are diffusional transport constraints affecting cumene reactivity under the tested conditions. On the other hand, a good correlation between the cumene conversion and external surface ($S_{meso}$) has been established. These results agree well with the work of Zhao et al. [17] who found that the diffusion rate of cumene in mesoporous ZSM-5 is by 2 - 3 orders of magnitude faster than that in conventional ZSM-5, which doubled the cumene conversion over mesoporous ZSM-5 despite its lower Brønsted acidity. Al-Khattaf et al. [18] reported that under the diffusion-controlled regime, the larger the external surface, the higher the catalyst effectiveness and consequently the catalytic activity. Taking these findings into account, the improved cumene conversion over the hierarchical ZSM-5 samples in this work can be attributed to the enhanced acid site utilisation due to the increased accessibility and physical transport provided by substantial mesoporosity. For MZ-0.8AAT, the cumene conversion drops though the considerable fraction of mesopores are already available. The lower activity of MZ-0.8AAT can be explained by a sharp decrease in its surface density of strong BS in this sample as confirmed by the py-IR data. Hence, the introduction of mesoporosity combined with the preservation of microporous characteristics, i.e. strong BS plays a key role for the superior catalytic activity in a strong acid catalysed reaction like cumene cracking.

## 4. Conclusions

We evidenced that one can improve the catalytic performance of commercially available ZSM-5 zeolites in the cracking of petroleum feedstock by simple, post synthesis modification involving alkaline and subsequent acid treatment. The key is to optimise the synthetic parameter, i.e. the NaOH concentration to maximise the generation of mesoporosity ($S_{meso}$) without the significant loss of intrinsic zeolite characteristics (strong Brønsted acidity). A subsequent acid washing step is of crucial importance to completely remove aluminium debris for uncovering the micro-/mesoporous network. Most notably, the alkaline treatment of commercial Al-rich ZSM-5 in 0.5 NaOH, followed by the strong acid washing in 0.5M HCl, was found to be optimal for the preparation of hierarchical ZSM-5 (HZ-0.5AAT) containing the substantial mesoporosity ($S_{meso}$ = 297$m^2$/g) with the preserved intrinsic zeolite features (74% surface density of strong Brønsted acid sites). The gas phase cracking of cumene revealed that the introduction of mesoporosity indeed increases the reactivity of commercial ZSM-5 zeolites when the surface density of strong Brønsted sites is mainly retained. In fact, the cumene conversion upon 1 hour on-stream over HZ-0.5AAT (72%) was noticeably higher than that over commercial ZSM-5 (63%) even though the latter samples possessed a higher surface density of strong Brønsted acid sites. These findings might stimulate future works on the preparation and application of hierarchical ZSM-5 materials as advanced catalysts for the oil refining and petrochemical industry.

## References

1. Michael Stöcker. *Gas phase catalysis by zeolites*. Microporous and Mesoporous Materials. 2005; 82(3): p. 257 - 292.

2. Avelino Corma. *State of the art and future challenges of zeolites as catalysts*. Journal of Catalysis. 2003; 216(1 - 2): p. 298 - 312.

3. Marcello Rigutto. *Cracking and hydrocracking*. Zeolites and Catalysis: Synthesis, Reactions and Applications. Wiley-VCH. 2010; 18: p. 547 - 584.

4. Lei Zhang, Adri N.C.van Laak, Petra E.de Jongh, Krijn P.de Jong. *Textural characterization of mesoporous zeolites*. Zeolites and Catalysis: Synthesis, Reactions and Applications. Wiley-VCH. 2010; 9: p. 237 - 282.

5. Javier Pérez-Ramírez, Claus H.Christensen, Kresten Egeblad, Christina H.Christensen, Johan C.Groen. *Hierarchical zeolites: Enhanced utilisation of microporous crystals in catalysis by advances in materials design*. Chemical Society Reviews. 2008; 37: p. 2530 - 2542.

6. Maria Milina, Sharon Mitchell, David Cooke, Paolo Crivelli, Javier Pérez-Ramírez. *Impact of pore connectivity on the design of long-lived zeolite catalysts*. Angewandte Chemie International Edition. 2015; 54(5): p. 1591 - 1594.

7. Sander van Donk, Andries H.Janssen, Johannes

H.Bitter, Krijn P.de Jong. *Generation, characterization and impact of mesopores in zeolite catalysts.* Catalysis Reviews: Science and Engineering. 2003; 45(2): p. 297 - 319.

8. Johan C.Groen, Jacob A.Moulijn, Javier Pérez-Ramírez. *Desilication: on the controlled generation of mesoporosity in MFI zeolites*. Journal of Materials Chemistry. 2006; 16: p. 2121 - 2131.

9. Jiří Čejka, Svetlana Mintova. *Perspectives of micro/mesoporous composites in catalysis.* Catalysis Reviews: Science and Engineering. 2007; 49(4): p. 457 - 509.

10. Yu Liu, Thomas J.Pinnavaia. *Aluminosilicate mesostructures with improved acidity and hydrothermal stability*. Journal of Materials Chemistry. 2002; 12: p. 3179 - 3190.

11. Vu Xuan Hoan, Matthias Schneider, Ursula Bentrup, Dang Thanh Tung, Phan Minh Quoc Binh, Nguyen Anh Duc, Udo Armbruster, Andreas Martin. *Hierarchical ZSM-5 materials for an enhanced formation of gasoline-range hydrocarbons and light olefins in catalytic cracking of triglyceride-rich biomass*. Industrial & Engineering Chemistry Research. 2015; 54(6): p. 1773 - 1782.

12. Vu Xuan Hoan, Norbert Steinfeldt, Udo Armbruster, Andreas Martin. *Improved hydrothermal stability and acidic properties of ordered mesoporous SBA-15 analogs assembled from nanosized ZSM-5 precursors*. Microporous and Mesoporous Materials. 2012; 164: p. 120 - 126.

13. Hiroshi Mochizuki, Toshiyuki Yokoi, Hiroyuki Imai, Seitaro Namba, Junko N.Kondo, Takashi Tatsumi. *Effect of desilication of H-ZSM-5 by alkali treatment on catalytic performance in hexane cracking*. Applied Catalysis A: General. 2012; 449: p. 188 - 197.

14. A.Corma, BW.Wojciechowski. *The catalytic cracking of cumene.* Catalysis Reviews: Science and Engineering. 1982; 24(1): p. 1 - 65.

15. Masaru Ogura, Shin-ya Shinomiya, Junko Tateno, Yasuto Nara, Mikihiro Nomura, Eiichi Kikuchi, Masahiko Matsukata. *Alkali-treatment technique-new method for modification of structural and acid-catalytic properties of ZSM-5 zeolites*. Applied Catalysis A: General. 2001; 219(1 - 2): p. 33 - 43.

16. Kreste Egeblad, Christina H.Christensen, Marina Kustova, Claus H.Christensen. *Templating mesoporous zeolites*. Chemistry of Materials. 2008; 20(3): p. 946 - 960.

17. Liang Zhao, Baojian Shen, Jinsen Gao, Chunming Xu. *Investigation on the mechanism of diffusion in mesopore structured ZSM-5 and improved heavy oil conversion*. Journal of Catalysis. 2008; 258(1): p. 228 - 234.

18. S.Al-Khattaf, H.de Lasa. *The role of diffusion in alkyl-benzenes catalytic cracking*. Applied Catalysis A: General. 2002; 226(1 - 2): p. 139 - 153.

# INFLUENCES OF CATALYTIC TEMPERATURES AND Ru-LOADED CATALYSTS ON WASTE TIRE PYROLYSIS

Nguyen Anh Dung
*Hanoi University of Mining and Geology*
*Email: nguyenanhdung@humg.edu.vn*

**Summary**

*This paper investigates the effects of Ru/MCM-41 catalysts in the pyrolysis of waste tire using a semi-batch reactor. The pure silica support MCM-41 was synthesised via silatrane route. Prior to evaluating the activity of Ru/MCM-41 catalysts, the influences of MCM-41 and catalytic temperature were studied. The results indicated a strong impact of MCM-41 and catalytic temperature on the yield and nature of pyrolysis products. Oil yield first decreased then increased with catalytic temperature. However, the highest catalytic temperature produced the oil having a higher poly-aromatic content. Ru/MCM-41 catalyst produced much lighter oil and dramatically decreased the concentration of poly- and polar-aromatics in the oil but also decreased the yield of oil. And the catalytic activity of Ru/MCM-41 was found to increase with Ru content in the tested range of ruthenium loading. The increase in catalytic activity was discussed in relation with catalyst characterisations.*

***Key words:*** *Pyrolysis, waste tire, bifunctional catalyst, Ru, MCM-41.*

## 1. Introduction

Tires are designed to be resistant to chemical, biological and physical degradation. Meanwhile, the world production of waste tire is approximately 6 x $10^6$ tons/year, and nearly 70% of these waste are simply dumped in the open or in the land-filled [1, 2]. Moreover, fires at tire deposits have been reported to be very difficult to control and generate high levels of pollution to the soil, atmosphere and water [3].

Thus, over recent years, tire pyrolysis, a recycling process, has attracted significant renewed attention. It essentially involves degradation of the tire components by exposure to high temperatures in the absence of oxygen. The result is a carbonised char, condensable oil and a gas fraction. Gas fraction has been reported to have high calorific value [4], and high hydrogen content [2, 5, 6], whereas the tire-derived oil was shown to be similar, to a certain extent, to the commercial petroleum naphtha [7]. However, the high concentration of aromatic hydrocarbons (HCs) [7 - 9], especially polycyclic HCs (PAHs), has limited its application as a fuel. As a result, several studies have been done with focus on the possibilities for the production of chemical feedstock from the tire-derived oil rather than fuel. For instance, Williams and Brindle [10, 11] and Boxiong et al. [12] reported the high selectivity toward single ring aromatic HCs in the light fractions by catalytic pyrolysis of waste tire using ZSM-5 and USY zeolites as catalysts, respectively. Our previous study [13], a first step in the attempts to study the possibility of fuel production from waste tire, has shown that the mordenite-catalysed pyrolysis of waste tire produced the oil having high selectivity toward gasoline, kerosene and gas oil fractions. However, a relative high amount of poly- and polar-aromatics still existed in the oil. And the amount of aromatics increased with increasing acid properties of the catalyst. As a result, a new catalyst should be rationally designed and tested for waste tire-to-fuel process.

Bifunctional catalysts are extensively studied for aromatic reduction [14]. Metals can catalyse the hydrogenation of the feedstock, making it more reactive for cracking and heteroatom (sulfur, oxygen) removal [15]. And a high level of aromatic hydrogenation at moderate hydrogen pressures can be achieved with noble metals catalysts [16, 17]. The intrinsically high hydrogenation activity of noble metal might help reducing steric effects that impede the direct elimination of the sulfur heteroatom [18, 19]. However, noble metals display a low resistance to sulfur poisoning limiting their applications. The sulfur tolerance of a noble metal supported catalyst may be enhanced by (i) using acidic carriers [20], (ii) changing the metal particle size, or (iii) alloying with other metals [21]. Considering the metallic nature, Ru was reported to have a better sulfur tolerance than Pt, Pd or Pd-Pt catalysts in hydrogenation and ring opening of tetralin on noble metal supported on zirconium doped mesoporous silica catalysts due to the low density of states at the Fermi level of this metal [22]. Also, previous studies and the references therein on the conversion of hydrocarbons over supported and unsupported catalysts have established the order of catalytic activities for a considerable number of metals; these studies found ruthenium the most active metal investigated [23, 24]. In addition, Ru supported on

HMOR was found to exhibit higher activity in terms of PAHs removal and light oil production than other metals (Pt, Rh, Re) supported on HMOR catalysts [25] in waste tire pyrolysis. On the other hand, due to the size of the aromatic molecules, especially the PAHs, a large pore material consequently should be used as the support of the bifunctional catalyst. Pure silica MCM-41, which has a mild acidic property, was shown to exhibit good activity for the degradation of waste plastic [26 - 27]. The carbon number distribution of the derived oil shifted to lower number, and the authors also observed the carbenium ion cracking mechanism over this material [27]. Besides, catalytic temperature strongly affected the products obtained from catalytic pyrolysis of waste tire [10, 28].

The aim of this work is to investigate the influences of Ru-supported pure silica MCM-41 catalyst on the products obtained from waste tire pyrolysis. For this purpose, a pure silica MCM-41 was synthesised via silatrane route. Then, pyrolysis of waste tire using MCM-41 as a catalyst was conducted to study the effects of catalytic temperature to find the optimum condition. Subsequently, a series of Ru-supported catalysts, prepared by impregnation technique with various Ru loading, were subjected to waste tire pyrolysis to evaluate their influence on the yields and the nature of the evolved products.

## 2. Experiment

### *2.1. Catalyst preparation*

To synthesise pure silica MCM-41, silatrane was first synthesised using the method of Wongkasemjit's group [29]. The silatrane precursor was added to a solution containing CTAB, NaOH, and TEA, followed by adding water with vigorous stirring [30]. The obtained crude product was filtered and washed with water to obtain a white solid. Then, the white solid was dried at room temperature and calcined at 580°C for 6 hours to obtain mesoporous MCM-41.

Ru-supported catalysts were prepared by the conventional wetness impregnation technique. An appropriate amount of precursor solution of $RuCl_3.xH_2O$ (FLUKA) was loaded to the MCM-41, followed by drying in an oven at 110°C for 3 hours, and then calcined at 580°C for 2 hours. Subsequently, it was pelletised and sieved to obtain particle sizes in the range of 400 - 425µm. Prior to the catalytic activity testing, each catalyst was reduced by hydrogen at 400°C for 3 hours.

### *2.2. Catalyst characterisation*

XRD patterns were obtained using the Riguku D/Max 2200H with a scanning speed of 0.5 degree/min and 2θ from 1.5 degree to 60 degree. The composition of the Ru on the support was determined by the Inductively Coupled Plasma (ICP) technique using a Perkin Elmer Optima 4300 PV machine. The surface area and pore size distribution of the studied catalysts were characterised by $N_2$ physical adsorption using a Sorptomatic 2900 equipment. Hydrogen chemisorption at room temperature was carried out in a Micromeritics 2900 apparatus, after the in-situ reduction of sample at 500°C (10°C.min$^{-1}$) for 1 hour, under a flow of $H_2$. Dispersion data was calculated by assuming a stoichiometry H/Ru = 1 [17]. Temperature-programmed desorption (TPD) using $NH_3$ was carried out in a TPD/TPR Micromeritics 2900 machine. Approximately, 0.1g of sample was first pretreated in He at 550°C for 30 minutes. Then, the system was cooled to 100°C, and the $NH_3$ adsorption was performed using $NH_3/N_2$ for 1.5 hours followed by the introduction of He to remove the physically adsorbed $NH_3$ for 30 minutes at 100°C. Finally, the system was cooled to 50°C, and then the temperature program desorption was started from 50°C to 600°C with a heating rate of 5°C/min. TPR of Ru-supported catalysts was conducted using the same Micromeritic 2900 equipment from room temperature to 500°C with a heating rate of 5°C/min. Temperature program oxidation (TPO) using also the Micromeritics 2900 machine was performed from room temperature to 900°C (10°C/min), and the final temperature was held for 30 minutes. The amount of coke was then determined from the area under the curve and calculated by the software supplied with the machine. The catalyst characterisation was done at the Petroleum and Petrochemical College, Chulalongkorn University, Bangkok, Thailand.

### *2.3. Pyrolysis of waste tire*

The detail of pyrolysis process was described elsewhere [13]. Briefly, the pyrolysis of waste tire was carried out in the lower zone of the reactor, where the temperature was set at 500°C. Then, the evolved product was carried by a nitrogen flow to the upper zone packed with a catalyst. This zone was controlled at various catalytic temperatures (350, 400 and 450°C) in order to investigate the influence of catalytic temperature. The obtained product was next passed through an ice-salt condensing system containing 3 condensers in order to separate incondensable compounds from the liquid product. The solid and liquid products were weighed to determine the product distribution. The

amount of gas was then determined by mass balance. Prior to being analysed, the liquid product was dissolved in n-pentane to precipitate asphaltenes. The obtained maltenes was analysed by FTIR and liquid adsorption chromatography [31]. In the later process, saturated hydrocarbons, mono-, di-, poly- and polar aromatics in the maltenes were fractionated. Finally, a Varian CP 3800 Simulated Distillation Gas Chromatograph (SIMDIST GC) equipped with FID was used to analyse the obtained maltene and hydrocarbon fractions according to the ASTM D2887 method to determine simulated true boiling point curves. The petroleum fractions were then cut based on their boiling point, including naphtha (< 200°C), kerosene (200 - 250°C), gas oil (250 - 370°C) and residue (> 370°C).

## 3. Results and discussion

### 3.1. Catalyst characterisation

Figure 1 illustrates the XRD patterns of the synthesised MCM-41 and Ru-supported samples. As seen in the figure, the structure of MCM-41 did not change after incorporation of ruthenium and no peak of ruthenium species was observed. Probably the amount of Ru loaded was below the detectable range of the XRD equipment and/or ruthenium was highly dispersed in all samples.

The physical properties of the fresh catalysts and the amount of coke of the used ones were summarised in Table 1. Accordingly, ICP analysis indicated a very good consistence between the targeted and true values of metal loaded in all samples. The BET surface area of silica MCM-41 is very high, and the average pore diameter is approximately 2.6nm, which is similar to the values reported in [30]. $H_2$-chemisorption results showed that the mean diameter of ruthenium particles for all samples is about 1.9nm, and the diameter increases with increasing ruthenium loading. In addition, all Ru-supported samples have a high metal dispersion of 65.2 - 68.5%. However, the dispersion of ruthenium slightly decreases with increasing concentration of ruthenium in the sample. Furthermore, the incorporation of Ru slightly decreased the surface

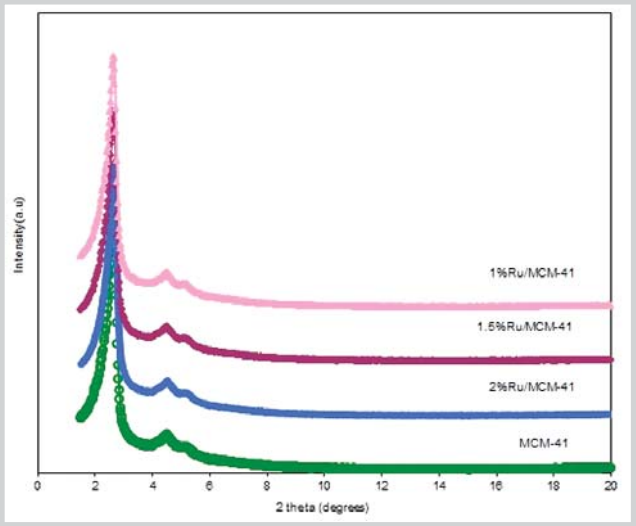



***Figure 1.*** *XRD patterns of the MCM-41 and Ru/MCM-41 catalysts*

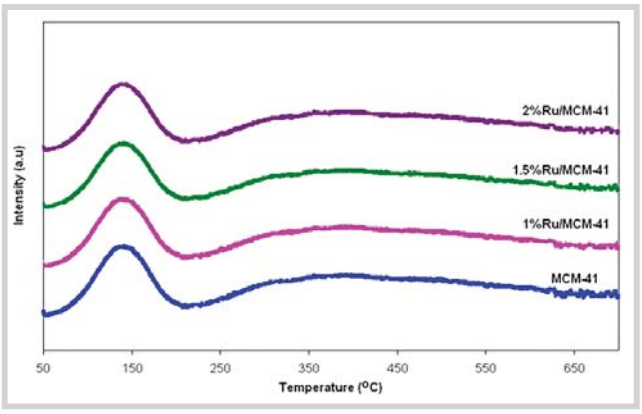



***Figure 2.*** *TPD-$NH_3$ profiles of Ru/MCM-41 catalysts*

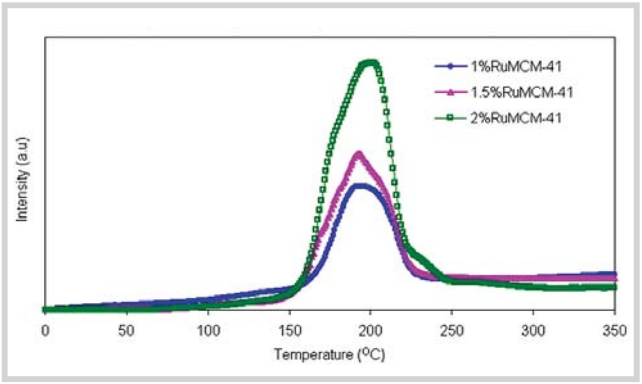



***Figure 3.*** *TPR profiles of Ru/MCM-41 catalysts at various loading percentages*

***Table 1.*** *Physical and chemical properties of MCM-41 and Ru-supported catalysts*

| Samples | %wt Ru | Dispersion (%) | Ru particle size[b] (nm) | BET Surface area ($m^2.g^{-1}$) | Pore diameter (nm) | Coke ($g.g^{-1}$ catalyst) | Asphaltenes ($g.g^{-1}$ oil) |
|---|---|---|---|---|---|---|---|
| MCM-41 (350°C)[a] | - | - | | 1454 | 2.61 | 0.084 | 0.00064 |
| MCM-41 (400°C)[a] | - | - | | 1454 | 2.61 | 0.097 | 0.00053 |
| MCM-41 (450°C)[a] | - | - | | 1454 | 2.61 | 0.108 | 0.00073 |
| 1%Ru/MCM-41 | 0.98 | 68.5 | 1.88 | 1450 | 2.57 | 0.119 | 0.00048 |
| 1.5%Ru/MCM-41 | 1.51 | 67.9 | 1.90 | 1448 | 2.56 | 0.126 | 0.00041 |
| 2%Ru/MCM-41 | 2.02 | 65.2 | 1.98 | 1439 | 2.51 | 0.124 | 0.00022 |

area of the support in association with a reduction in average pore diameter, possibly caused by the diffusion of Ru into the pore.

The strength and distribution of acid sites of all prepared catalysts determined by TPD-$NH_3$ are given in Figure 2. It can be seen that the profile of MCM-41 shows 2 desorption peaks with maxima at 150°C and 350°C, respectively. These peaks are broad and low intensive suggesting a good distribution of the acidic sites as well as the low amount of acidic sites. As this zeolite material is composed of pure silica, the acid sites must be contributed from the silanol groups lining the wall of the channels as suggested by Seddegi et al. [27]. The incorporation of ruthenium slightly decreases the intensity of the peaks, possibly caused by the diffusion of ruthenium particles into the zeolite channels, thus blocking some acidic sites. The total acid sites of Ru-supported catalysts are comparable.

Figure 3 depicts the TPR profiles of all samples. Accordingly, the locations of the peaks in TPR profiles of all samples with different Ru loadings are similar, but the intensity increases with increasing Ru content. And, Ru-supported MCM-41 exhibits a main reduction peak at 190°C, which is higher than Ru-supported on mesoporous silica doped with zirconium [32], indicating a stronger metal support interaction. Consequently, from $H_2$-chemisorption analysis the high dispersion of Ru in all Ru-supported samples (> 65%) was observed (Table 1), which is well consistent with XRD results. Moreover, as indicated in Table 1, the amount of coke of the spent catalysts obtained from TPO analysis shows that Ru-supported catalysts produced a higher amount of coke than MCM-41.

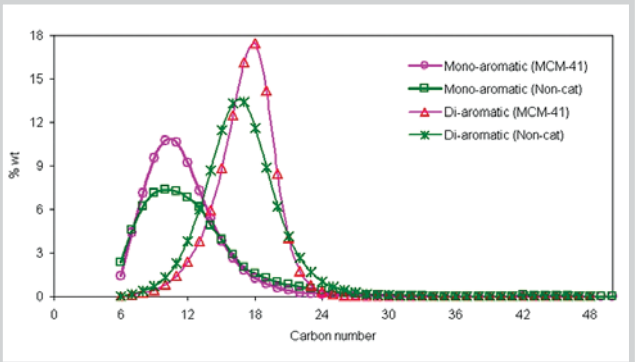



***Figure 4.*** *Carbon number distribution of mono- and di-aromatics in oils obtained from thermal and catalytic pyrolysis using MCM-41*

### *3.2. Thermal and catalytic pyrolysis of waste tire*

The pyrolysis products obtained from thermal and catalytic pyrolysis over MCM-41 are summarised in Table 2. It can be seen that the gas yield obtained from MCM-41 is much higher than that produced from thermal pyrolysis. In addition, with respect to thermal pyrolysis, the oil generated over MCM-41 has higher naphtha and kerosene, and the poly- and polar-aromatic contents in the oil are lower. These results might be ascribed to the cracking activity of the catalyst [13]. Besides, saturates in the derived oil decrease when using MCM-41. This is well consistent with the results obtained from FTIR analysis, as depicted in Figure 4. It can be seen that the infrared absorption bands of interest are observed around the range of C-H stretching vibration of $-CH_2-$ and $-CH_3$ groups approximately between 3,000$cm^{-1}$ and 2,800$cm^{-1}$ [33]. The peak at 3,030$cm^{-1}$ represents the aromatic C-H stretching, whereas the one at 2920$cm^{-1}$ represents the symmetric aliphatic C-H stretching, and the ratio of the two peaks correlates with the aromaticity of the hydrocarbon compounds [34]. And obviously, as compared to thermal pyrolysis, MCM-41 generated the oil having the higher ratio of $I_{3030cm}$-1/$I_{2920cm}$-1; thus, it has lower saturated hydrocarbons [33, 34].

On the other hand, the use of MCM-41 leads to a dramatic increase in the concentrations of mono- and di-aromatics (Table 2). Figure 4 illustrates the carbon number distribution of mono- and di-aromatics. Accordingly, MCM-41 causes the shifts of these compounds distribution to higher carbon number, indicating the formation of heavier aromatics. It is well accepted that aromatic hydrocarbons are not easy to be converted in a secondary cracking reaction [35, 36]. Meanwhile, alkylation reaction can be promoted by a Lewis acid catalyst [37, 38], and MCM-41 was reported to favour the alkylation reaction

***Table 2.*** *Products obtained from thermal and catalytic pyrolysis using MCM-41**

| Yield (%wt) | Non-cat | MCM-41 | Content (%wt) | Non-cat | MCM-41 | Yield (%wt) | Non-cat | MCM-41 |
|---|---|---|---|---|---|---|---|---|
| Naphtha | 13.02 | 18.81 | Sat-HCs | 53.81 | 48.21 | Gas | 10.33 | 14.56 |
| Kerosene | 8.81 | 9.95 | Mono-aromatics | 13.24 | 17.18 | Liquid | 44.02 | 38.02 |
| LGO | 7.80 | 4.83 | Di-aromatics | 9.88 | 20.37 | Solid | 45.65 | 45.42 |
| GO | 7.62 | 2.28 | Poly-aromatics | 8.99 | 6.55 | | | |
| Residues | 6.77 | 2.15 | Polar-aromatics | 12.68 | 7.69 | | | |

**Catalytic temperature: 350°C*

***Table 3.*** *Pyrolysis products obtained at various catalytic temperatures*

| Catalyst temperature (°C) | Product distribution (%wt) | | | Yields ofpetroleumcuts (%wt) | | | | Chemicalcompositions (%wt) | |
|---|---|---|---|---|---|---|---|---|---|
| | Gas | Liquid | Solid | Naphtha | Kerosene | Gas Oil | Residues | Poly-aromatics | Polar-aromatics |
| Non-Cat, 350 | 10.33 | 44.02 | 45.65 | 13.02 | 8.81 | 15.42 | 6.77 | 8.99 | 12.68 |
| 350 | 14.56 | 38.02 | 45.42 | 18.81 | 9.95 | 7.11 | 2.15 | 6.55 | 7.69 |
| 400 | 23.52 | 32.05 | 45.24 | 16.49 | 8.38 | 5.88 | 1.11 | 6.45 | 8.05 |
| 450 | 13.52 | 42.04 | 44.44 | 15.64 | 10.61 | 13.08 | 2.35 | 8.21 | 11.69 |

of previously formed aromatic rings [39]. Therefore, it is proposed that probably MCM-41 promotes not only the cracking of saturated HCs but also the alkylation of the already-generated aromatics. As a result, heavier mono- and di-aromatics are produced, leading to the increment of mono- and di-aromatic concentration in the tire-derived oils.

### *3.3. Influences of catalytic temperatures*

Table 3 summarises the product yields, the petroleum fractions and compositions of the oils produced by pyrolysis with MCM-41 catalyst at various catalyst temperatures. Accordingly, catalyst temperature does not influence the solid yield since the pyrolysis conditions were kept constant, and the tire was completely decomposed at 500°C [2]. However, catalyst temperature strongly affects the yields of other products. As seen from Table 3, the yield of gaseous products first increases at the expense of the liquid yield as the catalyst temperature rises from 350°C to 400°C, which is attributed to greater and deeper cracking reactions. Further increasing this temperature to 450°C causes a reduction in the yield of gaseous product in accordance with an increase in the yield of the oil. Liquid adsorption chromatography analysis also shows an increase in poly- and polar-aromatics with catalyst temperature (Table 3). Possibly, a considerable amount of olefins including conjugated olefins and aromatics, etc, produced during pyrolysis, might undergo cyclisation and alkylation followed by dehydrogenation to produce (heavier) aromatics when the acid catalyst was used [11, 40]. Note that these reactions are favoured at high reaction temperatures [6] and aromatic content in the pyrolytic oil increased when a zeolite with a large pore diameter was used [13]. Therefore, the very high catalyst temperature together with the meso-pores of the MCM-41 should be responsible for the increment of liquid yield as well as the formation of heavier aromatics from olefins and/or the lighter ones. On the other hand, it was elucidated that aromatic and alkene species have a greater predisposition to being involved in pathways to coke formation because of their ability to easily be involved in hydrogen transfer and cyclisation reactions [41]. As a result, a higher amount of coke is produced as the catalyst temperature rises (Table 1). And the high amount of coke formed can cause deactivation of the catalyst; thus, reducing its cracking activity leading to a reduction in the yield of gas product.

It can be seen in Table 3 that, regardless of the catalyst temperature, the yield of naphtha fraction from catalytic pyrolysis is higher than that from thermal pyrolysis. And the variation in catalyst temperature alters the contents of petroleum fractions in the pyrolytic oils; that is, increasing this temperature decreases naphtha in consistence with an increment in kerosene and gas oil as well as residue, suggesting the existence of the recombination of light molecules and leading to the formation of heavier compounds, and a consequent higher liquid yield. This well coincides with the fact that heavy molecules such as poly- and polar-aromatics jump up at the catalyst temperature of 450°C (Table 3). Running at the highest catalyst temperature in the testing range yields the highest amount of gas oil and kerosene. Besides, under the catalyst temperature of 400°C, the production of naphtha, kerosene and gas oil decreases, which is attributed to the high cracking activity under this condition, as mentioned previously.

Since light oils are commercially valuable, from these results together with the fact that aromatic hydrogenation is thermodynamically favoured at low temperatures [32], the catalyst temperature of 350°C was selected for further study on the effects of Ru loading.

### *3.4. Effects of Ru-loading amount*

In this section, the effects of Ru supported on pure silica MCM-41 and the amount of Ru loading (1.0, 1.5 and 2%wt) on the yields and the nature of the products obtained from pyrolysis of waste tire were studied.

#### *3.4.1. Product distribution*

Figure 5 illustrates the effects of Ru loading amount on the product distribution. The data of MCM-41 and

non-catalytic pyrolysis were also included for comparison purpose. It can be seen that the gas yield increases dramatically at the expense of liquid yield when the catalysts were used, especially the ones with Ru loading. For instance, the gas yield obtained from pyrolysis in the absence of a catalyst is approximately 3 times less than that obtained when 2%Ru/MCM-41 was used. The promotion effects of Ru incorporation on cracking activity might be attributed to the combination of metal and acid properties of the bifunctional Ru-supported MCM-41 catalyst. The high hydrogenation activity of Ru [15] probably hydrogenated aromatic HCs, which were reported to be predominant in the products obtained from pyrolysis of waste tire [7 - 9, 11], and then these hydrogenated compounds might undergo catalytic cracking by MCM-41 producing lighter HCs. Free hydrogen is liberated from the pyrolysis products as reported in many studies [2, 5, 6], and/or is generated during the reforming reactions [2, 6]. As indicated by XRD, and $H_2$-chemisorption analysis, Ru is highly dispersed in all Ru-supported catalysts. The high dispersion of Ru leads not only to the formation of small Ru particles, inducing some preferential exposed planes, and then favouring hydrogenation properties [42], but also to the better transportation of the reactant/product from the acid sites to the metal sites, and vice versa [16]. That probably explains the higher cracking activity of Ru supported catalysts as compared to MCM-41. Additionally, the gas yield was found to gradually increase with increasing Ru content. 2%Ru/MCM-41 produced the highest yield of gas in line with a lowest liquid yield. This might be attributed to a good balance between metal and acid sites, as a result of the high concentration of ruthenium at approximately the same dispersion, which was reported to be a crucial factor controlling the activity of a bifunctional catalyst [43]. Also, the high activity of Ru-supported catalysts leads to a drastic reduction in asphaltenes (Table 1).

*3.4.2. Pyrolytic oil*

The effect of Ru loading amount can be further depicted from the petroleum cuts as shown in Figure 6. From the figure, the use of catalysts decreases gas oil and residues in accordance with the increment in the light fractions; naphtha and kerosene. The oils obtained over Ru-supported catalysts have higher content of light fractions as compared to that produced over MCM-41. This is again attributed to their bifunctionality. Moreover, the contents increase with increasing Ru loading. As compared to 1.5%Ru/MCM-41, 2%Ru/MCM-41 produces

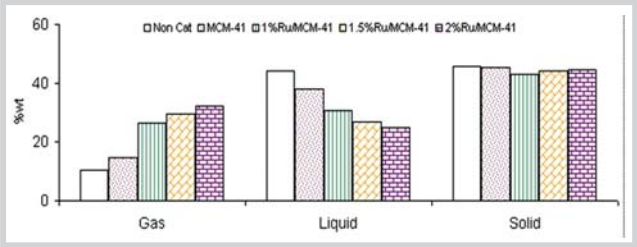



***Figure 5.*** *Effect of Ru loading amount on product distribution*

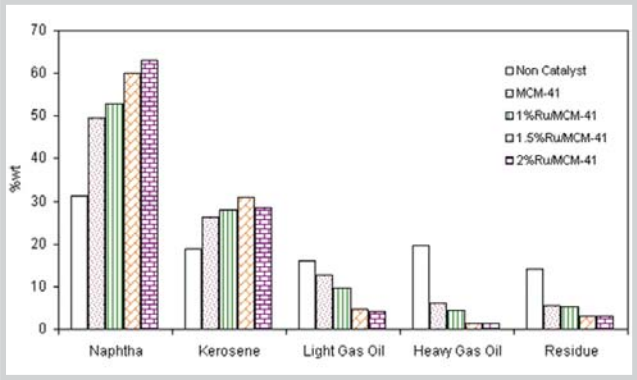



***Figure 6.*** *Petroleum cuts of pyrolytic oils obtained from using various Ru percentages*

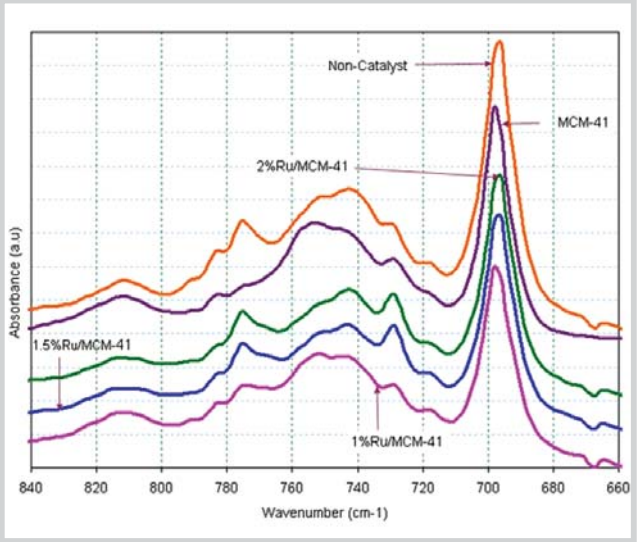



***Figure 7.*** *IR spectra of pyrolytic oils obtained from thermal and catalytic pyrolysis*

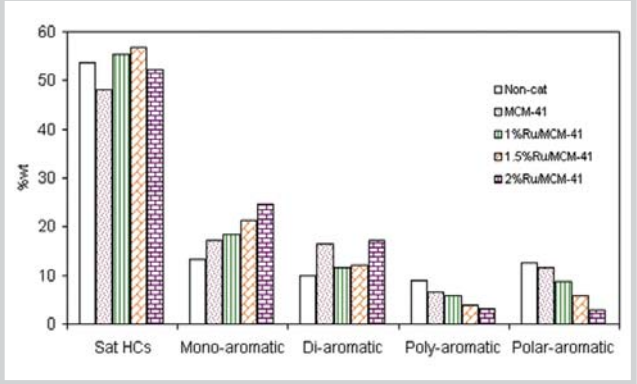



***Figure 8.*** *The chemical compositions of pyrolytic oils obtained from thermal and catalytic pyrolysis*

the oil having slightly higher naphtha and less kerosene whereas the heavier gas oil fractions remain constant, indicating that 2%Ru/MCM-41 further cracks or transforms kerosene to naphtha and light gases.

Figure 8 illustrates the FTIR spectra of the derived oils. In the figure, bands at the wave number of 740cm$^{-1}$ and 700cm$^{-1}$ indicate the presence of poly-aromatics including biphenyl [32, 44]. As such, Ru-supported catalysts produce the oils having the lowest band intensity, indicating their low poly-aromatic contents. And the polycyclic aromatics decrease with increasing ruthenium loading. This is well consistent with the results obtained from liquid adsorption chromatography, as depicted in Figure 9. Besides, from the figure, a gradual increase in mono-aromatics in accordance with a decrease in poly- and polar-aromatics is observed as the ruthenium content increases. Ruthenium based catalyst was found to exhibit high hydrogenation activity [15], and its activity increased with increasing ruthenium loading [30, 45]. Akhemedov and Al-Khowaiter [46] found that Ru/ZSM-5 demonstrated much higher C-C bond cleavage selectivity in cycloalkanes in comparison with alkanes. Meanwhile, the hydrogenation of aromatics occurs mostly over the metallic function of the catalyst, although the acid sites have some hydrogenation activity [47], but the rate is considerably lower than that of metal sites [48]. It was also reported that hydrogenation of polycyclic aromatics is more preferable than single-ring aromatics [48 - 50] and generally yields partial hydrogenated products [51]. In the present study, Ru is well dispersed in all samples, as indicated by XRD, $H_2$-chemisorption analysis. Therefore, it is likely that increasing Ru loading benefits a higher hydrogenation activity, promoting conversion of poly-aromatics to (partial) hydrogenated compounds, which would further undergo ring-opening and/or cracking over acid sites. As a consequence, higher concentration of mono-aromatics and light fractions are achieved.

On the other hand, the increasing ruthenium loading also leads to the gradual reduction in polar-aromatics (Figure 8). Several explanations might be extended to explain the polar-aromatic reduction having occurred in the cases of Ru-supported catalysts. The increasing ruthenium content would prevent polar-aromatic formation due to the enhanced hydrogenation activity [52]. At the same time, side cracking reaction that produces polar-aromatics with lower molecular weights [53, 54] might also be a candidate. And, the high amount of coke generated on the spent Ru-supported catalysts (Table 1) as a result of the accumulation of polar-aromatic compounds [53] should not be excluded. Besides, the increase in hydrogenation activity with increasing ruthenium content in the catalyst might promote the hydrodesulfurisation (HDS) reactions, causing the reduction of polar-aromatics. This is more likely to occur since the HDS of the feed containing both polar-aromatics and other polycyclic aromatics mainly followed the HYD pathway due to the competition adsorption on the active sites [55]. And, it is also well-known that the HDS reactions via HYD pathway lead to the formation of mono-aromatic [56]. That probably explains the gradual increase in mono-aromatics at the expense of polar-aromatics as observed in Figure 8.

Finally, the reason for a high concentration of di-aromatics in the oil obtained over 2%Ru/MCM-41 (Figure 8) is not clear. However, from the FTIR analysis (Figure 7, the bands at the wave number of around 700cm$^{-1}$), it seems that the high di-aromatics content might be attributed, or at least partially, to the high concentration of bi-phenyl and its substituted compounds [47]. Therefore, it is possible that the presence of high amount of Ru sites on the very large surface of MCM-41, to a certain extent, decreases the steric hindrance, resulting in a promotion effect on the occurrence of the HDS reaction via DDS route, which is well known to produce di-aromatics [56]. Pawelec et al. [57] found that the HDS of 4,6 dimethyl-dibenzothiophene on CoMo/P/Ti-HMS (Hexagonal Mesoporous Silica material_HMS) catalysts occurred via (i) dealkylation, resulting in dibenzothiophene formation; and (ii) isomerisation (main route) to produce 3,6 dimethyl-DBT, and eventually 3,4' dimethyl-biphenyl and 3,4' methylcyclohexyl toluene products. However, no study on Ru-supported pure silica MCM-41 have been published for the ability of this catalyst to drive the HDS of 4,6 dimethyl-DBT via the isomerisation route as introduced by Pawelec [57]. But, to study this is out of the scope of this research work. Therefore, a further study is needed to elucidate this issue.

## 4. Conclusions

Catalytic temperatures strongly influenced the product distribution and the nature of the products obtained from the MCM-41 catalysed-pyrolysis of waste tire. The oil yield first decreased, and then increased with catalyst temperature. Under the highest studied catalyst temperature, the highest poly- and polar-aromatics were

produced. In addition, increasing catalyst temperature decreased the yield of naphtha in accordance with the increment of heavier fractions. These phenomena might be attributed to the combination effects of high catalyst temperature, the meso-pore and acid properties of MCM-41, leading to the preference occurrence of alkylation, aromatisation and Diel-Alder reactions.

Ru was highly dispersed in all Ru-supported catalysts. The incorporation of Ru on the surface of MCM-41 was found to have promotion effects on the catalytic activity. And the catalytic activity increased with increasing Ru loading, which was attributed to a better hydrogenation activity. Gas yield gradually increased at the expense of the liquid yields with Ru content in the bifunctional catalysts. Furthermore, Ru-supported catalysts produced much lighter oils as compared to MCM-41 and non-catalytic pyrolysis. A higher selectivity toward light petroleum fractions was also observed over a catalyst having higher concentration of ruthenium metal sites. That was explained by the promotion in the hydrogenation of both poly- and polar-aromatics, as Ru loading increased, followed by ring-opening and/or cracking producing lower molecular weight hydrocarbons.

**References**


1. S.Galvagno, S.Casu, T.Casabianca, A.Calabrese, G.Cornacchia. *Pyrolysis process for the treatment of scrap tyres: preliminary experimental results*. Waste Management. 2002; 22(8): p. 917 - 923.

2. C.Berrueco, E.Esperanza, F.J.Mastral, J.Ceamanos. P.García-Baicaicoa. *Pyrolysis of waste tyres in an atmospheric static-bed batch reactor: Analysis of the gases obtained*. Journal of Analytical and Applied Pyrolysis. 2005; 74(1 - 2): p. 245 - 253.

3. UK Environment Agency. *Tires in the environment*. 1998.

4. Mahmood M.Barbooti, Thamer J.Mohamed, Alla A.Hussain, Falak O.Abas. *Optimization of pyrolysis conditions of scrap tires under inert gas atmosphere.* Journal of Analytical and Applied Pyrolysis. 2004; 72(1): p. 165 - 170.

5. E.Aylón, R.Murillo, A.Fernández-Colino, A.Aranda, T.García, M.S.Callén, A.M.Mastral. *Emissions from the combustion of gas-phase products at tyre pyrolysis*. Journal of Analytical and Applied Pyrolysis. 2007; 79(1 - 2): p. 210 - 214.

6. Paul T.Williams, David T.Taylor. *Aromatization of tyre pyrolysis oil to yield polycyclic aromatic hydrocarbons*. Fuel. 1993; 72(11): p. 1469 - 1474.

7. B.Benallal, C.Roy, H.Pakdel, S.Chabot, M.A.Poirier. *Characterization of pyrolytic light naphtha from vacuum pyrolysis of used tyres comparison with petroleum naphtha*. Fuel. 1995; 74(11): p. 1589 - 1594.

8. Adrian M.Cunliffe, Paul T.Williams. *Composition of oils derived from the batch pyrolysis of tyres*. Journal of Analytical and Applied Pyrolysis. 1998; 44(2): p. 131 - 152.

9. Paul T.Williams, Richard P.Bottrill. *Sulfur-polycyclic aromatic hydrocarbons in tyre pyrolysis oil*. Fuel. 1995; 74(5): p. 736 - 742.

10. P.T.Williams, A.J.Brindle. *Catalytic pyrolysis of tyres: influence of catalyst temperature*. Fuel. 2002; 81(18): p. 2425 - 2434.

11. P.T.Williams, A.J.Brindle. *Aromatic chemicals from the catalytic pyrolysis of scrap tyres*. Journal of Analytical and Applied Pyrolysis. 2003; 67(1): p. 143 - 164.

12. S.Boxiong, W.Chunfei, G.Binbin, W.Rui, Liangcai. *Pyrolysis of waste tyres with zeolite USY and ZSM-5 catalysts*. Applied Catalysis B: Environmental. 24 2007; 73(1 - 2): p. 150 - 157.

13. N.A.Dung, A.Mhodmonthin, S.Wongkasemjit, S.Jitkarnka. *Effects of ITQ-21 and ITQ-24 as zeolite additives on the oil products obtained from the catalytic pyrolysis of waste tire.* Journal of Analytical and Applied Pyrolysis. 2009; 85(1 - 2): p. 338 - 344.

14. Alois Lugstein, Andreas Jentys, Hannelore Vinek. *Hydroisomerization and cracking of n-octane and C8 isomers on Ni-containing zeolites*. Applied Catalysis A: General. 1999; 176(1): p.119 - 128.

15. M.A.Ali, T.Kimura, Y.Suzuki, M.A.Al-Saleh, H.Hamid, T.Inui. *Hydrogen spillover phenomenon in noble metal modified clay-based hydrocracking catalysts*. Applied Catalysis A: General. 2002; 277(1 - 2): p. 63 - 72.

16. D.Eliche-Quesada, J.M.Meria-Robles. E.Rodriguez-Castellon, A.Jimenez-Lopez. *Influence of the incorporation of palladium on Ru/MCM hydrotreating catalysts*. Applied Catalysis B: Environmental. 2006; 65(1 - 2): p.118 - 126.

17. D.Eliche-Quesada, M.I.Macias-Ortiz, J.Jimenez-Jimenez, E.Rodriguez-Castellon, J.Jimenez-Lopez. *Catalysts based on Ru/mesoporous phosphate heterostructures (PPH) for hydrotreating of aromatic hydrocarbons*. Journal of Molecular Catalysis A: Chemical. 2006; 225(1 - 2): p. 41 - 48.

18. J.B.McKinley. *Catalysis*. New York: Reinhold. 1957.

19. T.A.Pecoraro, R.R.Chianelli. *Hydrodesulfurization catalysis by transition metal sulfides*. Journal of Catalysis. 1981; 67: p. 430 - 445.

20. J.Barbier, E.Lamy-Pitara, P.Marecot, J.P.Boitiaux, J.Cosyns, F.Verna. *Role of sulfur in catalytic hydrogenation reactions*. Advances in Catalysis. 1990; 37: p. 279 - 318.

21. Joeng-Kyu Lee, Hyun-Ku Rhee. *Sulfur tolerance of zeolite beta-supported Pd-Pt catalysts for the isomerization of n-hexane*. Journal of Catalysis. 1998; 177: p. 208 - 216.

22. E.Rodriguez-Castellon, J.Merida-Robles, L.Diaz, P.Maireles-Torres, J.J.Jones, J.Roziere, A. Jimenez-Lopez. *Hydrogenation and ring opening of tetralin on noble metal supported on zirconium doped mesoporous silica catalysts*. Applied. Catalysis. A: General. 2004; 260: p. 9 - 18.

23. S.Gao, L.D.Schmidt. *Effect of oxidation-reduction cycling on $C_2H_6$ hydrogenolysis: Comparison of Ru, Rh, Ir, Ni, Pt, and Pd on $SiO_2$*. Journal of Catalysis. 1989; 115(2): p. 356 - 364.

24. Vagif M.Akhmedov, S.H.Al-Khowaiter. *Hydro-conversion of hydrocarbons over Ru-containing supported catalysts prepared by metal vapor method*. Applied Catalysis A: General. 2000; 197(2): p. 201 - 212.

25. Nguyen Anh Dung. *Catalytic pyrolysis of waste tire using noble metals-supported HMOR catalysts*. Petrovietnam Journal. 2015; 6: p. 43 - 50.

26. M.A.Uddin, Y.Sakata, A.Muto, Y.Shiraga, K.Koizumi, Y.Kanada, K.Murata. *Catalytic degradation of polyethylene and polypropylene into liquid hydrocarbons with mesoporous silica*. Microporous and Mesoporous Materials. 1998; 21: p. 557 - 564.

27. Z.S.Seddegi, U.Budrthumal, A.A.Al-Arfaj, A.M.Al-Amer, S.A.I.Barri. *Catalytic cracking of polyethylene over all-silica MCM-41 molecular sieve*. Applied Catalysis A: General. 2002; 225: p. 167 - 176.

28. Boxiong Shen, Chunfei Wu, Rui Wang, Binbin Guo, Cai Liang. *Pyrolysis of scrap tyres with zeolite USY*. Journal of Hazardous Materials. 2006; 137: p. 1065 - 1073.

29. W.Charoenpinijkarn, M.Suwankruhasn, B.Kesapabutr, S.Wongkasemjit, A.M.Jamieson. *Sol-gel processing of silatranes*. European Polymer Journal. 2001; 37(7): p. 1441 - 1448.

30. N.Thanabodeekij, S.Sadthayanon, E.Gulari, S.Wongkasemjit. *Extremely high surface area of ordered mesoporous MCM-41 by atrane route*. Materials Chemistry and Physics. 2006; 98: p. 131 - 137.

31. G.Sebor, J.Blazek, M.F.Nemer. *Optimization of the preparative separation of petroleum maltenes by liquid adsorption chromatography*. Journal of Chromatography A. 1999; 847: p. 323 - 330.

32. Eliche-Quesada, J.M.Merida-Robles, E. Rodríguez-Castellon, A. Jiménez-Lopez. *Ru, Os and Ru-Os supported on mesoporous silica doped with zirconium as mild thio-tolerant catalysts in the hydrogenation and hydrogenolysis/hydrocracking of tetralin*. Applied Catalysis A: General. 2005; 279(1 - 2): p. 209 - 221.

33. S.H.Wang, P.R.Griffiths. *Resolution enhancement of diffuse reflectance i.r. spectra of coals by Fourier self-deconvolution: 1. C-H stretching and bending modes*. Fuel. 1985; 64: p. 229 - 236.

34. C.A.Islas-Flores, E.Buenrostro-Gonzalez, C.Lira-Galeana. *Fractionation of petroleum resins by normal and reverse phase liquid chromatography*. Fuel. 2006; 85: p. 1842 - 1850.

35. Z. Liu, X. Meng, C. Xu, J. Gao *Secondary cracking of gasoline and diesel from heavy oil catalytic pyrolysis*. Chinese Journal of Chemical Engineering. 2007; 15(3): p. 309 - 314.

36. X.Meng, C.Xu, J.Gao, Lili. *Studies on catalytic pyrolysis of heavy oils: Reaction behaviors and mechanistic pathways*. Applied Catalysis A: General. 2005; 294( 2): p. 168 - 176.

37. John J.McKetta. *Chemical processing handbook*. CRC Press. 1993.

38. Z.Zhao, W.Qiao, X.Wang, G.Wang, Z.Li, L.Cheng. *Effect of alkaline earth metals on catalytic performance of HY zeolite for alkylation of α-methylnaphthalene with long-chain olefins*. Microporous and Mesoporous Materials. 2006; 94(1 - 3): p. 105 - 112.

39. G.San Miguel, J.Aguado, D.P.Serrano, J.M.Escola. *Thermal and catalytic conversion of used tyre rubber and its polymeric constituents using Py-GC/MS*. Applied Catalysis B: Environmental. 2 May 2006; 64(3 - 4): p. 209 - 219.

40. K.H.Lee, Y.W.Lee, B.H.Ha. *Catalytic cracking of vacuum gas oil on the dealuminated mordenites*. Journal of Catalysis. 1998; 178(1): p. 328 - 337.

41. P.B.Venuto, T.E.Habib. *Fluid catalytic cracking with zeolite catalysts*. Marcel Dekker, New York. 1979.

42. R.M.Navarro, P.Castaño, M.C.Álvarez-Galván, B.Pawelec. *Hydrodesulfurization of dibenzothiophene and a SRGO on sulfide Ni(Co)Mo/Al$_2$O$_3$ catalysts. Effect of Ru and Pd promotion*. Catalysis Today. 2009; 143(1 - 2): p. 108 - 114.

43. A. Soualah, J.L. Lemberton, L. Pinard, M. Chater, P. Magnoux, K. Moljord. *Hydroisomerization of long-chain n-alkanes on bifunctional Pt/zeolite catalysts: Effect of the zeolite structure on the product selectivity and on the reaction mechanism*. Applied Catalysis A: General. 2008; 336(1 - 2): p. 23 - 28.

44. C.Jäger, F.Huisken, H.Mutschke, Th.Henning, W.Poppitz, I.Voicu. *Identification and spectral properties of PAHs in carbonaceous material produced by laser pyrolysis*. Carbon. 2007; 45(15): p. 2981 - 2994.

45. D.Eliche-Quesada, E.Rodríguez-Castellón, A.Jiménez-López. *Hydrodesulfurization activity over supported sulfided ruthenium catalysts. Influence of the support*. Microporous and Mesoporous Materials. 2007; 99(3): p. 268 - 278.

46. V.M.Akhmedov, S.H.Al-Khowaiter. *Hydroconversion of hydrocarbons over Ru-containing supported catalysts prepared by metal vapor method*. Applied Catalysis A: General. 2000; 197(2): p. 201 - 212.

47. O.Cairon, K.Thomas, A.Chambellan, T.Chevreau. *Acid-catalysed benzene hydroconversion using various zeolites: Brönsted acidity, hydrogenation and side-reactions*. Applied Catalysis A: General. 2003; 238(2): p. 167 - 183.

48. P.Castano, B.Pawelec, J.L.G.Fierro, J.M.Arandes, J.Bilbao. *Aromatics reduction of pyrolysis gasoline (PyGas) over HY-supported transition metal catalysts.* Applied Catalysis A: General. 2006; 315: p. 101 - 113.

49. A.Corma, A.Martínez, V.Martínez-Soria. *Hydrogenation of aromatics in diesel fuels on Pt/MCM-41 Catalysts*. Journal of Catalysis. 1997; 169(2): p. 480 - 489.

50. S.Jongpatiwut, Z.Li, D.E.Resasco, W.E.Alvarez, E.L. Sughrue, G.W.Dodwell. *Competitive hydrogenation of poly-aromatic hydrocarbons on sulfur-resistant bimetallic Pt-Pd catalysts*. Applied Catalysis A: General. 2004; 262(2): p. 241 - 253.

51. M.Jacquin, D.J.Jones, J.Roziere, S.Albertazzi, A.Vaccari, M.Lenarda, L.Storaro, R.Ganzerla. *Novel supported Rh, Pt, Ir and Ru mesoporous aluminosilicates as catalysts for the hydrogenation of naphthalene*. Applied Catalysis A: General. 2003; 251(1): p. 131 - 141.

52. N.A. Dung, R. Klaewkla, S. Wongkasemjit, S. Jitkarnka. *Light olefins and light oil production from catalytic pyrolysis of waste tire.* Journal of Analytical and Applied Pyrolysis. 2009; 86(2): p. 281 - 286.

53. A.Corma, C.Martinez, G.Ketley, G.Blair. *On the mechanism of sulfur removal during catalytic cracking*. Applied Catalysis A: General. 2001; 208(1 - 2): p. 135 - 152.

54. J.A.Valla, A.A.Lappas, I.A.Vasalos. *Catalytic cracking of thiophene and benzothiophene: Mechanism and kinetics*. Applied Catalysis A: General. 2006; 297(1): p. 90 - 101.

55. H.Pakdel. D.M.Pantea, C.Roy. *Production of Dl-limonene by vacuum pyrolysis of used tires*. Journal of Analytical and Applied Pyrolysis. 2001; 57(1): p. 91 - 107.

56. H.Wang, R.Prins. *Hydrodesulfurization of dibenzothiophene and its hydrogenated intermediates over sulfided Mo/γ-Al$_2$O$_3$*. Journal of Catalysis. 2008; 258(1): p. 153 - 164.

57. B.Pawelec, J.L.G.Fierro, A.Montesinos, T.A.Zepeda. *Influence of the acidity of nanostructured CoMo/P/Ti-HMS catalysts on the HDS of 4,6-DMDBT reaction pathways.* Applied Catalysis B: Environmental. 2008; 80(1 - 2): p. 1 - 14.

# WHAT FUTURE GAS PRICE MECHANISM FOR VIETNAM?

Rebecca Keller
*IHS*
*Email: Rebecca.Keller@ihs.com*

**Summary**

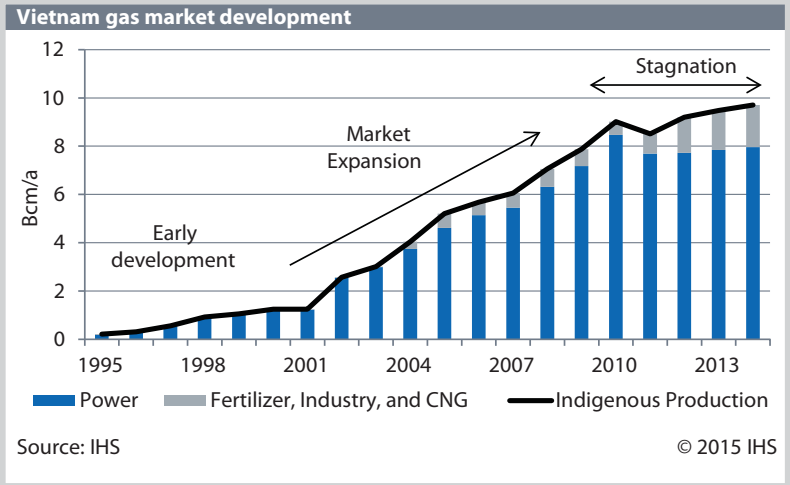
*Gas market expansion proceeded in Vietnam through 2010 despite managed gas pricing, as most indigenous gas reserves could be produced at a relatively low cost. But, as new sources of supply are higher cost, Vietnam must transition to a new pricing mechanism or risk market stagnation and supply declines in the longer term. Vietnam is not alone in this situation, and can draw from lessons learned from other markets in Asia to determine the appropriate pricing mechanism for the market context and government policy objectives. Successful models include gradual introduction of market orientation and price increases.*

***Key words:*** *Gas pricing, LNG.*

## 1. Introduction

Vietnam enjoyed strong gas market expansion in the mid-2000s, through integrated gas-to-power and fertiliser projects which served as long-term offtakers for offshore fields. From 2000 to 2010, annual production grew by over 20% on average, with sales priced at relatively low levels set by the government. Prices were negotiated on a bilateral basis for each project and approved by the government and were initially in the range of USD 1 - 4/MMBtu. From a policy perspective, the government aims to keep prices at a level that is affordable for the price-sensitive power and fertiliser sectors, which account for over 90% of demand. In Vietnam, power generators face regulated pricing for electricity sales which constrains their ability to use higher-cost gas feedstock, while they also faced fuel competition with low-cost generation from coal and hydro power.

This pricing mechanism worked for market expansion initially because offshore gas projects were relatively low-cost fields to develop, especially for associated gas. Vietnam was not alone in this approach; many other developing countries in Asia also put in place low, regulated pricing to support initial development of their domestic gas markets. But, unlike Vietnam, many of these markets have moved towards more market-oriented pricing mechanisms to promote supply growth.




## 2. Assessing Vietnam's current gas pricing mechanism

Lack of indigenous gas resources or import potential is not to blame for market stagnation. The BP Statistical Review of World Energy reported the country has over 20Tcf (0.6Tcm) of gas reserves as of end-2014 [1]. Vietnam has several large offshore gas discoveries which could be developed to support greenfield power and petrochemicals projects. In addition to domestic supply, Vietnam could benefit from tapping into the global liquefied natural gas (LNG) market, which is entering a period of supply abundance and a softening of prices caused by lower oil prices and a number of new LNG export projects starting in Australia and North America.

Lack of gas demand potential is also not hindering market growth. Rising power demand from strong economic growth is creating a huge need for new power capacity, while there is also scope for gas to meet growing demand in the industrial and petrochemicals sectors. The government has long recognised natural gas' role as a valuable fuel in the supply mix. Vietnam's Gas Master Plan (GMP), last released in 2011, targeted gas demand of 1.6 to 2.0Bcf/d by 2015 and 2.1 to 2.6Bcf/d from 2016 - 2026 [2]. Several new gas-fired power plants were identified in Vietnam's Power Development Plan (PDP)

VII (2011 - 2030) to achieve a balanced power mix with coal, the targeted primary generation source [3].

Rather, the gas market has been flat because of delays in sanctioning proposed indigenous gas and LNG import projects, whose successful development hinges on an adoption of a new gas pricing framework. Other supportive government policy is also required, but the need to establish new pricing mechanisms is one of the primary sources of project delay.

In Vietnam, regulated pricing at recent levels (USD 2 - 5/MMBtu) is seen as inadequate by upstream operators to economically develop new gas projects. More difficult-to-develop resources require a premium compared to fields developed in the past. The proposed Block B gas project offshore Southwest Vietnam is one such example. Before Chevron divested its stakes to Petrovietnam in mid-2015, it proposed peak gas flows of 490MMcf/d to be delivered to onshore power plants. This would have expanded the market by ~50% and been a key source of power generation to meet rising electricity demand. But, project sanctioning faced years of delay over negotiations on gas price formation and the field development plan. Chevron was reportedly seeking gas prices in the range of USD 9 - 10/MMBtu, which would have been difficult for baseload power plants to accept based on the current regulated electricity pricing. Another large gas discovery, ExxonMobil's Ca Voi Xanh find, is also likely to be higher cost than current production, due to the need to process the field's high carbon dioxide content. Additional investment to develop associated gas pipeline and downstream infrastructure in the relatively undeveloped central region would lead to further price build-up for offtakers.

Similarly, LNG imports into Vietnam will be higher-priced than current production, even under relatively weak market conditions which started in late 2014. As of mid-2015, both long-term contracted LNG and spot cargoes are being delivered to Asian buyers at USD 7 - 9/MMBtu, the lowest levels seen in years. Delivered costs to end-users would reflect USD 1 - 3/MMBtu of additional charges, making this gas stream much more expensive than current supply.

To realise market expansion and develop known gas discoveries and proposed LNG imports, Vietnam will need to transition to a new price mechanism which addresses the higher cost of new supply. This issue has been acknowledged by the government and was referenced in the GMP 2011, which proposed transitioning away from the current managed policy towards a "competitive wholesale market". Without new investment, Vietnam's gas supply is at risk from production declines within 4 - 5 years, which if unaddressed could lead to gas shortages and low utilisation factors at gas-based fertiliser and power plants. There is also the risk that Vietnam's power generation mix will become too heavily dependent on coal, with resulting environmental and health consequences.

**3. Gas price transition: Lesson learned from Asian markets**

When determining an appropriate pricing mechanism which works in the local market context, Vietnam can draw from experiences of other countries, which provide examples of different paths to price reform. Based on economic theory, price formation should be market-oriented, set by supply and demand conditions and reflective of costs in the long run. But in practice, gas pricing mechanisms are non-uniform globally, and competitive traded gas hubs exist only in mature markets. Common approaches for pricing are cost-plus schemes, fixed price levels with built-in cost escalation over time, or indexation to competing fuels such as oil or even coal.

For emerging markets, energy pricing evolves over time, as markets develop and consumers' ability to pay increases. Regulated pricing is typical at first, to meet objectives of energy affordability, and has been employed across Southeast Asia, India, and China. But once regulations are in place, it is difficult to enact reform, with resistance from end-users accustomed to lower pricing. The consequences of delaying reforms are high in the long run: risking stranded gas resources, under-utilisation gas-fired power plants, shortages in other sectors, and a higher reliance on fuels which are more costly (oil products) or have higher carbon emissions (coal). In addition, if direct subsidies are in place, this creates a high financial burden on the government and diverts state investment from infrastructure and social spending. Subsidies and regulated pricing create market distortions, altering consumer behaviour and risking unsustainable demand growth.

In Asia, price reform has typically occured when countries face a need to develop more difficult and costly indigenous resources or imports to grow supply. In particular, many countries have found that introducing LNG imports requires a new pricing mechanism to

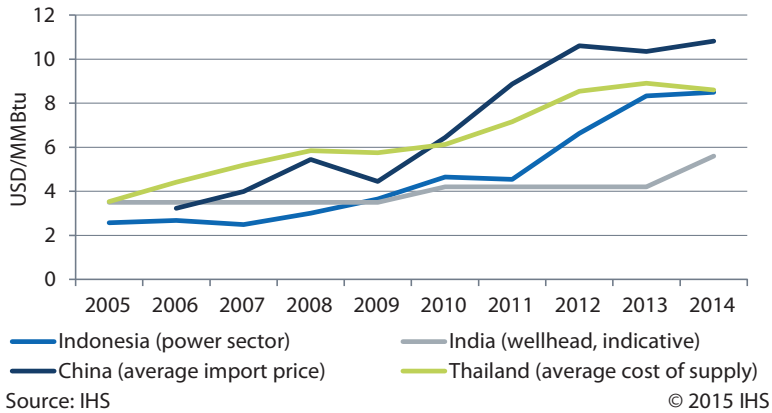
integrate costlier gas into the supply mix. Vietnam is experiencing similar conditions, and will need to follow the path of other markets on price reforms to realise similar supply growth.

In Southeast Asia, Indonesia is one of the leading examples of gas reform success, while Vietnam can also draw lessons from the experiences of China, India, and Thailand. In Indonesia and China, the move towards market orientation has been gradual but steady. Indonesian energy policy targets greater use of gas in a number of sectors, including power, industry, and transport, to reduce the use of oil products and provide a more balanced and sustainable energy mix. But to expand supply and develop domestic gas resources, the government realised it needed to raise pricing along the value chain. Upstream operators had long voiced concerns that wellhead prices were not enabling cost recovery for more difficult fields. Similarly, Indonesia priced domestic LNG at the Asian benchmark, or the regional market price, for sales to local power, industrial, and fertiliser consumers. While price hikes are resisted by some end-users, overall the gas market has grown since reforms began.

China has introduced some reforms, but its gas market remains heavily regulated so that the government can prioritise key sectors and regions for gas supply and preferential pricing. Under this scheme, sales prices have lagged supply costs, but this began to improve once reforms were introduced in 2013. Since then, China has taken several moves to introduce more market factors in price formation. For example, the government has liberalised LNG imports, enacted direct negotiation for industrial gas offtakers, and introduced some regional trading platforms, such as the Shanghai Petroleum Exchange which began trading LNG volumes in 2012.

Thailand provides an example of how another mechanism, gas price pooling can integrate higher-cost gas in the supply mix. The country's Energy Industry Act of 2008 stipulated that tariffs should reflect costs and provide a reasonable return on investment. As a result, prices follow a market-based formula based on oil products pricing which is meant to ensure consistent margins for suppliers. While the market historically enjoyed low-cost gas from indigenous production in the Gulf of Thailand, supply costs have gradually risen for indigenous gas and oil-linked imports from LNG and Myanmar pipeline gas. Average wellhead prices have followed a steady upward trajectory, from about USD 3/MMBtu in 2005 to USD 6 - 8/MMBtu since 2012. While LNG was imported for USD 15 - 16/MMBtu in 2013 - 2014 and pipeline gas was in the USD 10 - 12/MMBtu range, the impact on consumers was mitigated by the weighted average cost of gas scheme. End-users have still experienced price increases, but in an incremental fashion which is easier to accommodate.

**Gas price formation: Asian markets in transition**




Source: IHS © 2015 IHS

India, by contrast, has delayed adjustment of wellhead gas prices to reflect higher development costs of new source fields, and has seen stagnant/declining production as a result. The market turned quickly to LNG as a result, but importers have faced issues finding consumers who can afford higher-cost imports. To accommodate price-sensitive but priority sectors such as fertilisers and power plants, the government has provided support in the form of gas price pooling. It has also subsidised higher gas feedstock costs, a policy which is difficult to sustain in the long run because of the drain on government finances.

## 4. Conclusions

Examples of more successful reform paths, such as those taken by Indonesia, China, and Thailand, can provide lessons learned for Vietnam as it determines a new pricing mechanism to enable market growth. As these markets became exposed to international, market-based LNG pricing, they enacted mechanisms to integrate higher-cost LNG imports into the domestic gas supply mix. This was done gradually to avoid an abrupt impact on end-users accustomed to lower pricing.

Ultimately Vietnam can not avoid a move towards greater market orientation. When establishing a new pricing policy,

it is critical to adopt a scheme which enables adequate return on investment to encourage future projects. This would help attract private exploration and production (E&P) companies to Vietnam which can expedite project development for more costly or difficult projects through investment and technology transfer.

Energy affordability objectives, which have been paramount in Vietnam, should be balanced with those of energy security and sustainability. This does not necessarily mean that affordability targets must completely be sidelined. For example, many gas markets in Asia continue to apply price discrimination by end-use sector to address price sensitivity issues or encourage gas usage. Rather, the government must consider its targets of affordability against detrimental long-term consequences of delayed price reform: market stagnation or decline, stranded gas resources, and higher reliance on costlier or higher-carbon fuels.

**References**

1. BP. *BP statistical review of world energy*. www.bp.com.

2. Prime Minister. *Decision approving the Master Plan to develop Vietnam's gas industry until 2015, with orientations towards 2025*. Decision No. 459/QD-TTg dated 30 March 2011.

3. Prime Minister. *Decision approving the Master Plan to develop national power system during the 2011 - 2020 period with vision towards 2030*. Decision No. 1208/QD-TTg dated 21 July 2011.

# CLEANER PRODUCTION AND APPLICATION IN THE VIETNAM PETROLEUM INDUSTRY

MSc. Nguyen Van Tuan, MSc. Nguyen Lan Huong
*Vietnam Oil and Gas Group*
*Email: tuanv@pvn.vn*

**Summary**

*Cleaner Production (CP) was first introduced in Vietnam in 1995 by the United Nations Environmental Programme (UNEP). According to UNEP, CP is the continuous application of an integrated preventive environmental strategy to processes, products, and services in order to increase efficiency and reduce risks to humans and the environment. The demonstration case studies have figured out that CP can give the opportunities to reduce from 10 - 15% of energy and input material consumption in production. CP brings about not only economic benefit but also environmental one to help improve production efficiency of both big and small companies.*

*This paper introduces the concepts, methodology and benefits of Cleaner Production, its application and practice in the Vietnam National Oil and Gas Group.*

***Key words:*** *Cleaner Production, CP, waste minimisation, emissions, initiatives.*

## 1. Cleaner Production Concept

Cleaner Production (CP) was first introduced in Vietnam by the United Nations Environmental Programme (UNEP) in 1995. According to UNEP, CP is the continuous application of an integrated preventive environmental strategy to processes, products, and services in order to improve ecological productivity and reduce risks to humans and the environment.

Accordingly, CP for products includes reducing negative impacts during the whole life cycle of a product, from design to its disposal. For production processes, CP includes material and energy conservation, toxic material elimination and reduction of the quantity and toxicity of all wastes at source. For services, CP is to incorporate environmental concerns into designing and delivering services.

The objective of CP is to avoid pollution by utiliszing resources, materials and energy with the highest efficiency. Thus, a certain additional proportion of materials and energy which ought to be discarded will be converted into finished products. Therefore, CP not only brings economic benefits to companies, but also helps protect the environment.

Basically, CP is similar to "Waste Minimisation", "Pollution Prevention" or "Green Productivity". However, the approach and methodology of each concept are different.

CP brings economic benefits and reduces waste through pollution prevention measures, which are different from end-of-pipe waste treatment measures. With these benefits, CP is an important step for companies to establish and apply the Environmental Management System ISO 14000.

## 2. Cleaner Production Methodology

To implement CP, we have to conduct CP assessment. CP assessment is a series of activities conducted to identify options that can bring efficiency to production. The CP assessment often focuses on answering the following questions:

- Where waste and emissions are generated;
- Why waste and emissions are generated;
- How waste and emissions can be minimised and eliminated in the company.

CP assessment is a systematic approach to investigate the existing production process and identify opportunities to improve the process or products.

A CP assessment process is divided into 6 steps: (1) Getting started; (2) Analysing process steps; (3) Generating CP options; (4) Selecting CP options; (5) Implementing CP options; (6) Maintaining CP. These steps are divided into 18 specific tasks (Figure 1).

CP implementation is a journey rather than a destination, when a CP assessment is finished, other assessments will be started to improve current conditions or continue with other selected options. CP does not specify limits but requires continuous improvement from a company.

### 3. Cleaner Production benefits

CP brings not only economic benefits but also environmental one, and is of great significance for a company; especially the industrial companies, whether small or big. The case studies have showed that most companies have the potential to reduce from 10 - 15% of energy and input material consumption.

Benefits brought by CP include:

- Improved production efficiency;
- More efficient utiliszation of raw materials, water and energy;
- Recovery of valuable by-products;
- Less pollution;
- Lower costs for waste disposal and waste water treatment;
- Improved image for companies;
- Improved safety and occupational health.

### 4. Cleaner Production application in Vietnam

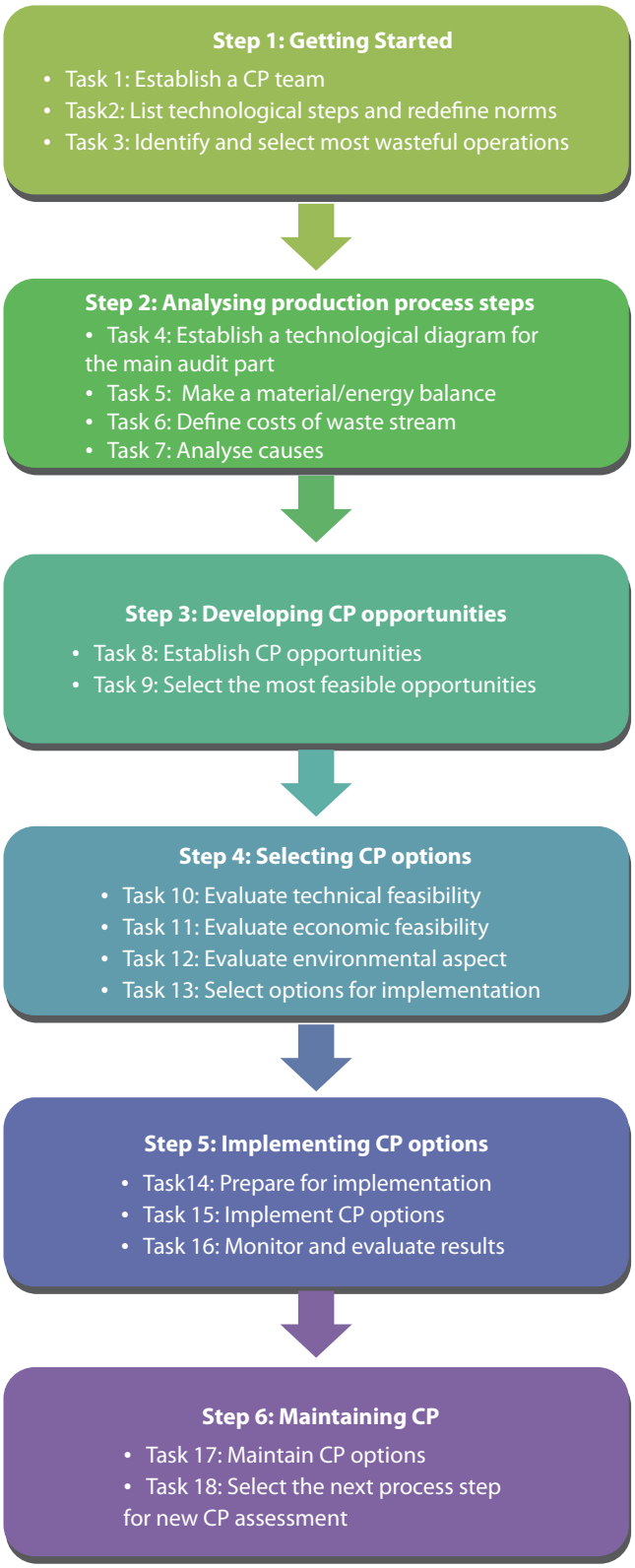
On 22 September 1999, the Minister of Science, Technology and Environment (now the Minister of Science and Technology), on behalf of the Government of Vietnam, signed the International Declaration on Cleaner Production.

In view of the economic and environmental benefits that CP brings about, on 7 September 2009, the Prime Minister signed Decision No. 1419/QD-TTg approving the Cleaner Production Strategy in the Vietnamese Industry to the year of 2020; in which sets the targets by 2015:

- 50% of the industrial companies are aware of the CP benefits in the industrial production;
- 25% of the industrial companies apply CP; the CP applied industrial companies save from 5 - 8% of energy, fuel and raw material consumption per unit of product.

And by the year of 2020:

- 90% of industrial companies are aware of the CP benefits in the industrial production;
- 50% of the industrial companies apply CP; the CP applied companies save from 8 - 13% of energy, fuel and raw material consumption per unit of product;
- 90% of the medium and large companies have established a specialised body responsible for CP.




To implement the Prime Minister's Decision No. 1419/QD-TTg, the Ministry of Industry and Trade has promulgated directives to guide the provincial Departments of Industry and Trade and the industrial companies to develop and implement the Action

Programme on Cleaner Production in order to achieve the targets of the Strategy for Cleaner Production approved by the Prime Minister. According to the statistics on the Ministry of Industry and Trade's website on Cleaner Production, many provinces and cities in Vietnam have been promoting CP application in their industrial sectors. In Hanoi, 54 enterprises have applied CP, of which 16 enterprises have reduced the fuel and raw material consumption per unit of product by over 5%.

CP application is bringing practical benefits to various industrial sectors such as brewery industry, tea processing, leather and footwear, paper and pulp; plastic recycling, steel industry; and building materials, etc.

**5. Cleaner production application in the Vietnam petroleum industry**

Thoroughly aware of the economic and environmental benefits that CP brings about, the Vietnam Oil and Gas Group (PVN), in implementing the guidelines of the Ministry of Industry and Trade, has developed and approved the Action Plan for implementing the Cleaner Production Strategy in Industry toward the year of 2020 by Decision No. 9702/QD-DKVN dated 31 December 2013. PVN's Action Plan has set the targets:

By the year of 2015:

- 50% of the enterprises under PVN having the CP potential shall be aware of the CP benefits;

- 25% of the enterprises under PVN having the CP potential shall apply CP in their production and shall save the energy and material consumption from 3 - 5%;

- 25% of the enterprises under PVN shall have CP staff;

- 70% of the CP responsible staff of PVN will be trained and capable to disseminate, guide, consult and support the CP application in their enterprises.

And from 2016 to 2020:

- 100 % of the enterprises under PVN having the CP potential shall be aware of the CP benefits;

- 50% of the enterprises under PVN having the CP potential shall apply CP in their production and shall save the energy and material consumption from 5 - 8%;

- 50% of the enterprises under PVN shall have CP staff;

- 100 % of the CP responsible staff of PVN will be trained and capable to disseminate, guide, consult and support the CP application in their enterprises.

PVN's CP Action Plan also figures out 6 specific tasks and pinpoint the measures to successfully implement the tasks and the entire plan.

However, since the CP Action Plan was approved by the PVN's President and CEO, the implementation has been behind the planned schedule. Up to now, one of the Action Plan's most important tasks - basic and advanced training for CP staff from PVN affiliates - has not been started yet. Besides objective reasons and the capability of the unit which was appointed as the implementing body of the Plan, there are also subjective reasons which come from some of the PVN functional divisions, as well as the inefficient internal co-ordination.

Although the basic and advanced training courses to provide a more systematic and professional methodology for CP have not really been launched yet, many industrial enterprises under PVN, such as Binh Son Refining and Petrochemical Company Limited (BSR), Petrovietnam Fertilizer and Chemicals Corporation (PVFCCo), and PetroVietnam Camau Fertilizer Company Limited (PVCFC) have been very interested in saving raw materials and energy consumption, as well as, reducing emissions into the environment through technical innovations and systematic application of initiatives. Every year, engineers of these enterprises have generated hundreds of initiatives, bringing about the savings of billion VND. In 2012, only 5 industrial enterprises under PVN generated and applied 319 initiatives, bringing about the savings of 394 billion VND in the first year of application. In 2013, 302 initiatives in PVN's enterprises saved in total 1,703 billion VND in the first year of application. Many initiatives already applied in PVN's affiliates are in fact a type of cleaner production practice in the Vietnam petroleum industry.

While the survey data for CP assessment of each enterprise under PVN is unavailable, the number of measures registered and the initiatives recognised and applied every year suggest that the potential for CP application inside the PVN's industrial enterprises is huge. The CP application, as demonstrated above, obviously will not only bring practical economic and environmental benefits but also help improve the image for a strong PVN brand among the community. Thus, the CP application is

an objective demand inside PVN and its affiliates, and also a requirement from the Government and the Ministry of Industry and Trade to successfully implement Decision No. 1419/QD-TTg approved by the Prime Minister. What remains is awareness.

In the coming period, the Vietnam National Oil and Gas Group is to determine to boost the implementation of its CP Action Plan, considering it a measure among others to be resolutely deployed by PVN to reduce costs and improve the efficiency of production and business in the context of unpredictable crude oil price decline; and a contribution to the environmental protection and sustainable development of PVN as set out by its Development Strategy.

**References**

1. Vietnam Cleaner Production Centre - Hanoi University of Science and Technology. *Cleaner Production guidelines for SMEs.*

2. Prime Minister. *Decision approving the "Cleaner Production Strategy in Industry toward the year of 2020"*. Decision No. 1419/QD-TTg dated 7 September 2009.

3. Vietnam Oil and Gas Group. *Decision approving and issuing the Action Plan for implementing the Cleaner Production Strategy in Industry toward the year of 2020 of the Vietnam Oil and Gas Group*. Decision No. 9702/QD-DKVN dated 31 December 2013.

4. Ministry of Industry and Trade. http://www.sxsh.vn.



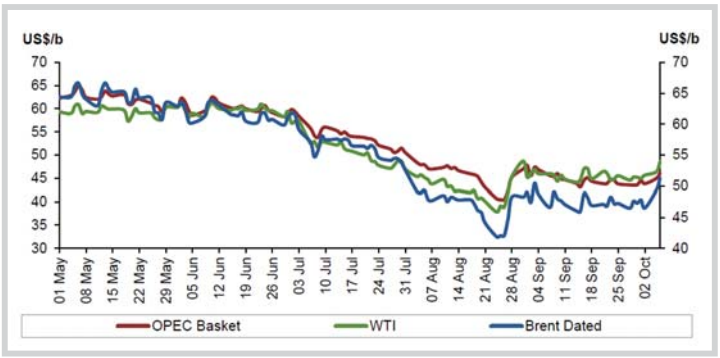
# OIL AND GAS GLOBAL MARKET

**Oil market forecast**

At the end of the market day on October 15, 2015, OPEC Reference Basket stood at USD 45.05/barrel, representing an increase from last month of USD 1.92/barrel. Brent crude oil spot prices increased by USD 3.1/barrel to USD 49.01/barrel while WTI crude oil spot price was at USD 46.28/barrel, up USD 1.7/barrel from last month. This could be a positive sign for oil market compared to September as fundamental factors, that have weighed on the market for more than a year, are starting to show signs of alleviation. However, the crude oil price is forcasted to remain uncertainties. In OPEC's October Oil Market Report (OMR), released on October 12, 2015, crude oil futures were up after two months of steep declines. ICE Brent settled up 33UScent at USD 48.54/barrel, while Nymex WTI jumped by USD 2.58 to USD 45.47/barrel. Compared to a year ago, both remain significantly lower year-to-date at USD 51/barrel and USD 56.61/barrel, respectively. Speculators' overall bullish bets on crude oil grew over the month as long positions in futures and options rose, while the group's short positions, or bets on lower oil prices, fell. The Brent premium over WTI eased considerably over the month, by more than USD 2, as the US marker was supported by inventory draws at its pricing hub, while Brent was pressured by oversupply. The Brent - WTI spread narrowed from USD 5.30/barrel in August to USD 3.05/barrel in September, its narrowest since January.

There are some reasons that drive the uncertain oil market into something significantly more complex.

First is the strength of oil consumption growth. In EIA's Short-term Energy and Winter Fuels Outlook released on October 6, 2015 the oil demand in non-OECD is projected to grow by 0.9 million barrels/day in 2015 and by 1.2 million barrels/day in 2016. China continues to be the main driver of non-OECD oil consumption growth, despite the slowdown in the country's economic growth beginning in the second half of 2014 and with continuing signs of




*Source: OPEC Monthly Oil Market Report - October 2015*

***Figure 1:*** *Crude oil price movement from May to October 2015*

***Table 1.*** *Crude oil futures prices (USD/barrel)*

| Name | Last | Change | Open | High | Low |
|---|---|---|---|---|---|
| WTI (November 2015) | 47.66 | 0.56 | 47.46 | 47.84 | 47.35 |
| WTI (December 2015) | 48.17 | 0.56 | 47.97 | 48.35 | 47.85 |
| WTI (January 2016) | 48.89 | 0.57 | 48.67 | 49.04 | 48.56 |
| WTI (February 2016) | 49.45 | 0.51 | 49.27 | 49.56 | 49.17 |
| Brent (November 2015) | 50.5 | 0.64 | 50.3 | 50.69 | 50.05 |
| Brent (December 2015) | 50.87 | 0.62 | 50.8 | 51.08 | 50.46 |
| Brent (January 2016) | 51.55 | 0.62 | 51.54 | 51.71 | 51.32 |
| Brent (February 2016) | 51.61 | -2.55 | 54.60 | 54.65 | 51.61 |

*Source: Barchart.com - October 13, 2015*

weakening in its economy. China's consumption growth is expected to average 0.3 million barrels/day in 2015 and in 2016. Iran is expected to experience an uptick in economic activity and petroleum consumption in 2016, assuming implementation of the Joint Comprehensive Plan of Action (JCPOA) between Iran and the five permanent members of the United Nations Security Council plus Germany (P5+1) announced on July 14.

After falling by 0.3 million barrels/day in 2014, OECD petroleum and other liquids consumption is expected to rise by 0.5 million barrels/day in 2015 and by 0.2 million barrels/day in 2016, reaching an average of 46.4 million barrels/day, the highest annual average level of OECD consumption since 2010. The increase in 2015 stems from both economic and weather factors, with the United States contributing most of the annual consumption growth. US consumption is expected to grow by an average of 0.3 million barrels/day in 2015 and by 0.1 million barrels/day in 2016. Several other OECD countries saw economic conditions improve as they emerged from recessions, particularly countries in Asia and, to a lesser extent, in Europe. In addition, colder-than-normal weather early in 2015 across OECD Europe contributed to a projected 0.1 million barrels/day increase in consumption in 2015.

Second is the pace and volume at which Iranian oil re-enters the market beside the production of OPEC members and the responsiveness of non-OPEC production to low oil prices, especially the US. In the October OMR, OPEC predicted that non-OPEC oil supply is estimated to average 57.24 million barrels/day in 2015, revised down by 0.16 million barrels/day from last month's estimation, on the prediction that US supply declines are likely to accelerate, given the persistently low oil prices. OECD Americas and Africa oil supply were revised down, whereas in other regions, particularly OECD Europe, Other Asia, Latin America and the FSU, supply figures were revised up, partially offsetting the downward revisions. Non-OPEC oil supply in 2016 is now forecast at an average of 57.11 million barrels/day, a contraction of 0.13 million barrels/day from 2015 levels. This is 0.29 million barrels/day lower than the previous forecast of OPEC and is based on an expected steeper production decline in US shale plays, and legacy wells outnumbering newly drilled wells, as well as the negative effects of capex cuts in different regions of the world. Non-OPEC production growth in 2015 is largely attributable to investments made when oil prices were higher. Redirection of investment is also helping to maintain or grow production levels in non-OPEC producing countries. Companies have reduced exploration investment, and are directing a greater share of investment toward currently producing fields. This redirection of investment helps maintain production levels in the short term, but could result in lower future production.

EIA forecasts OPEC crude oil production to increase by 0.8 million barrels/day to 37.31 million barrels/day in 2015 and to remain relatively flat at 37.60 million barrels/day in 2016, led by OPEC's two largest producers: Saudi Arabia and Iraq. Iraq is expected to be the largest contributor to OPEC production growth in 2015.

In 2016, additional OPEC crude oil supply is expected to come from Iran, which is forecast to increase production if international sanctions targeting its oil sector are suspended. According to the Guardian, Ali Kardor, director of investment affairs and financial provision at National Iranian Oil Co. (NIOC), said Iran currently produces 3 million barrels/day, of which 1.3 million barrels/day are exported but they expected to increase to 2.3 million barrels/day in May or June 2016.

Saudi Arabia and other OPEC member countries are not expected to reduce production to accommodate additional Iranian volumes, although some producers will see production declines in the near term.

The global production is predicted to continue to outpace the demand, leading to strong inventory builds throughout the forecast period. Global oil inventory builds in the second quarter of 2015 averaged 2.3 million barrels/day, compared with 1.8 million barrels/day in the first quarter of the year. The pace of inventory builds is expected to slow in the second half of the year, to roughly 1.5 million barrels/day. In 2016, inventory builds are expected to slow to an average of 0.8 million barrels/day. Surplus capacity is typically an indicator of market conditions, and surplus capacity below 2.5 million barrels/day indicates a relatively tight oil market, but the current and forecast levels of global inventory builds make the projected low surplus capacity level in 2015 less significant.

Finally, a weakening dollar and Russia's military involvement in Syria is attributed to the crude oil market. Oil prices rose sharply over the dollar weakened due to the message from the September policy meeting minutes of the US Federal Reserve System (FED) released, on October 8 which showed that Fed officials held off on raising interest rates because of concerns about low

inflation. The USD index, which measures the value of the USD relative to other currencies, had down 0.4% yesterday. Falling in dollar often impacts to raise oil prices. Besides, Russia's military operations in Syria could increase geopolitical tensions and the risk of a crude oil supply disruption from the Middle East over the long term.

Fundamental business conditions for integrated oil and gas companies will worsen before signs of improvement appear late next year, according to a Moody's Investors Service assessment based on reduced expectations for crude oil and natural gas prices. Moody's expects earnings before interest, taxes, depreciation, and amortisation (EBITDA) for the global integrated oil and gas industry to contract by 20% or more this year and to recover only modestly in 2016.

"This view is based on our expectations of revenue and cash flow declines and a negative free cash flow profile for the industry in 2015," the firm says. "We expect the industry's free cash flow to remain negative in 2016."

Free cash flow is the difference between cash flow from operations and investments. Moody's expects total free cash flow for the integrated companies it rates to be negative by as much as USD 80 billion this year, compared with a negative USD 26 billion in 2014.

"The cash flow gap at recent pricing levels should ease somewhat in 2016 to the area of USD 55 billion," says Moody's. The firm assigned the global integrated oil and gas industry a negative investment rating, indicating expectations for worsening business fundamentals during the next 12 - 18 months. Companies rated by Moody's are ExxonMobil Corp., Chevron Corp., Royal Dutch Shell PLC, Total SA, Statoil ASA, BG Energy Holdings, BP PLC, Eni SPA, OMV AG, and Repsol SA.

The ratings firm expects cuts in capital spending by integrated companies next year to be larger than the 10 - 20% reductions this year. Because some companies, including Total and Chevron, continue to invest heavily in large projects, Moody's says, "if oil prices continue to fall, the industry's negative free cash flow profile could increase in 2016". Still, cuts in spending and operating costs as well as asset sales will cushion the effect of lower oil prices.

Moody's notes that full-cycle costs rose to about USD 50/barrel of oil equivalent for the companies over the past 4 years, while the ratio of per-barrel cash margins to 3-year average finding and development costs-a metric called the leveraged full-cycle ratio - has fallen from 2.54:1 in 2011 to 1.56:1 in 2014 and 1.25:1 in the 12 months ending in June.

Costs are falling, however, in response to spending cuts and overcapacities in drilling and other service industries. The big operators are renegotiating and canceling rig contracts, improving supply-chain management, and standardising project design. "We expect the benefits of lower costs to fully show up towards the end of 2016, bringing upstream margins and returns more in line with lower oil prices," Moody's says.

Most of the integrated companies are increasing asset sales "to cover negative cash flow, improve capital discipline, bolster cash, and support disciplines," the firm notes. The companies it tracks divested more than USD 35 billion of assets in both 2013 and 2014. The total could reach USD 40 - 60 billion in 2015 - 2016. The price assumptions Moody's adopted in August for West Texas Intermediate crude are USD 50/barrel this year, USD 52/barrel in 2016, and USD 60/barrel in 2017. Its Brent assumptions for those years are USD 55/barrel, USD 57/barrel, and USD 65/barrel.

**Impact of low oil prices on the global petroleum activities**

According to the 2015 World Oil's survey of international petroleum agencies and operators, in recent years (2014 - 2015) the upstream of the oil and gas industry has plunged into a second downturn in a 15-year global E&P spending upcycle after several years stabilised at a high level. In 2014, global spending amounted to USD 729 billion, but this year it seems to be below USD 700 billion. The decline is significantly in the drilling field.

**North America**

The forecast of 2015 offshore drilling worldwide reveals that in North America the well numbers could drop to 252 from 355 wells in 2014, of which US holds 184 wells. Despite gas prices are low, in 2014, US gas well numbers rose to 514,782 from 485,000 active producing gas wells in 2013 and remain approximately unchanged in 2015. In this region, overall, one trend we will be watching will be a shift from oil as a preferred target to natural gas, as the price of crude has dropped below the level where unconventional oil plays can be economically produced but gas has maintained a modest but more reliable price for a long time.

***Table 2.*** *Worldwide supply and demand (million barrel/day)*

| No | Demand/Supply | 2014 | 2015 | | | | | 2016 |
|---|---|---|---|---|---|---|---|---|
| | | | 1st Quarter | 2nd Quarter | 3rd Quarter | 4th Quarter | Year | |
| **A** | **Demand** | **92.7** | **93.5** | **93.7** | **95.0** | **95.5** | **94.4** | **95.8** |
| 1 | **OECD** | **45.7** | **46.5** | **45.3** | **46.5** | **46.7** | **46.2** | **46.4** |
| | Americas | 24.1 | 24.2 | 24.1 | 24.8 | 24.8 | 24.5 | 24.7 |
| | Europe | 13.4 | 13.4 | 13.5 | 13.8 | 13.5 | 13.6 | 13.6 |
| | Asia Oceania | 8.2 | 8.8 | 7.7 | 7.8 | 8.3 | 8.1 | 8.1 |
| 2 | **Non-OECD** | **47.1** | **47.1** | **48.4** | **48.5** | **48.8** | **48.2** | **49.4** |
| | FSU | 4.9 | 4.6 | 4.8 | 5.0 | 4.9 | 4.8 | 4.8 |
| | Europe | 0.7 | 0.7 | 0.7 | 0.7 | 0.7 | 0.7 | 0.7 |
| | China | 10.6 | 10.8 | 11.2 | 10.9 | 11.2 | 11.0 | 11.4 |
| | Other Asia | 12.0 | 12.4 | 12.5 | 12.2 | 12.7 | 12.5 | 12.9 |
| | Americas | 6.8 | 6.7 | 6.9 | 7.0 | 7.0 | 6.9 | 7.0 |
| | Middle East | 8.1 | 7.7 | 8.3 | 8.7 | 8.1 | 8.2 | 8.4 |
| | Africa | 4.0 | 4.1 | 4.1 | 4.0 | 4.2 | 4.1 | 4.2 |
| **B** | **Supply** | **93.7** | **95.0** | **96.3** | | | | |
| 1 | **OECD** | **22.9** | **23.7** | **23.5** | **23.3** | **23.4** | **23.5** | **23.3** |
| | Americas | 19.0 | 19.9 | 19.6 | 19.5 | 19.6 | 19.6 | 19.5 |
| | Europe | 3.3 | 3.4 | 3.5 | 3.3 | 3.3 | 3.4 | 3.2 |
| | Asia Oceania | 0.5 | 0.4 | 0.4 | 0.5 | 0.5 | 0.5 | 0.5 |
| 2 | **Non-OECD** | **29.8** | **30.3** | **30.2** | **29.9** | **30.0** | **30.1** | **29.7** |
| | FSU | 13.9 | 14,0 | 14.0 | 13.9 | 13.9 | 13.9 | 13.7 |
| | Europe | 0.1 | 0.1 | 0.1 | 0.1 | 0.1 | 0.1 | 0.1 |
| | China | 4.2 | 4.3 | 4.4 | 4.3 | 4.3 | 4.3 | 4.2 |
| | Other Asia | 3.5 | 3.6 | 3.6 | 3.6 | 3.7 | 3.6 | 3.6 |
| | Americas | 4.4 | 4.6 | 4.6 | 4.5 | 4.6 | 4.6 | 4.7 |
| | Middle East | 1.3 | 1.3 | 1.2 | 1.2 | 1.2 | 1.2 | 1.2 |
| | Africa | 2.3 | 2.3 | 2.3 | 2.3 | 2.3 | 2.3 | 2.2 |
| 3 | **Processing gains** | **2.2** | **2.2** | **2.2** | **2.2** | **2.2** | **2.2** | **2.3** |
| 4 | **Global biofuel** | **2.2** | **1.8** | **2.4** | **2.8** | **2.4** | **2.3** | **2.4** |
| 5 | **OPEC** | **36.6** | **36.9** | **38.1** | | | | |
| | Crude | 30.3 | 30.5 | 31.5 | | | | |
| | NGLs | 6.4 | 6.5 | 6.5 | 6.6 | 6.7 | 6.6 | 6.8 |
| 6 | **Non-OPEC** | **57.0** | **58.1** | **58.3** | **58.2** | **58.0** | **58.1** | **57.7** |

*Source: International Energy Agency - September Oil Market Report 2015*

The US has long pushed for liberalised trade, with US-produced crude being the biggest exception since the shock of the 1973 Arab oil embargo led Congress to ban oil exports under nearly all circumstances. The House now votes as early as September to lift the oil-export ban, with Senate action anticipated early next year, which would mark a milestone few saw coming. But while freely exporting US oil may come as a shock to some, it probably won't cause much of an economic stir, especially with global oil prices now below USD 50/barrel.

Thanks to the fracking revolution, the US is no longer the energy-dependent nation it was for most of the past 50 years. Oil production since 2007 has shot up more than 80% to 9.5 million barrels/day. The US still imports a lot of oil, but the share from foreign sources, 27%, is at its lowest level since 1985. According to the Wall Street Journal, the US is already exporting more than a half-million barrels of crude a day to Canada, the biggest exemption under the ban. That is 14 times as much as in 2007, but still just 5.2% of US oil produced a day.

More than a dozen American oil companies contend that allowing unfettered oil exports would eliminate market distortions and streamline US production. Many US refineries, heavily concentrated along the Gulf Coast,

are best tooled to handle medium-and heavy-grade oil imported from the Middle East and elsewhere. The US oil is lighter and best refined with different equipment. Many US refineries can refine the lighter oil but only at an additional cost.

Because of this mismatch and the export ban, US-based refineries have been buying domestic crude at a discount compared with oil elsewhere and still selling refined products at higher prices on the world market. The US government doesn't limit exports of refined products; these exports have more than doubled since 2007.

Most economists say allowing oil exports would likely prompt a chain of market interactions that could result in bringing down the price of gasoline, whose national monthly average last month - USD 2.88/gallon - was the lowest July level since 2010. Exporting oil would encourage more US drilling, which would boost supplies, putting downward pressure on the global price of oil. That would ease the price of gasoline traded in world markets. Eventually, that could cut US pump prices by up to US 12 cents a gallon, according to several recent studies.

Drilling activity in Canada is set to drop 30% this year to 7,778 wells, of which 7,765 wells are onshore and 13 wells offshore. Investment in Canada's oil sands extraction industry is dropping, and shale operators in the Horn River and Montney are cutting back on drilling. Exploratory drilling fell down almost 7%. Canadian producers continue to drill longer wells, with total meters drilled rising to 24.76 million last year. Oil sands operators are shelving projects, making layoffs, and looking for cost-savings. In addition, as oil sands production shifts increasingly to in situ recovery, rather than mining, the array of technical options continues to grow, as operators become increasingly innovative in extracting bitumen. Regardless of short-term issues, oil sands production is still expected to reach 3.0 million barrels/day before the end of 2015. Because oil sands represent the enormous value to the Canadian economy, the Canadian Energy Research Institute estimates that oil sands investments and revenues will add approximately CAD 3.87 trillion to Canada's GDP between 2014 and 2038. Therefore the total investment in oil sands development will top CAD 514 billion in that time frame. Land sales saw a modest resurgence in 2014, but still well behind the record CAD 5 million collected in 2008. Because land inventories are a consistent indicator of future drilling activity; the decrease in land sale volumes indicates that although there are some positive signs in Canada, it would be premature to suggest that any big increase is imminent.

According to Mexico's National Commission on Hydrocarbons (CNH), of the 21 exploratory wells drilled in Mexico during the first three quarters of 2014, only seven had commercially viable oil or gas production. CNH also said that state firm Pemex originally had intended to drill 53 exploratory wells, and was not only far behind in its drilling schedule, but also experiencing a very low success rate. In response to declining production, Mexico is ending Pemex's monopoly and holding licensing rounds to encourage foreign investment. Due to that this year, 2015, will very likely be the most important year in the modern history of Mexico's oil and gas industry. This is not only because implementation of the New Energy Reform Law will begin, but also because this law is much desired and anticipated by the government to stimulate economic growth. Pemex is releasing 14 contracts up for bids in the Gulf of Mexico, for which success is now in question, given that the price of crude oil has dropped. On its own initiative, Pemex is expected to drill 593 wells during 2015, an increase of 19.1% from 2014. From now on, Mexico is betting on big investments in its first round of exploration bids, Round One, to try to shore up its faltering oil and gas production. In this Round One, 169 blocks will be offered for bidding, of which 109 are exploration projects, and 60 are for extraction. Pemex hopes to attract annual investments of CAD 12.6 billion for four years. The blocks cover an area of 28,500km$^2$ of which 91% are exploration areas, and the remaining 9% are oil fields for development and production. The 2P reserves and prospective resources up for bidding represent a volume of 3.8 billion barrels of oil equivalent and 14.6 billion barrels of oil equivalent, respectively.

**Europe**

Drilling activity in Western Europe reflects weakness in its economy, with an 11.8% decrease to just 480 wells. Overall, activity in the North Sea is expected to decrease 12.4%, to 365 wells. Oil production took another tumble, avering 2.77 million barrels/day, a 0.6% decline.

In 2014, the UK unveiled the results of the nation's 28$^{th}$ offshore licensing round. Awards for an initial tranche of 134 licenses, covering 252 blocks, were announced on November. This year, the UK also launched its 14$^{th}$ onshore licensing round. The license offers were made public during the first half of 2015. Lower oil prices are sure to bring further the upstream budget cuts, particularly for

E&P activities. The number of exploration wells is expected to decrease 20%.

In January 2015, Norwegian officials offered ownership interests in 54 new production licences. Forty-three companies were awarded ownership interests in one or more licenses; 23 of these will be offered operatorships. On January 20, Norway announced its 23rd licensing round, comprising 57 blocks, or parts of blocks. These are distributed with 34 blocks in the South-eastern Barents sea and the Norwegian sea. The government aims to award the licenses during first-half 2016.

Activity throughout Eastern Europe is expected to drop 2,7% to 8,281 wells. Drilling in the region is dominated by Russia, which accounts for 83% of all new wells. Thank to a surge in Russian output, regional production increased 0.7% to 13.5 million barrels/day. In response to the Ukrainian crisis, Russia was hit with the US and EU sanctions, which are carry forward and hinder the nation's ability to exploit its shale resources and Arctic deposits. Nevertheless as Russian companies stepped up drilling last year, the country's production in December 2014 rose to post-Soviet record of 10.667 million barrels/day, indicating that the country has yet to feel the effects of sanctions. Drilling this year is expected to ease off slightly, losing 2.0% to 6,867 wells.

Last September, Rosneft and ExxonMobil struck oil in the Kara Sea with the Universitetskaya-1 wildcat. Then, in January 2015, ExxonMobil began production at the Sakhalin-1project's Arcutun-Dagi field, the last of three fields to be developed. Peak production from the field should reach 90,000 barrels/day.

In other countries, Kazakhstan's Kashagan oil project in the Caspian Sea will definitely resume output by 2017. Production may even resume in 2016. In January 2015, the Croatian government granted 10 licenses for exploration in the Adriatic Sea.

**Africa**

The investments for sustaining production levels and increasing reserves have been inadequate at best, even in countries with relative economic and social stability. The bright spot lies offshore, in the western regions and in deep water. Falling oil prices have made outside investors even more reluctant to commit to projects. Accordingly, African drilling is predicted to decline 10.7%, to 1,408 wells. Oil production slipped 9.1%, averaging 7.78 million barrels/day during 2014.



**Nigeria,** the largest economy of Africa (surpassing South Africa in 2013), has experienced a decline in crude production since second-half 2013, falling an estimated 80,000 barrels/day by the end of 2014. To add further pain to a grim situation, Nigerian officials reported that rampant theft from oil pipelines, along with sabotage by insurgents, was costing the country 300,000 barrels of oil/day. Stepped-up patrols and air surveillance have had only a modest impact on the loss. Nigeria's abundant natural gas reserves lack gathering infrastructure, meaning that up to USD 3 billion in potential gas revenues are being flared. The country produces about 4 billion $ft^3$ of gas/day.

Offshore, Shell's Bonga North West project began producing oil last August. Oil from Bonga North West is transported by a new subsea pipeline to the Bonga FPSO export facility. Ultimately, the project should add 40,000 barrels/day to Nigeria' offshore production. Nevertheless, unless there is a dramatic reversal in crude oil prices or unprecedented investment, many observers expect that



crude production may continue to decline at annual rates of 15% to 20%. Production averaged 2.14 million barrels/day last year. Drilling will remain stagnant at 125 wells.

**Algeria** is Africa's third-largest producer and has experienced production declines similar to Nigeria and Angola. By the end of 2014, Algerian output was averaging 1.12 million barrels/day, which is a 16% decline from the 2005 - 2010 average. Collapsing crude prices have hit the nation particularly hard, because the government depends on petroleum for 97% of its export revenues. In a major effort to reverse the five-year decline, Algeria announced an initiative to invest USD 100 billion in the energy sector by 2020, with an emphasis on the country's large shale deposits in the Benue Trough region. Disappointingly, the most recent licensing round only awarded four out of 31 available blocks. This was the lowest success rate of any of the four rounds undertaken since Algeria's 2005 Hydrocarbon Law, despite tax incentives created for foreign operators.

An ongoing military conflict in **Libya** continues to stifle development. The petroleum industry collapsed after the Libyan dictatorship was overthrown three years ago. Production recovered modestly in the next two years, only to disintegrate again in the wake of the civil war, bottoming out last spring to an estimated 215,000 barrels of oil/day. The conflict continues to revolve around control of below the country's own consumption level. The fighting has taken a toll on drilling, as well, with a 54.4% reduction to just 57 wells expected.

**Egypt** has gone from being a net energy export to a net importer. Highly subsidised fuel has left the government with a deepening debt, and motivated to develop its petroleum resources. In early January 2015, the Egyptian Petroleum Ministry reported that it had signed exploration agreements, for both oil and natural gas, offshore in the Gulf of Suez and in the Western Desert. The ministry signed deals worth about USD 270 million with Shell, BP, Eni and smaller companies. Also about USD 124 million in grants were allocated for drilling 41 wells.

Last fall, Egypt signed exploration deals worth USD 187 million, covering 7 exploration areas. In recent years foreign companies have been hesitant to explore for petroleum in Egypt waters, because the amount the government pays barely covers investment costs. Oil production averaged 691,000 barrels/day, down 4,3%. Drilling is forecast to fall 12%, to 441 wells.

**Middle East**

With OPEC decision to maintain the current production level, active well numbers in the Middle East will increase 11.2%, to 3,053 wells, of which 277 are offshore. Regional oil production continued its slow movement upward, rising about 1%, to 24.8 million barrels/day.

Saudi Arabia has 16% of the world's proved oil reserves, is the largest exporter of total petroleum liquids in the world and possesses the world's largest crude oil production capacity. Saudi Arabia's long-term goal is to further develop its lighter crude oil potential, and maintain current levels of production by offsetting declines in mature fields with newer fields. Saudi Aramco said that it will conduct additional drilling at existing fields to help compensate for the natural declines from mature fields. Saudi Arabia is also expanding its natural gas production capabilities throughout the Kingdom. Therefore, Saudi Arabia drilling will remain nearly even, at 573 wells.

Collected by **Ha Phong**

# TENTATIVE TRAINING COURSES AT CENTRE FOR PETROLEUM TRAINING AND INFORMATION

| No. | Course | Code | Duration | Tentative time | Venue |
|---|---|---|---|---|---|
| **I** | **Petroleum E&P** | | | | |
| 1 | Seismic amplitude analysis and interpretation | EXP_2042_E | 4 days | Nov. 2015 | HN |
| 2 | Carbonate reservoir system in SE Asia | EXP_4044_E | 3 days | Nov. 2015 | HN |
| 3 | Hydrocarbon potential evaluation and reserve calculation | EXP_2024 | 4 days | Nov. 2015 | HN |
| 4 | Tectonic analysis | EXP_3004 | 4 days | Nov. 2015 | HN/HCM |
| 5 | Fractures and faults analysis + field trips | EXP_4005 | 4 days | Nov. 2015 | HN |
| 6 | Advanced geo-chemistry | EXP_2010 | 3 days | Nov. 2015 | HN/HCM |
| 7 | Application of chemical methods and chemical systems for workover and reservoir stimulation | MDS_2007 | 2 days | Nov. 2015 | HN |
| 8 | EOR applications for oilfields in Vietnam | PRD_4002 | 3 - 5 days | Dec. 2015 | HN/HCM |
| 9 | Applied reservoir engineering | EXP_2043_E | 3 days | Jan. 2016 | HN |
| 10 | Advanced reservoir engineering | EXP_2044_E | 3 days | Jan. 2016 | HN |
| 11 | Petrographic analysis on carbonate rocks | EXP_4054_E | 3 - 5 days | Jan. 2016 | HN/HCM |
| **II** | **Petroleum economics and management** | | | | |
| 12 | Contracts for petroleum products distribution | EBA_2031 | 2 days | Oct. 2015 | HN/HCM |
| 13 | Enterprise assessment and re-structure | EBA_2039 | 3 days | Oct. 2015 | HN/HCM |
| 14 | Advanced market forecast | EBA_2023 | 5 days | Oct. 2015 | HN/HCM |
| 15 | Risk management in E&P | EBA_2027 | 4 days | Nov. 2015 | HN/HCM |
| 16 | Suply chain management | EBA_1018 | 5 days | Nov. 2015 | HN |
| 17 | Scientific project management | EBA_2017 | 4 days | Nov. 2015 | HN/HCM |
| 18 | PMI project management | EBA_2040 | 3 - 5 days | Nov. 2015 | HN/HCM |
| **III** | **English** | | | | |
| 19 | English for petroleum industry | ENG_5002 | 60 hours | Oct. 2015 | HN/HCM |
| **IV** | **Other fields** | | | | |
| 20 | Communication skill | SSK_2018 | 3 days | Oct. 2015 | HN/HCM |
| 21 | Fundamentals of petroleum industry | INT_1001 | 2,5 days | Nov. 2015 | HN/HCM |
| 22 | E&P for non-technical professionals (12 modules) | | 3 days/module | 2015-2016 | HN/HCM |

*Note: For any further information, please contact us at the following address:*


*CENTRE FOR PETROLEUM TRAINING AND INFORMATION*

***In Hanoi:***

*14th floor, VPI Tower, 167 Trung Kinh Str., Yen Hoa Ward, Cau Giay Dist.*

*Tel: (+84-4) 37843061/ext: 1420; Fax: (+84-4) 37824950*

***In Ho Chi Minh city:***

*04 Nguyen Thong Str., 7th Ward, 3rd Dist.*

*Tel: (+84-8) 39301394; Fax: (+84-8) 39301394*

***Email: cpti@vpi.pvn.vn***

***Website: http://vpi.pvn.vn/vn/Training.aspx***